



Durham E-Theses

Quark mixing and Kaon transitions

Webb, James

How to cite:

Webb, James (1984) *Quark mixing and Kaon transitions*, Durham theses, Durham University.
Available at Durham E-Theses Online: <http://etheses.dur.ac.uk/7578/>

Use policy

The full-text may be used and/or reproduced, and given to third parties in any format or medium, without prior permission or charge, for personal research or study, educational, or not-for-profit purposes provided that:

- a full bibliographic reference is made to the original source
- a [link](#) is made to the metadata record in Durham E-Theses
- the full-text is not changed in any way

The full-text must not be sold in any format or medium without the formal permission of the copyright holders.

Please consult the [full Durham E-Theses policy](#) for further details.

QUARK MIXING AND KAON TRANSITIONS

The copyright of this thesis rests with the author.
No quotation from it should be published without
his prior written consent and information derived
from it should be acknowledged.

QUARK MIXING AND KAON TRANSITIONS

THESIS SUBMITTED TO
THE UNIVERSITY OF DURHAM

BY

JAMES WEBB, B.Sc. (DURHAM)

FOR THE DEGREE OF DOCTOR OF PHILOSOPHY

DEPARTMENT OF PHYSICS

DURHAM UNIVERSITY

AUGUST 1984



-5. NOV. 1984

- 3 -

CONTENTS

	<u>Page</u>
Acknowledgements	iii
Abstract	iv
Chapter 1 The Standard Model	1
1.1 Gauge Theories - QED and QCD	1
1.2 Spontaneous Symmetry Breaking and the GWS Model	5
1.3 Beyond the Standard Model	11
Chapter 2 The Necessary Top Quark	14
2.1 Flavour Changing Neutral Currents	14
2.2 Experimental Constraints on the Quark Mixing Matrix	18
2.3 Anomalous Ward Identities	20
2.4 Experimental Evidence for the t-Quark	22
Chapter 3 The $K^0 - \bar{K}^0$ Transition Amplitude	25
3.1 Formalism	25
3.2 Experimental Information	29
3.3 $K^0 - \bar{K}^0$ Amplitude: Dispersive Contributions	35
3.4 $K^0 - \bar{K}^0$ Amplitude: The Box Diagram	39
3.5 $K^0 - \bar{K}^0$ Amplitude: Double Penguin Diagram	45

	<u>Page</u>	
Chapter 4	Phenomenological Applications of the	
	$K^0 - \bar{K}^0$ Transition	47
	4.1 Phenomenology: 1966 - 1983	47
	4.2 B-Meson Decay	53
	4.3 Phenomenology: 1983 - 1984	58
	4.3.1 Limits on B	58
	4.3.2 Bounds on t-Quark Mass	63
	4.3.3 Maximal CP-Violation	67
Chapter 5	Analysis of the $K^0 - \bar{K}^0$ Transition	
	Amplitude	68
	5.1 Introduction	68
	5.2 The Box Diagram Contribution	69
	5.3 Penguin Diagram Contributions	73
	5.4 Dispersive Contributions to δm	75
	5.5 Conclusions	78
Chapter 6	Conclusions	80
References		86

ACKNOWLEDGEMENTS

I would like to thank Fred Gault for his collaboration, advice and support throughout the period in which this research was undertaken. My thanks go to him and to Alan Martin for reading the manuscript.

I am also grateful to V.Barger and J.Trampetić for useful comments and to L.-L.Chau for useful telegrams. I thank the members of the particle physics group at Durham - Fred Gault, Alan Martin, Peter Collins, Mike Pennington, Stuart Grayson, Tim Spiller, Anthony Worrall, Nigel Glover, Anthony Allan, Neil Speirs, King Lun Au, Martin Carter and Tony Peacock - for their various views on particle physics in general and this work in particular.

I am grateful to the SERC for financial support.

Finally, I would like to dedicate this thesis to my parents, without whom it would not have been possible!

ABSTRACT

The phenomenological applications of strangeness changing neutral currents, particularly the $K^0 - \bar{K}^0$ transition, are reviewed. In the Standard Model there are three possible contributions to this transition: the box diagram, the double penguin and the long distance dispersive amplitudes. The results obtained from a phenomenological study of the $K^0 - \bar{K}^0$ amplitude are shown to depend critically on the assumptions made about the relative magnitudes of each of these contributions.

Upper and lower bounds on the size of the hadronic matrix element (B) of the box diagram amplitude are derived, assuming that this amplitude is the dominant contribution to the $K^0 - \bar{K}^0$ transition. No interesting upper bound can be derived under other assumptions.

Measurements of the B-meson lifetime and partial decay widths are used to restrict the allowed ranges for the parameters θ_2 and θ_3 of the quark mixing matrix. This information is used, together with an analysis (under various assumptions) of the $K^0 - \bar{K}^0$ mass matrix, to derive lower bounds on the mass of the t-quark (m_t) as a function of the parameter B . These bounds can also be regarded as lower bounds on B as a function of m_t .

The information from B-meson decays is used to determine the box diagram contribution to the $K_L - K_S$ mass difference. For $B \ll 1$ this is significantly less than the experimental result. The double penguin amplitude is also estimated and a possibly large contribution to δm is found. There is no compelling phenomenological reason to include a substantial contribution to δm from long distance dispersive amplitudes.

CHAPTER 1

THE STANDARD MODEL

1.1 Gauge Theories - QED and QCD

The strangeness changing neutral currents $K^0 \rightarrow n\pi$, $K_L \rightarrow \mu^+\mu^-$ and particularly $K^0 \leftrightarrow \bar{K}^0$ have been, in the past, a useful source of information about weak interactions. In the standard model these transitions are understood to occur as a result of the mixing between the quarks which are the basic constituents of hadrons. In this work a study is made of the information about quarks and their relation to hadrons that can be gained through a phenomenological analysis of such transitions. The reliability of this information is also investigated.

All known particle interactions are now thought to be described by gauge theories, which have risen to pre-eminence in particle physics as the result of two factors. The first is their renormalizability (i.e. that divergences in non-lowest order calculations can be removed in a well defined way); the second is the remarkable success of one particular gauge theory, namely Quantum Electrodynamics (QED). The agreement of the QED prediction for the anomalous magnetic moment of the muon with the experimental result is better than 1 part in 10^5 .

QED describes the interaction of a spin- $\frac{1}{2}$ fermion with a spin-1 photon. The Lagrangian for this theory is

$$L = \bar{\Psi}(i\gamma^\mu(\partial_\mu + ieA_\mu) - m)\Psi - \frac{1}{4}F^{\mu\nu}F_{\mu\nu} \quad (1.1)$$



where ψ is the fermion field, A_μ is the photon field and $F_{\mu\nu}$ is the electromagnetic field strength tensor

$$F_{\mu\nu} = \partial_\nu A_\mu - \partial_\mu A_\nu$$

This Lagrangian is invariant under global (position independent) phase transformations

$$\psi \rightarrow \exp(-i\alpha) \psi$$

This invariance implies that the phase α has no physical meaning and can, therefore, be chosen arbitrarily. However, it is unnatural to fix α uniquely over all space and time and it is more satisfactory to have the possibility of choosing it locally, i.e. to require the Lagrangian to be invariant under

$$\psi \rightarrow \exp(-i\alpha(x)) \psi$$

This invariance is obtained if A_μ transforms under the local phase transformation as

$$A_\mu \rightarrow A_\mu + \frac{1}{e} \partial_\mu \alpha(x)$$

which is the usual gauge transformation for the electromagnetic vector potential.

The requirement of local gauge invariance has two important consequences. The first is that the coupling of the photon to the fermion is restricted to be of the "minimal" form given above. The second consequence is that a mass term for the photon of the type $M^2 A_\mu A^\mu$ is forbidden. The masslessness of the photon leads to the $1/r$ form for the coulomb potential. The impressive success of QED in describing the interaction of electrons and photons leads one to believe that the gauge invariance of QED is not only a formal property of the theory, but is an essential ingredient of it. Consequently, it is natural to attempt to describe weak and strong

interactions in terms of a gauge theory.

The principle of local gauge invariance was generalized by Yang and Mills /1/ in 1954. In QED one is dealing with the very simple gauge symmetry of the abelian U(1) group whose generators are constants. The original Yang-Mills theory was a theory of strong interactions with the SU(2) group of isospin as the gauge symmetry, involving the proton and neutron as fundamental fermions. The modern version of this theory is Quantum Chromodynamics (QCD) /2,3/ in which the fundamental fermions are quarks lying in a triplet representation of an SU(3) group called colour. The SU(3) group has eight generators T^a ($a=1,8$) which have representations as traceless 3×3 matrices and form a Lie algebra

$$[T^a, T^b] = if^{abc} T^c$$

where the f_{abc} are the structure constants of the algebra.

The basic Lagrangian of QCD is

$$L = \bar{q}^j (i \gamma^\mu (\delta_{jk} \partial_\mu + ig(T_a^a)_{jk} A_\mu^a) - m \delta_{jk}) q^k - \frac{1}{4} G_{\mu\nu}^a G_a^{\mu\nu} \quad (1.2)$$

where q^k ($k=1,3$) is a colour triplet of quarks of mass m ; A_μ^a ($a=1,8$) is an octet of massless vector gauge bosons called gluons with field strength tensor $G_{\mu\nu}^a$; g is the dimensionless strong interaction coupling constant. Since SU(3) is a non-abelian group, the gauge transformations are more complicated. The QCD Lagrangian is invariant under the infinitesimal gauge transformations

$$q^k \rightarrow q^k - i\alpha^a(x) (T_a^a)^k_j q^j$$

$$A_\mu^a \rightarrow A_\mu^a + f_{bc}^a \alpha^b(x) A_\mu^c + \frac{1}{g} \partial_\mu \alpha^a(x)$$

if the field strength tensor is given by

$$G_{\mu\nu}^a = \partial_\nu A_\mu^a - \partial_\mu A_\nu^a - gf_{bc}^a A_\mu^b A_\nu^c$$

From this equation it can be seen that the gluon kinetic energy term, $G_{\mu\nu}^a G_a^{\mu\nu}$, contains triple and quartic gluon interactions. In this self-coupling of the gauge bosons (which is a consequence of the non-abelian nature of the gauge group) QCD is very different from the abelian QED. These gluon self-interactions are important because their existence ensures the unitarity of some basic scattering processes, e.g. $q\bar{q} \rightarrow gg$ and $gg \rightarrow gg$ (where, here, "g" represents a gluon).

Higher order corrections to the basic quark-gluon coupling leads to the idea of a "running" coupling constant, i.e. the coupling g depends on momentum in a very definite way. The coupling "constants" $\alpha_s = g^2/4\pi$ at two different momentum scales Q^2 and μ^2 are related by

$$\alpha_s(Q^2) = \frac{\alpha_s(\mu^2)}{1 + \frac{\beta_0 \alpha_s(\mu^2)}{4\pi} \ln(Q^2/\mu^2)} \quad (1.3)$$

where

$$\beta_0 = 11 - \frac{2}{3}n_f$$

and n_f is the number of fermions. If $n_f \leq 16$ ($\beta_0 > 0$) then $\alpha_s(Q^2) < \alpha_s(\mu^2)$ for $Q^2 > \mu^2$. This property is known as asymptotic freedom since $\alpha_s(Q^2) \rightarrow 0$ as $Q^2 \rightarrow \infty$. It is this property of QCD which enables sensible perturbative calculations to be performed at high Q^2 despite the fact that at long distances α_s is not small (presumably leading to the confinement of quarks and gluons inside hadrons). The running coupling constant can also be expressed as

$$\alpha_s(Q^2) = \frac{4\pi}{\beta_0 \ln(Q^2/\Lambda^2)} \quad (1.4)$$

where Λ is a momentum scale which (approximately) delineates the boundary of the non-perturbative regime. The value of Λ can be extracted from data on deep inelastic scattering /4,5/ with some uncertainties, and is in the range

$$0.1 \leq \Lambda(\text{GeV}) \leq 0.5$$

Higher order calculations in QCD produce corrections which are proportional to $\alpha_s^n(\mu^2) \ln^n(Q^2/\mu^2)$ where μ^2 is the renormalisation scale. When only the terms with $n=m+1$ are retained the calculation is in the "leading logarithm approximation". In $O(\alpha_s)$ calculations the leading logarithms can be absorbed by replacing $\alpha_s(\mu^2)$ with the running coupling constant $\alpha_s(Q^2)$.

Like QED, QCD has performed well (though less spectacularly) when confronted by experiment /3/. This leads to the hope that weak interactions are also described by a gauge theory. However, in the case of weak interactions the postulated vector bosons are massive, as demonstrated by the short range of the interaction, and gauge invariance forbids an explicit mass term of the form $M^2 A_\mu A^\mu$. So, if weak interactions are to be described by a gauge theory, a more subtle method of introducing a vector boson mass must be found. This can be achieved by the (ad hoc) method of spontaneous symmetry breaking.

1.2 Spontaneous Symmetry Breaking and the GWS Model

The existence of massive vector bosons implies that the gauge symmetry of weak interactions has been broken. A simple way to describe this symmetry breaking would be to add explicitly non-invariant terms to the Lagrangian, such as the mass term given above. However, this method destroys some of the important features of the original gauge theory - its unitarity and renormalizability /6/.

An alternative way in which the gauge symmetry can be broken, referred to as spontaneous symmetry breaking, gives masses to the vector bosons and yet retains the important properties of the original theory. The idea is to have a theory where the Lagrangian is still exactly symmetric under the group transformations but it gives rise, for dynamical reasons, to a ground state which is not invariant. Non-invariance of the ground state (vacuum) leads to a well defined pattern of symmetry breaking effects.

Glashow /7/ was the first to propose that the underlying field theory of weak interactions was an SU(2)xU(1) gauge theory which included QED as well. This idea was taken up later by Weinberg /8/ and Salam /9/ who included the Higgs mechanism /10/ for spontaneous symmetry breaking. The resulting theory is referred to as the Glashow-Weinberg-Salam (GWS) theory, and it is renormalizable /11/.

The Lagrangian of a basic SU(2)xU(1) gauge theory involving four vector bosons (one for each generator of SU(2)xU(1)) coupled to an SU(2) doublet of complex scalar fields is

$$L = (D_\mu \phi)^\dagger (D^\mu \phi) - V(\phi^\dagger \phi) - \frac{1}{4} F_{\mu\nu}^a F_a^{\mu\nu} - \frac{1}{4} G_{\mu\nu} G^{\mu\nu} \quad (1.5)$$

where $F_{\mu\nu}^a$ (a=1,3) is the field strength tensor for the triplet of gauge fields (W_μ^a) corresponding to the SU(2) group and $G_{\mu\nu}$ is the tensor for the gauge field (B_μ) of the U(1) group. The "covariant derivative" of the scalar field (ϕ) is given by

$$D_\mu \phi = \left(\partial_\mu + ig \frac{1}{2} t_a W_\mu^a + ig' \frac{1}{2} B_\mu \right) \phi$$

where t_a are the three Pauli matrices. The two coupling constants g and g' are independent since the gauge symmetry is a direct product of the two groups. The scalar potential is given by

$$V(\phi^+\phi) = \mu^2 \phi^+\phi + \lambda (\phi^+\phi)^2$$

where $\lambda > 0$ so that V is bounded from below, but the sign of μ^2 is undetermined. If μ^2 represents the usual mass term for a scalar field, i.e. $\mu^2 > 0$, then V has a minimum at $\phi^+\phi = 0$ and the ground state is invariant under the full gauge group. However, if $\mu^2 < 0$, then V has a minimum when $\phi^+\phi = v^2/2$ with $v^2 = -\mu^2/\lambda$. When the particle content of the theory is determined with respect to this vacuum it is found that three of the scalars have become the longitudinal components of the gauge bosons which have gained masses.

Defining

$$\phi(x) = \frac{1}{\sqrt{2}} \begin{pmatrix} 0 \\ v + \sigma(x) \end{pmatrix}$$

such that $\phi_{\text{vacuum}} = v/\sqrt{2}$ as above, the term in the Lagrangian involving the covariant derivatives of the scalar field gives

$$\begin{aligned} (D_\mu \phi)^\dagger (D^\mu \phi) &= \frac{1}{2} (\partial_\mu \sigma) (\partial^\mu \sigma) + \frac{1}{2} (\frac{1}{2} g v)^2 (W_\mu^1 W_\mu^1 + W_\mu^2 W_\mu^2) \\ &\quad + \frac{1}{2} (\frac{1}{2} v)^2 ((g W_\mu^3 - g' B_\mu) (g W_\mu^3 - g' B_\mu)) \\ &\quad + \text{higher order terms} \end{aligned}$$

Defining

$$W_\mu^\pm = \frac{1}{\sqrt{2}} (W_\mu^1 \pm i W_\mu^2)$$

and

$$\begin{aligned} Z_\mu &= \cos\theta_W W_\mu^3 - \sin\theta_W B_\mu \\ A_\mu &= \sin\theta_W W_\mu^3 + \cos\theta_W B_\mu \end{aligned}$$

with

$$\tan\theta_W = g'/g$$

gives

$$\begin{aligned}
 (D_\mu \phi)^\dagger (D^\mu \phi) &= \frac{1}{2} (\partial_\mu \sigma) (\partial^\mu \sigma) + M_W^2 (W_\mu^+ W_\mu^- + W_\mu^- W_\mu^+) \\
 &+ M_Z^2 (Z_\mu Z^\mu) + \text{higher order terms}
 \end{aligned}
 \tag{1.6}$$

This shows that two of the gauge bosons have gained a common mass

$$M_W = \frac{1}{2} g v \tag{1.7}$$

whilst a third has a mass

$$M_Z = M_W / \cos \theta_W \tag{1.8}$$

and a fourth is massless. This last boson is identified with the photon and the others are the weak interaction bosons (W^\pm , Z). The identification of A_μ with the photon leads to the relations

$$g \sin \theta_W = e = g' \cos \theta_W \tag{1.9}$$

The existence of a massless gauge boson (the photon) demonstrates the presence of an unbroken U(1) symmetry as required by QED.

Equation (1.6) contains the usual kinetic term for a scalar particle (σ). This is the Higgs scalar and its mass is given from $V(\phi^\dagger \phi)$ to be $|\mu|^2$. This mass is not determined by the theory and is left as a free parameter.

Fermions are introduced in left handed doublets and right handed singlets of the SU(2) group, e.g. for the leptons e and ν_e

$$\begin{pmatrix} \frac{1}{2}(1 - \gamma_5) \nu_e \\ \frac{1}{2}(1 - \gamma_5) e \end{pmatrix} ; \frac{1}{2}(1 + \gamma_5) e ; \frac{1}{2}(1 + \gamma_5) \nu_e$$

For this reason the SU(2) group is labelled with a subscript L: $SU(2)_L$. The fermions each have a U(1) hypercharge quantum number Y and, after spontaneous symmetry breaking, the combination

$$Q = \frac{1}{2}(t_3 + Y)$$

is identified as the electric charge of the fermion. The fermions are given a Yukawa coupling to the scalar ϕ which, after spontaneous symmetry breaking, gives a mass to the fermions (an explicit mass term is forbidden by the chiral nature of the gauge group). The case of quarks is complicated by the fact that the mass eigenstates are not identical to the weak interaction eigenstates, but are related to them by a unitary transformation. This is discussed in Chapter 2.

The amplitude for the decay $\mu \rightarrow e \bar{\nu}_e \nu_\mu$ as given by the GWS theory at low momentum transfer ($k^2 \ll M_W^2$) is (the Feynman rules for the GWS theory can be found in ref./12/)

$$A = g^2 (\bar{\nu}_\mu \gamma^\lambda (1 - \gamma_5) \mu) (\bar{e} \gamma_\lambda (1 - \gamma_5) \nu_e) / 8M_W^2$$

which coincides with the (V - A) current x current prediction if

$$\frac{G_F}{\sqrt{2}} = \frac{g^2}{8M_W^2} \tag{1.10}$$

Using this and equation (1.9) leads to an expression for the W-boson mass, with $\alpha = e^2/4\pi$

$$M_W = \left(\frac{\pi\alpha}{\sqrt{2}G_F} \right)^{\frac{1}{2}} \frac{1}{\sin\theta_W} = \frac{37.3}{\sin\theta_W} \text{ GeV}$$

and consequently

$$M_Z = \frac{M_W}{\cos\theta_W} = \frac{74.6}{\sin 2\theta_W} \text{ GeV}$$

Measurements of $\sin\theta_W$ give /13/

$$\sin^2\theta_W = 0.229 \pm 0.010$$

which leads to $M_W = 70$ GeV and $M_Z = 89$ GeV. Radiative corrections alter these estimates to give /14/

$$M_W = 82 \pm 2.4 \text{ GeV}$$

$$M_Z = 93 \pm 1.6 \text{ GeV}$$

These vector bosons have been discovered at the $p\bar{p}$ collider in CERN. Their masses have been measured to be /15,16/

$$M_W = 80.9 \pm 1.5 \text{ GeV}$$

$$M_Z = 95.6 \pm 1.4 \text{ GeV}$$

(1.11)

which are in remarkable agreement with the theoretical predictions.

The GWS theory of weak and electromagnetic interactions is in good agreement with experiment both at low /17/ and high /15,16/ energies. Nevertheless, the theory contains some unsatisfactory features:

- i) the ad hoc introduction of scalar particles to induce the spontaneous symmetry breaking;
- ii) the couplings of these scalars to the fermions in the theory must all be different so that the fermions obtain different masses after the symmetry breaking. These couplings are a priori undetermined in the theory;
- iii) the observed parity violation of weak interactions is put in by hand - the fermions left and right handed pieces transform differently under the SU(2) gauge group.

In an attempt to overcome these problems people have been led to consider extensions of the standard model. Some of these extended theories are described in the next section.

1.3 Beyond the Standard Model

The Standard Model is based on an $SU(3) \times SU(2) \times U(1)$ gauge theory which has been successful in describing observed interactions. However, a number of theoretical problems have motivated the construction of many theories which contain the Standard Model as a low energy approximation.

One fruitful approach is grand unification: at energies greater than some scale M_X particle interactions are described by a gauge theory based on (in most cases) a single group. This group contains the standard $SU(3) \times SU(2) \times U(1)$ as a subgroup and a simple example is the $SU(5)$ theory of Georgi and Glashow /18/. The extra degree of symmetry in these theories provides relations between some of the free parameters of the Standard Model. For example, the quantity $\sin\theta_W$ is predicted in the $SU(5)$ model mentioned above and the result is in reasonable agreement with experiment /19/.

The technique of spontaneous symmetry breaking is also used in Grand Unified Theories (GUTs). At a scale M_X the GUT symmetry is broken, either directly or indirectly, to the standard group. This is effected by a set of scalar particles which are introduced in addition to those used to break the GWS group down to $U(1)_{e.m.}$. The gauge bosons which are not associated with the generators of the standard $SU(3) \times SU(2) \times U(1)$ group gain masses $\sim M_X$. In the $SU(5)$ model M_X is about 10^{15} GeV.

In GUTs quarks and leptons sit in the same multiplets of the gauge group. One consequence of this is that the bosons with masses $\sim M_X$ after the first symmetry breaking can cause transitions which violate baryon number. The $SU(5)$ theory of Georgi and Glashow

predicts that protons should decay with a lifetime $\tau_p \sim 10^{26}$ to 10^{31} years in a dominant decay mode of $p \rightarrow e^+ \pi^0$ /20/. Experiments to detect proton decay are in progress /21/ and the results of the IMB experiment /22/ give a lower bound on τ_p which is at the upper limit of the range in the SU(5) model. This may indicate that the simplest SU(5) model is ruled out. If this is the case, one must turn to other groups, such as SO(10), or to a more complicated Higgs structure.

One feature of low energy weak interactions which is not explained either in the Standard Model or in the SU(5) GUT is parity violation. A possible solution to this problem is found in left-right symmetric models (LRS models) based on the gauge group $SU(2)_R \times SU(2)_L \times U(1)$ /23/. These models contain an extra three gauge bosons related to the generators of the $SU(2)_R$ group (W_R^+ , Z_R^0). The standard gauge bosons are labelled W_L^+ , W_L^- , Z_L^0 , γ and the three neutral particles (Z_R^0 , Z_L^0 , γ) are mixtures of the basic gauge bosons as in the standard GWS theory.

At high energies this theory is parity conserving and parity violation is introduced via spontaneous symmetry breaking. The symmetry breaking occurs in two stages: first the full group is broken down to the GWS group at a scale M_{W_R} , then the GWS group is broken at the usual scale $M_{W_L} \sim 80$ GeV. The observed parity violation arises as a consequence of $M_{W_R} > M_{W_L}$. Present data on beta decay and non-leptonic kaon decay require $M_{W_R} \gg 300$ GeV /24,25/.

LRS theories are compatible with grand unification. In particular the GUT group SO(10) contains $SU(2) \times SU(2) \times U(1)$ as a subgroup. The more natural incorporation of parity violation together with the recent results on proton decay perhaps make an SO(10) theory a better candidate for a GUT.

The existence of scalar particles in all the theories described above poses a number of theoretical problems. One such problem is the need to maintain a hierarchy of mass scales ($M_W \ll M_X$) when higher order corrections are included. Supersymmetry /26/ has been proposed as a solution to those problems.

Supersymmetry is a theory which relates bosons to fermions. This has the unfortunate consequence that each boson and fermion in a standard theory must be given a partner differing by half a unit of spin to make the theory supersymmetric. That is, the existence of squarks (scalar quarks), sleptons (scalar leptons) and gauginos (spin- $\frac{1}{2}$ gauge particles) is predicted. If supersymmetry were exact each of these new particles would have the same mass as its standard counterpart. As this is experimentally not the case, supersymmetry, if it exists, must be broken.

Supersymmetry also provides the possibility of including gravitational interactions in the form of Supergravity /27/. Such theories can have interesting consequences at low energies, particularly for the phenomenon of spontaneous symmetry breaking /28/. Supersymmetric theories of weak interactions can be constructed /29/.

In conclusion, the standard model of weak interactions based on an $SU(3) \times SU(2) \times U(1)$ gauge theory agrees well with low energy experiments. Nevertheless, this theory has some theoretical problems and solutions for these are sought by extending the GWS theory in various directions. The possibility exists that some alternatives can be ruled out by consideration of low energy data.

CHAPTER 2

The Necessary Top Quark

2.1 Flavour Changing Neutral Currents

As mentioned in Chapter 1, the quark sector of the GWS theory of weak interactions is complicated by the fact that the weak eigenstates are not identical with the mass eigenstates. Prior to the discovery of the J/ψ resonance, low energy hadron spectroscopy required the existence of three quarks: u, d, s /30/. Weak interactions couple the u-quark to the combination /31/

$$d_w = \cos\theta_c d + \sin\theta_c s \quad (2.1)$$

where θ_c is the Cabibbo angle, the magnitude of which is given by /32/

$$\cos\theta_c = 0.9737 \pm 0.0025 \quad (2.2)$$

This device also allows the retention of a universal low energy coupling constant /32/

$$G_F = (1.16632 \pm 0.00002) \times 10^{-5} \text{ GeV}^{-2} \quad (2.3)$$

This Cabibbo mixing is satisfactory for all charged current interactions (involving the exchange of a W boson). However, it causes some problems in the neutral current sector (involving, at lowest order, the exchange of a Z^0). Here the Cabibbo theory leads to amplitudes $\sim G_F \sin\theta_c \cos\theta_c$ for flavour changing neutral currents (FCNCs), (e.g. $K^0 \rightarrow \mu^+ \mu^-$, $K \rightarrow \pi \nu \bar{\nu}$, $K^0 \rightarrow \gamma\gamma$, $K \rightarrow \pi \gamma\gamma$, $K \rightarrow \pi e^+ e^-$) which contradicts the observed /33/ suppression of

such processes.

The standard remedy for this failure was proposed by Glashow, Iliopoulos and Maiani (GIM) /34/. They introduced a fourth quark - the c-quark - which couples to the combination of d- and s-quarks

$$s_w = \cos\theta_c s - \sin\theta_c d$$

which is orthogonal to equation (2.1). In the GWS theory the gauge boson W_μ^3 couples to a quark current associated with the SU(2) generator t_3 . This current is

$$\begin{aligned} J_\mu &= (\bar{u} \gamma_\mu (1 - \gamma_5) u - \bar{d}_w \gamma_\mu (1 - \gamma_5) d_w) \\ &\quad + (\bar{c} \gamma_\mu (1 - \gamma_5) c - \bar{s}_w \gamma_\mu (1 - \gamma_5) s_w) \\ &= (\bar{u} \gamma_\mu (1 - \gamma_5) u - \bar{d} \gamma_\mu (1 - \gamma_5) d) \\ &\quad + (\bar{c} \gamma_\mu (1 - \gamma_5) c - \bar{s} \gamma_\mu (1 - \gamma_5) s) \end{aligned}$$

which is diagonal in the mass eigenstates. As the current coupled to the Z^0 is a linear combination of J_μ and the electromagnetic current, which is also flavour diagonal, FCNCs are forbidden at tree level. This suppression is natural in the sense of Glashow and Weinberg /35/ in that it is independent of the value of θ_c .

FCNCs are also suppressed to $O(G_F \alpha)$ by the GIM mechanism provided that $m_c \ll M_W$, where m_c and M_W are the masses of the c-quark and the W boson respectively. Gaillard and Lee /36/ used this property in the context of the strangeness changing neutral current $K^0 \leftrightarrow \bar{K}^0$ to estimate m_c . Their result was $m_c \sim 1.5$ GeV which is approximately half the mass of the J/ψ ($c\bar{c}$) resonance.

In the quark sector of the GWS theory the analogues of the lepton - neutrino doublets are

$$\begin{pmatrix} u \\ d_w \end{pmatrix} ; \begin{pmatrix} c \\ s_w \end{pmatrix} \tag{2.4}$$

In these doublets the weak eigenstates of the charge $Q = +\frac{2}{3}$ quarks are identical with the mass eigenstates, and the d- and s-quarks are mixed. Identical results would be obtained if the mass eigenstates of the d- and s- quarks had been used and the u- and c-quarks had been mixed. The form of equation (2.4) is the conventional choice.

In principle, there could be a similar Cabibbo mixing in the leptonic sector. However, there is no experimental evidence /37/ for such a mixing, which has no physical significance if the neutrinos are massless. Only one experiment has reported a positive result for a neutrino mass measurement /38/ but the results are inconclusive /37/.

Kobayashi and Maskawa (KM) extended the idea of Cabibbo mixing to six quarks in order to produce CP-violation /39/. A new pair (t, b) of quarks is introduced and the $Q = -\frac{1}{3}$ quark (b) mixes with the d- and s-quarks:

$$\begin{pmatrix} d_w \\ s_w \\ b_w \end{pmatrix} = \begin{pmatrix} V_{ud} & V_{us} & V_{ub} \\ V_{cd} & V_{cs} & V_{cb} \\ V_{td} & V_{ts} & V_{tb} \end{pmatrix} \begin{pmatrix} d \\ s \\ b \end{pmatrix}$$

where the mixing matrix V_{ij} is unitary ($V^\dagger V = 1$). In general a 3×3 unitary matrix can be parametrized by three angles (θ) and one complex phase (δ). Such a parametrization is

$$V = \begin{pmatrix} c_1 & s_1 c_3 & s_1 s_3 \\ -s_1 c_2 & c_1 c_2 c_3 + s_2 s_3 e^{-i\delta} & c_1 c_2 s_3 - s_2 c_3 e^{-i\delta} \\ -s_1 s_2 & c_1 s_2 c_3 - c_2 s_3 e^{-i\delta} & c_1 s_2 s_3 + c_2 c_3 e^{-i\delta} \end{pmatrix} \quad (2.5)$$

where $c_i = \cos\theta_i$, $s_i = \sin\theta_i$, $i = 1, 2, 3$. In the limit $\theta_2 = \theta_3 = \delta = 0$

this matrix reduces to the Cabibbo matrix with $\theta_1 = \theta_c$. Non-zero δ gives rise to CP-violation.

Many other parametrizations of the quark mixing matrix similar to the above exist in the literature /17,39 - 41/. They are related to the matrix given above by various transformations such as $\theta_i \rightarrow -\theta_i$ and $\delta \rightarrow \delta \pm \pi$. These differences have no physical significance but once the form of the KM matrix is fixed the angles are constrained by $0 \leq \theta_i \leq \pi/2$ and the phase is allowed to vary over the whole range $0 \leq \delta \leq 2\pi$.

The KM parametrization keeps the definition that $\cos\theta_c$ is the ratio between a $d \rightarrow u$ transition and the purely leptonic process $\mu \rightarrow \nu$. In the four quark model the ratio of $s \rightarrow u$ transitions to $d \rightarrow u$ transitions is $\tan\theta_c$ but this definition is no longer true in the six quark model. An alternative parametrization which retains the definition of $\tan\theta_c$ is given by Maiani /42/. The matrix then appears as

$$V = \begin{pmatrix} c_\beta c_\theta & c_\beta s_\theta & s_\beta \\ -s_\gamma c_\theta s_\beta e^{i\delta} - s_\theta c_\gamma & c_\gamma c_\theta - s_\gamma s_\beta s_\theta e^{i\delta} & s_\gamma c_\beta e^{i\delta} \\ -s_\beta c_\gamma c_\theta + s_\gamma s_\theta e^{-i\delta} & -c_\gamma s_\beta s_\theta - s_\gamma c_\theta e^{-i\delta} & c_\gamma c_\beta \end{pmatrix} \quad (2.6)$$

where the phase δ is not identical with the phase in the KM parametrization. Although the Maiani form has the advantage for recent phenomenology that the couplings of the b-quark are simple, the KM type parametrization of equation (2.5) will be used in this work because it is more familiar and widely used.

The unitarity of the KM matrix ensures that an extended version of the GIM mechanism operates. That is, FCNCs involving the b-quark are suppressed to $O(G_F \alpha)$. The discovery of the $\Upsilon(b\bar{b})$ resonance /43/

and subsequent observation of the decays of b-flavoured hadrons /44/ has tested this feature of the Standard Model. For example, if the b-quark were in a weak SU(2) singlet (i.e. had no t-quark partner), then the tree level decay $b \rightarrow d Z^0 \rightarrow d l^+ l^-$ would be allowed. Kane and Peskin /45/ have shown that this would lead to the bound

$$\frac{\Gamma(B \rightarrow l^+ l^- X)}{\Gamma(B \rightarrow l^+ \nu X)} \gg 0.12 \quad (2.7)$$

Data taken by the CLEO collaboration at CESR yields the upper bound /45/

$$\frac{\Gamma(B \rightarrow l^+ l^- X)}{\Gamma(B \rightarrow l^+ \nu X)} < 0.027 \quad (90\% \text{ c.l.}) \quad (2.8)$$

This convincingly excludes the possibility that the b-quark is in a left handed singlet, thus furnishing evidence for the existence of its partner the t-quark.

The observed suppression of FCNCs makes them a useful area for testing the Standard Model and possible extensions. In particular, the values of the KM matrix elements and the mass of the t-quark can be constrained. This type of analysis is discussed in Chapter 4, together with some constraints on left right symmetric and supersymmetric extensions of the GWS theory.

2.2 Experimental Constraints on the Quark Mixing Matrix

The experimental constraints on the KM matrix elements (prior to the information from B-meson decay) are summarized by Kleinknecht and Renk /46/ and by Pakvasa /47/. The additional constraints coming from the observation of B-meson decays are

discussed in Chapter 4.

The coupling parameter $|V_{ud}|$ can be determined from a comparison of nuclear beta decays with the muon decay rate. The result is

$$|V_{ud}| = 0.9737 \pm 0.0025$$

Kaon semileptonic decays give $|V_{us}| = 0.219 \pm 0.003$ whereas hyperon semileptonic decays give $0.223 \leq |V_{us}| \leq 0.230$. The discrepancy between these results is probably due to a lack of theoretical understanding of SU(3) symmetry breaking. A crude average of the two results gives

$$|V_{us}| = 0.224 \pm 0.006$$

The unitarity relation $|V_{ud}|^2 + |V_{us}|^2 + |V_{ub}|^2 = 1$ then gives

$$|V_{ub}| < 0.1$$

The unitarity limit on $|V_{cd}|$ from $|V_{ud}|$ above is $|V_{cd}| < 0.24$. A lower bound can be obtained from data on charm production in deep inelastic scattering. This bound is $|V_{cd}| > 0.2$. Summarizing

$$0.2 < |V_{cd}| < 0.24$$

Analysis of the same data provides a conservative lower bound $|V_{cs}| \geq 0.59$, while a much stronger bound of $|V_{cs}| > 0.8$ can be obtained from $D^+ \rightarrow \bar{K}^0 e^+ \nu_e$. Including the unitarity limit from $|V_{cd}|$, then

$$0.8 < |V_{cs}| < 0.98$$

The unitarity limit for $|V_{cb}|$ from these estimates of $|V_{cd}|$ and $|V_{cs}|$ is

$$|V_{cb}| < 0.57$$

Finally, the unitarity of the KM matrix can be used to limit the elements $|V_{ti}|$. The results are

$$0 < |V_{td}| < 0.13$$

$$0 < |V_{ts}| < 0.56$$

$$0.82 < |V_{tb}| < 1$$

A summary of the constraints on the elements of the KM matrix prior to results from B-meson decay is

$$|V| = \begin{pmatrix} 0.9737 \pm 0.0025 & 0.224 \pm 0.006 & 0.05 \pm 0.05 \\ 0.22 \pm 0.02 & 0.89 \pm 0.09 & 0.28 \pm 0.28 \\ 0.065 \pm 0.065 & 0.28 \pm 0.28 & 0.91 \pm 0.09 \end{pmatrix} \quad (2.9)$$

This form is based on the assumption that there are only three generations of quarks. If there were four or more generations then the lower bounds coming from the unitarity of the KM matrix would be relaxed. In particular, $|V_{tb}| = 0$ would be allowed. The observations of B-meson decays provide much tighter constraints on the elements of the KM matrix. These constraints are given in Chapter 4.

2.3 Anomalous Ward Identities

An argument within the GWS theory for the existence of the t-quark is that the theory is aesthetically more pleasing if all the fermions appear in SU(2) doublets. A more mathematical statement of this is the requirement that the triangle anomalies must vanish.

Ward Identities (i.e. relations between Green's functions) can be derived quite generally in quantum field theories. These relations might be expected to hold in all orders of perturbation theory, which is the case in QED. However, in theories where fermions have an axial coupling (containing a γ_5), it can be shown that an anomalous term appears in a Ward Identity when it is calculated at particular orders in perturbation theory /48,49/. The anomaly appears when divergent Feynman diagrams are considered since there is no regularization procedure which respects axial symmetries. That the anomaly is real and not just a calculational artefact is shown by the Current Algebra calculation of the width for $\pi^0 \rightarrow \gamma\gamma$. Without the anomalous term in the Ward Identity this width is zero /50/. With the anomalous term included the correct result is obtained /51/.

Although the anomaly is welcome in Current Algebra, its existence in a spontaneously broken gauge theory is disastrous. Gross and Jackiw /52/ have shown that, if anomalies are present, such a theory is not renormalizable. Therefore, the anomaly must vanish in a realistic theory.

In a gauge theory the coupling of fermions (ψ) to the gauge fields (W_μ^a), where a is the group index, is of the form

$$g \bar{\psi} \gamma^\mu (1 + \gamma_5) T_a^+ \psi W_\mu^a + g \bar{\psi} \gamma^\mu (1 - \gamma_5) T_a^- \psi W_\mu^a \quad (2.10)$$

T_a^+ and T_a^- are hermitian matrices which define the group structure of the vertices, and $T_a^+ \neq T_a^-$ in general. The diagrams which give rise to the anomaly involve a fermion triangle (Fig. 2.1). By taking the trace round the fermion triangle and summing the contributions from each diagram, one finds that the total anomaly

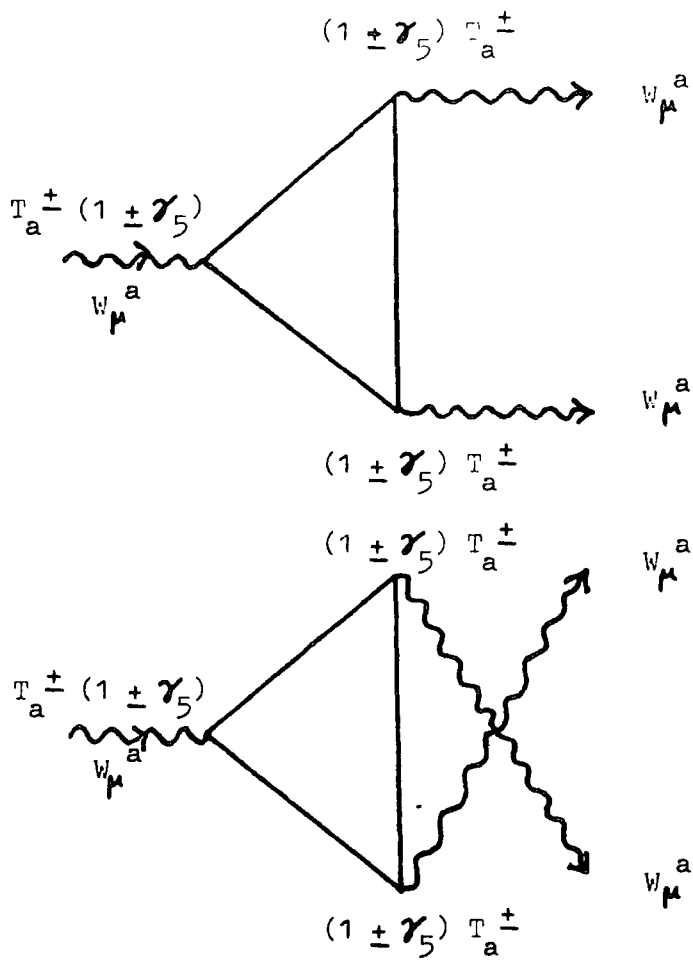


Figure 2.1

The diagrams for the triangle anomaly in a general gauge theory.

(A_{abc}) is proportional to

$$\begin{aligned} A_{abc} &= A_{abc}^+ - A_{abc}^- \\ &= \text{Tr} (\{ T_a^+, T_b^+ \} T_c^+) - \text{Tr} (\{ T_a^-, T_b^- \} T_c^-) \end{aligned} \quad (2.11)$$

Evidently the theory will be anomaly free if $A_{abc} = 0$ which can happen in three ways /53/:

i) $A^+ = A^- \neq 0$. The right and left handed anomalies cancel if T_a^+ and T_a^- are related by a unitary transformation.

ii) $A^+ = A^- = 0$. A representation of a Lie algebra is "safe" if its generators T_a satisfy this condition. The Lie algebras which have only safe representations have been listed /53/ and a gauge theory based on one of these will be anomaly free.

iii) Conditional cancellation. This case occurs when the condition $A^+ - A^- = 0$ places a restriction on the allowable quantum numbers for the particles in the theory. The GWS theory of weak interactions belongs to this class /54/. The condition for the GWS theory is

$$\sum_i Q_i = 0 \quad (2.12)$$

where the sum extends over all the particles in left handed doublets. This condition is satisfied by all the quarks and leptons within one generation (provided that the quarks come in three colours). Thus, if the GWS theory contains a third generation lepton (τ) with associated neutrino, then the b-quark must have a partner with $Q = +\frac{2}{3}$ (i.e. the t-quark).

2.4 Experimental Evidence for the t-Quark

Searches for the t-quark have been made both in e^+e^- and $p\bar{p}$ collisions. At PETRA the ratio

$$R = \frac{\sigma (e^+ e^- \rightarrow \text{hadrons})}{\sigma (e^+ e^- \rightarrow \mu^+ \mu^-)} = 3 \sum_i Q_i^2 \quad (2.13)$$

has been measured up to a centre of mass energy of 45.2 GeV /55/. Up to this energy there is no evidence either for a $t\bar{t}$ resonance or for the increase in R expected once the t-flavour threshold is crossed. As a result a lower bound on the t-quark mass has been derived /55/

$$m_t > 22.0 \text{ GeV} \quad (90 \% \text{ c.l. }) \quad (2.14)$$

A lower limit on the mass of a further $Q = -\frac{1}{3}$ quark is also given:

$$m_q > 21.0 \text{ GeV}$$

The absence of positive evidence for the t-quark in e^+e^- collisions has led to many attempts to place bounds on m_t from other information (see Chapter 4) and to models without a t-quark. These latter models are severely constrained by observations of B-meson decays (section 2.1).

At the $p\bar{p}$ collider the t-quark may be produced by QCD fusion, $p\bar{p} \rightarrow t\bar{t}$, or via the W, $p\bar{p} \rightarrow W \rightarrow t\bar{b}$. By considering the decay mode $t \rightarrow b e^+ \nu_e$ Barger, Martin and Phillips /56/ showed that early UA(1) observations /57/ of an electron with jets and missing energy could be interpreted as being due to a t-quark with mass 25 to 40 GeV. Recently, the UA(1) collaboration have presented evidence for the t-quark in the $W \rightarrow t\bar{b}$ channel and place its mass in the range

$$30 \leq m_t \text{ (GeV)} \leq 50 \quad (2.15)$$

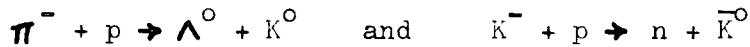
This determination of m_t will be useful for low energy weak interaction phenomenology which, until now, has had to accommodate an unknown value with correspondingly less certain results.

CHAPTER 3

THE $K^0 - \bar{K}^0$ TRANSITION AMPLITUDE

3.1 Formalism

The neutral kaon system can be described in essentially two ways /59 - 61/. The first is as a pair of states which are eigenstates of the strangeness operator. These are the states $|K^0\rangle$ with strangeness +1 and $|\bar{K}^0\rangle$ with strangeness -1 which are produced in strong interactions, for example



In terms of quark content these states are $|K^0\rangle = |d\bar{s}\rangle$ and $|\bar{K}^0\rangle = |\bar{d}s\rangle$. The action of the combined operation of parity and charge conjugation in this basis is given by

$$CP |K^0\rangle = \eta |\bar{K}^0\rangle \quad ; \quad \eta^2 = 1$$

A conventional choice /60/ is $\eta = +1$. The basis of CP eigenstates is then given by the linear combinations

$$|K_1\rangle = \sqrt{\frac{1}{2}} (|K^0\rangle + |\bar{K}^0\rangle) \quad \text{and} \quad |K_2\rangle = \sqrt{\frac{1}{2}} (|K^0\rangle - |\bar{K}^0\rangle) \quad (3.1)$$

where $|K_1\rangle$ has CP eigenvalue +1 and $|K_2\rangle$ has CP eigenvalue -1. This is the particle mixture theory of Gell-Mann and Pais /59/.

The CP conserving pionic decay products of these states are $K_1 \rightarrow 2\pi$ and $K_2 \rightarrow 3\pi$. The first of these decays has a high Q value and so K_1 has a short lifetime /33/

$$\tau_1 = (0.8923 \pm 0.0022) \times 10^{-10} \text{ s}$$

The second decay has a low Q value leading to a long lifetime for K_2 /33/

$$\tau_2 = (0.5183 \pm 0.0040) \times 10^{-7} \text{ s}$$

In 1964 Christenson, Cronin, Fitch and Turlay announced /62/ their discovery that the long-lived component of neutral kaons also decayed into two pions with a small probability (branching fraction 0.297 ± 0.023 % /33/). This result was confirmed by the observations of Abashian et al./63/. Following these results the kaon decay eigenstates were modified to include the effects of CP-violation

$$|K_S\rangle = (1 + |\rho|^2)^{-\frac{1}{2}} (|K_1\rangle + \rho |K_2\rangle) \quad (3.2a)$$

and

$$|K_L\rangle = (1 + |\rho|^2)^{-\frac{1}{2}} (|K_2\rangle + \rho |K_1\rangle) \quad (3.2b)$$

where ρ is a small parameter measuring the amount of the "wrong" CP component in the decay eigenstates. In terms of the strong interaction eigenstates these are

$$|K_S\rangle = \frac{1}{\sqrt{2(1 + |\rho|^2)}} \left\{ (1 + \rho) |K^0\rangle + (1 - \rho) |\bar{K}^0\rangle \right\} \quad (3.3a)$$

and

$$|K_L\rangle = \frac{1}{\sqrt{2(1 + |\rho|^2)}} \left\{ (1 + \rho) |K^0\rangle - (1 - \rho) |\bar{K}^0\rangle \right\} \quad (3.3b)$$

The time dependence of the two component kaon state vector

$$\Psi = \begin{pmatrix} K_1 \\ K_2 \end{pmatrix}$$

is given by /60,61/

$$i \frac{d\Psi_i}{dt} = (M_{ij} - \frac{i}{2}\Gamma_{ij})\Psi_j$$

with

$$M_{ij} = \langle K_i | H | K_j \rangle + \sum_n \frac{\langle K_i | H | n \rangle \langle n | H | K_j \rangle}{m_K - E_n} \quad (3.4)$$

and

$$\Gamma_{ij} = 2\pi \sum_n \langle K_i | H | n \rangle \langle n | H | K_j \rangle \delta(E_n - m_K) \quad (3.5)$$

In terms of these matrices the CP-violation parameter ρ is given by

$$\begin{aligned} \rho &= \frac{-i(\text{Im}M_{12} - (i/2)\text{Im}\Gamma_{12})}{(m_1 - m_2) - (i/2)(\gamma_1 - \gamma_2)} \\ &= \frac{-i(\text{Im}M_{12} - (i/2)\text{Im}\Gamma_{12})}{(m_S - m_L) - (i/2)(\gamma_S - \gamma_L)} \end{aligned} \quad (3.6)$$

where

$$m_i = M_{ii} ; \gamma_i = \Gamma_{ii} ; m_1 = m_S ; m_2 = m_L ; \gamma_1 = \gamma_S ; \gamma_2 = \gamma_L$$

are the masses and widths of the decay eigenstates.

The CP conserving $K_1 \rightarrow 2\pi$ amplitude is defined /60/ by

$$\langle 2\pi, I = j | T | K_1 \rangle = \sqrt{2} \exp(i\delta_j) \text{Re}A_j$$

and the CP-violating amplitude by

$$\langle 2\pi, I = j | T | K_2 \rangle = \sqrt{2} \exp(i\delta_j) \text{Im}A_j$$

where δ_j is the two pion final state strong interaction phase shift for a state with isospin $I = j$. Using these amplitudes, two complex observables can be defined:

$$\eta_{+-} = \frac{\langle \pi^+ \pi^- | T | K_L \rangle}{\langle \pi^+ \pi^- | T | K_S \rangle} = \epsilon + \epsilon'$$

$$\eta_{00} = \frac{\langle \pi^0 \pi^0 | T | K_L \rangle}{\langle \pi^0 \pi^0 | T | K_S \rangle} = \epsilon - 2\epsilon'$$
(3.7)

where

$$\epsilon = \rho + i(\text{Im}A_0 / \text{Re}A_0)$$

$$\epsilon' = \frac{i(\text{Im}A_2 / \text{Re}A_0)}{\sqrt{2}} \exp(i(\delta_2 - \delta_0))$$
(3.8)

The parametrization of CP-violation given above is redundant. There are four theoretical parameters ($\text{Im}K_{12}$, $\text{Im}\Gamma_{12}$, $\text{Im}A_0$, $\text{Im}A_2$), but there are, in fact, only three independent real experimental observables since the two complex observables η_{+-} and η_{00} are related by

$$\text{Re}(\eta_{+-} - \eta_{00}) \exp(-i(\delta_2 - \delta_0)) = 0$$

A standard convention /60/ given by Wu and Yang is to set $\text{Im}A_0 = 0$. In certain models the phase convention may be determined naturally so that a non-zero value of $\text{Im}A_0$ arises. However, a phase transformation can always be performed to recover the Wu-Yang convention. In this convention

$$\epsilon = \rho$$
(3.9)

3.2 Experimental Information

The non-conservation of strangeness in weak interactions allows $K^0 \leftrightarrow \bar{K}^0$ transitions, and the mixing of two degenerate states results in a mass splitting. The CP eigenstates $|K_1\rangle$ and $|K_2\rangle$ would have definite masses and lifetimes if CP invariance were a good symmetry. In fact this invariance does not hold but the corresponding corrections to mass and lifetime are negligibly small giving

$$\delta m = m_1 - m_2 = m_S - m_L \quad (3.10)$$

This mass difference is measured experimentally using the phenomena of interference and regeneration. Interference is a characteristic prediction of the particle mixture hypothesis. Assume that at time $t = 0$ a pure K^0 meson beam is produced, for example, in the reaction $\pi^- + p \rightarrow K^0 + \Lambda^0$. No \bar{K}^0 mesons are present at $t = 0$. The particle mixture hypothesis predicts that an initially pure K^0 state will become, after a time t

$$\begin{aligned} |\psi(t)\rangle &= \frac{1}{\sqrt{2}} (|K_1\rangle \exp(-i\lambda_1 t) + |K_2\rangle \exp(-i\lambda_2 t)) \\ &= \frac{1}{2} (|K^0\rangle (\exp(-i\lambda_1 t) + \exp(-i\lambda_2 t)) \\ &\quad + |\bar{K}^0\rangle (\exp(-i\lambda_1 t) - \exp(-i\lambda_2 t))) \end{aligned}$$

where $\lambda_i = m_i - (i/2)\gamma_i$. The probability of finding a \bar{K}^0 at time t is thus given by

$$\begin{aligned} P(\bar{K}^0, t) &= \frac{1}{4} (\exp(-\gamma_1 t) + \exp(-\gamma_2 t) \\ &\quad - 2 \exp(-\frac{1}{2}(\gamma_1 + \gamma_2)t) \cos(m_2 - m_1)t) \end{aligned}$$

The oscillatory time dependence represented by the last term can be detected in either of two ways. The first, advocated by Fry and Sachs

/64/, is by directly measuring the strangeness oscillation of a neutral kaon beam as a function of time through the detection of strong interactions which could only be induced by \bar{K}^0 , for example $\bar{K}^0 + p \rightarrow \Lambda^0 + \pi^+$. The second method, suggested by Zel'dovich /65/ and by Treiman and Sachs /66/, is through the observation of semi-leptonic (K_{13}) decays of neutral kaons. The $\Delta Q = \Delta S$ selection rule forbids the decays $K^0 \rightarrow e^- \bar{\nu} \pi^+$ and $\bar{K}^0 \rightarrow e^+ \nu \pi^-$ and allows only $K^0 \rightarrow e^+ \nu \pi^-$ and $\bar{K}^0 \rightarrow e^- \bar{\nu} \pi^+$. The oscillations of strangeness can, therefore, be detected by observing the number of electrons or positrons produced in K_{e3} decays.

The method of interference yields only the magnitude of the mass difference, leaving the sign undetermined. However, experiments based on the phenomenon of regeneration can be used to find both the magnitude and the sign of the mass splitting. Regeneration is a result of the differences in the nuclear properties of K^0 and \bar{K}^0 mesons. Assume that at $t = 0$ there is a beam consisting of K^0 mesons only. Decays $K_1 \rightarrow 2\pi$ will take place in this beam during a time $t \lesssim \tau_1 = 1/\gamma_1$. These decays will stop after $\tau_1 \ll t \ll \tau_2$ where $\tau_2 = 1/\gamma_2$, since all K_1 mesons will decay and leave a pure beam of K_2 mesons. If the beam is now directed at, say, a copper plate, $K_1 \rightarrow 2\pi$ decays will reappear behind the plate. What happens is the regeneration of K_1 mesons in matter.

Denoting the amplitude of the K^0 (\bar{K}^0) meson scattering on a nucleus by f (\bar{f}), a K_2 meson transforms after scattering into a linear superposition of K_2 and K_1

$$\begin{aligned} |K_2\rangle &= \frac{1}{\sqrt{2}} (|K^0\rangle - |\bar{K}^0\rangle) \xrightarrow{\text{scatt.}} \frac{1}{\sqrt{2}} (f|K^0\rangle - \bar{f}|\bar{K}^0\rangle) \\ &= \frac{1}{2}(f + \bar{f})|K_2\rangle + \frac{1}{2}(f - \bar{f})|K_1\rangle \end{aligned}$$

While \bar{K}^0 mesons are strongly absorbed by nuclei via processes such as $\bar{K}^0 + p \rightarrow \Lambda^0 + \pi^+$ and $\bar{K}^0 + n \rightarrow \Lambda^0 + \pi^0$, K^0 mesons can only undergo elastic and charge exchange scattering (due to baryon number and strangeness conservation) and therefore interact with appreciably smaller cross-sections. Thus $\bar{f} \neq f$ and a component of K_1 mesons has been regenerated in a beam of K_2 mesons.

When the regenerated K_1 mesons travel at a non-zero angle with respect to the incident beam, regeneration on different nuclei in the plate is incoherent. If, however, a K_1 meson travels forward, the amplitudes of regeneration on nuclei along the beam axis add up coherently. Measurement of the ratio of coherent to incoherent regeneration intensity makes it possible to determine δ_m with high accuracy. The interference of K_1 mesons regenerated in two (or more) plates can be used to find the sign of δ_m . Such experiments have established that $\delta_m = m_S - m_L < 0$ /67/.

The most precise value for δ_m obtained so far is /33,68/

$$\delta_m = -(0.5349 \pm 0.0022) \times 10^{10} \text{ h s}^{-1}$$

corresponding to

$$\delta_m = -(3.521 \pm 0.001) \times 10^{-14} \text{ GeV} \quad (3.11)$$

The discovery of CP-violation in 1964 was made when Christenson et al. observed the decay of the long lived component of a neutral kaon beam into two pions. A beam of " K_2 " mesons was allowed to regenerate a K_1 component in a bag of helium. Christenson et al. observed an excess of " $K_2 \rightarrow \pi^+ \pi^-$ " events in the forward direction over the number expected from coherent regeneration ($K_2 \rightarrow K_1 \rightarrow \pi^+ \pi^-$). They, therefore, concluded that they had observed the direct decay of the long lived neutral kaon into $\pi^+ \pi^-$ with a branching ratio

$$\frac{R(K_L \rightarrow \pi^+ \pi^-)}{R(K_L \rightarrow \text{all charged modes})} = (2.0 \pm 0.4) \times 10^{-3}$$

Using this result they estimated that

$$|\epsilon| = 2.3 \times 10^{-3} \quad (3.12)$$

$K_1 \rightarrow K_2$ mixing (CP-violation) results in a charge asymmetry in the semi-leptonic decays of the K_L meson

$$\delta = \frac{\Gamma(K_L \rightarrow e^+ \nu \pi^-) - \Gamma(K_L \rightarrow e^- \bar{\nu} \pi^+)}{\Gamma(K_L \rightarrow e^+ \nu \pi^-) + \Gamma(K_L \rightarrow e^- \bar{\nu} \pi^+)}$$

Using the $\Delta Q = \Delta S$ rule which forbids the decays $K^0 \rightarrow e^- \bar{\nu} \pi^+$ and $\bar{K}^0 \rightarrow e^+ \nu \pi^-$ and taking into account the equality $\Gamma(K^0 \rightarrow e^+ \nu \pi^-) = \Gamma(\bar{K}^0 \rightarrow e^- \bar{\nu} \pi^+)$ the asymmetry is given by

$$\delta = \frac{|1 + \epsilon|^2 - |1 - \epsilon|^2}{|1 + \epsilon|^2 + |1 - \epsilon|^2} = 2\text{Re } \epsilon$$

The world average experimental measurement for this asymmetry is /33,68/

$$\delta = (3.30 \pm 0.12) \times 10^{-3}$$

giving

$$\text{Re } \epsilon = (1.65 \pm 0.06) \times 10^{-3} \quad (3.13)$$

From this result and the estimate of Christenson et al. the phase of ϵ can be determined

$$\text{Arg } \epsilon = 44.2^\circ \pm 2.2^\circ \quad (3.14)$$

In addition to the parameter ϵ which describes the amount of

"wrong" CP component in the kaon decay eigenstates, there is another quantity, ϵ' , characterizing CP-violation. This describes CP-violation in the direct $K_2 \rightarrow 2\pi$ ($I = 2$) channel, and is given by

$$\epsilon' = \frac{i}{\sqrt{2}} (\text{Im}A_2/A_0) \exp(i(\delta_2 - \delta_0))$$

The phase of ϵ' is, therefore

$$\text{Arg}\epsilon' = \frac{1}{2}\pi + \delta_2 - \delta_0 = (37 \pm 6)^\circ \quad (3.15)$$

using the experimentally measured values for the $\pi\pi$ phase shifts /68/.

A suitable combination of the experimental observables η_{+-} and η_{00} yields the ratio of the magnitudes of ϵ and ϵ'

$$\left| \frac{\epsilon'}{\epsilon} \right| = \left| \frac{\eta_{+-} - \eta_{00}}{2\eta_{+-} + \eta_{00}} \right| \leq 0.02 \quad (3.16)$$

This ratio is a significant quantity for weak interaction phenomenology as will be shown in Chapter 5. Experiments are now in progress to determine this ratio more precisely /69,70/.

The experimental parameters δ_m and ϵ of the neutral kaon system are related to a theoretically calculable transition amplitude by simple expressions. In the $K_1 - K_2$ basis the mass matrix M_{ij} can be written /60/

$$\langle K_i | T | K_j \rangle = \begin{pmatrix} m_1 & im' \\ -im' & m_2 \end{pmatrix}$$

where the off-diagonal elements, $\pm im'$, are the CP-violating $K_1 \leftrightarrow K_2$ amplitudes. The $K^0 \rightarrow \bar{K}^0$ transition amplitude is then given by

$$\begin{aligned}\langle \bar{K}^0 | T | K^0 \rangle &= \frac{1}{2} \langle K_1 - K_2 | T | K_1 + K_2 \rangle \\ &= \frac{1}{2}(m_1 - m_2) + im'\end{aligned}$$

Similarly, the $\bar{K}^0 \rightarrow K^0$ amplitude is

$$\langle K^0 | T | \bar{K}^0 \rangle = \frac{1}{2}(m_1 - m_2) - im'$$

Thus

$$\begin{aligned}2\text{Re} \langle \bar{K}^0 | T | K^0 \rangle &= 2\text{Re} \langle K^0 | T | \bar{K}^0 \rangle \\ &= m_1 - m_2 = m_S - m_L = \delta m\end{aligned}\quad (3.17)$$

and

$$\begin{aligned}\text{Im} \langle \bar{K}^0 | T | K^0 \rangle &= -\text{Im} \langle K^0 | T | \bar{K}^0 \rangle \\ &= m' = \text{Im} A_{12}\end{aligned}$$

Taking the real part of equation (3.6) gives, in the Wu-Yang convention ($\epsilon = \rho$):

$$\begin{aligned}\text{Im} A_{12} &= \text{Re} \epsilon \left(\frac{\delta \pi}{2\delta m} + \frac{2\delta m}{\delta \pi} \right) \delta m + \text{Im} \Gamma'_{12} \left(\frac{\delta m}{\delta \pi} \right) \\ &= -2 \delta m \text{Re} \epsilon - \frac{1}{2} \text{Im} \Gamma'_{12}\end{aligned}$$

using the experimental result $\delta m \approx -\frac{1}{2} \delta \pi$. Now, the kaon semileptonic decays K_{e3} give /68/

$$\left| \frac{\text{Im} \Gamma'_{12}}{\text{Im} A_{12}} \right| < 0.02$$

Therefore

$$\text{Re} \epsilon = -\text{Im} A_{12} / 2\delta m = -m' / 2\delta m \quad (3.18)$$

The relations expressed in equations (3.17) and (3.18) will be used extensively in the following chapters.

3.3 $K^0 - \bar{K}^0$ Amplitude: Dispersive Contributions

Before the GWS theory of weak interactions was accepted there were many attempts to calculate the $K_L - K_S$ mass difference. As the standard current x current weak Hamiltonian contained only $\Delta S = 1$ interactions, the direct $K^0 - \bar{K}^0$ transition was set to zero.

Contributions to the mass difference occurred through decays to non-strange intermediate states, represented by the summation term in M_{ij} (equation(3.4)). Possible dispersive contributions are

$$\begin{aligned} K^0 &\leftrightarrow \pi e \nu \leftrightarrow \bar{K}^0 \\ K^0 &\leftrightarrow \rho, \omega, A_1 \leftrightarrow \bar{K}^0 \\ K^0 &\leftrightarrow n\pi \ (n > 1) \leftrightarrow \bar{K}^0 \\ K^0 &\leftrightarrow \pi^0, \eta, \eta' \leftrightarrow \bar{K}^0 \end{aligned}$$

If the $\Delta S = \Delta Q$ rule were exact the semileptonic intermediate states would not contribute to δm at all since one of the vertices would necessarily have to involve $\Delta S = -\Delta Q$. Even if the $\Delta S = \Delta Q$ rule is not exact, experiments indicate /68/ that $\Delta S = -\Delta Q$ transitions have much smaller amplitudes than $\Delta S = \Delta Q$ transitions. Therefore, the contributions of semileptonic modes to δm can be neglected.

Vector meson (ρ, ω, A_1) contributions are assumed to be small. For example, Oneda finds /71/ that the contribution of the ρ meson is only around 2% of the observed value due to angular momentum effects. Similarly one expects all vector meson contributions to be suppressed.

The first attempts to calculate the $K_L - K_S$ mass difference were made by considering the two pion intermediate state /72 - 76/. The sign of this contribution can easily be understood. Neglecting the effects of CP-violation /77/

$$\delta_m = \sum_n \left(\frac{|\langle K_1 | H | n \rangle|^2}{m_K - E_n} - \frac{|\langle K_2 | H | n \rangle|^2}{m_Y - E_n} \right) \quad (3.19)$$

therefore, the two pion contribution is given by

$$\delta_m|_{2\pi} = \frac{|\langle K_1 | H | 2\pi \rangle|^2}{m_K - E_{2\pi}}$$

since $K_2 \rightarrow 2\pi$ is forbidden. This contribution can have either sign, being positive when $E_{2\pi} < m_K$ and negative when $E_{2\pi} > m_K$. The sign is determined, in principle, by the relative strengths of the parts above and below the pole. The authors of references 72 to 76 consider the two pion, $I = 0$, intermediate state and neglect the $I = 2$ contribution because of the $\Delta I = \frac{1}{2}$ enhancement in weak interactions. A summary of their results is

$$- 3.0 < \frac{\delta_m|_{2\pi}}{\delta_m^{\text{expt.}}} < +3.2 \quad (3.20)$$

A recent evaluation of the two pion contribution /77/ using a subtracted dispersion relation for the self energy obtains the result $\delta_m|_{2\pi} = (0.64 \text{ to } 1.4) \times \delta_m^{\text{expt.}}$. Donoghue et al. /77/ also obtain the result $\delta_m|_{2\pi} = (1.4 \text{ to } 2.8) \times \delta_m^{\text{expt.}}$ based on a chiral perturbation theory calculation. Both these results are sensitive to the UV cut off employed, but both indicate that the part above the pole is stronger leading to an overall negative $\pi\pi$ contribution to δ_m . That is, the two pion contribution has the same sign as the experimental result.

An estimate of the one particle pseudoscalar (π^0, η, η') intermediate states was first obtained by Itzykson et al. /78/. In order to eliminate the unknown matrix element $\langle K^0 | H | \pi^0 \rangle$ they

computed the quantity

$$\frac{\delta m_{|\pi^0, \eta}}{\Gamma(K_1)} = \frac{16}{3} \cdot 4\pi f_\pi^2 \frac{m_\pi}{\sqrt{(m_K^2 - 4m_\pi^2)}} \cdot \frac{4m_K^2 - 3m_\eta^2 - m_\pi^2}{(m_K^2 - m_\pi^2)^2}$$

So, the π^0, η contribution to δm is given by deviations from the Gell-Mann-Okubo mass formula

$$4m_K^2 - 3m_\eta^2 - m_\pi^2 = 0$$

Inserting the experimental values for the masses gives

$$\frac{\delta m_{|\pi^0, \eta}}{\Gamma(K_1)} = 0.7$$

or

$$\delta m_{|\pi^0, \eta} = -1.4 \delta m_{\text{expt.}} \quad (3.21)$$

which has the wrong sign. However, this result depends on the exact (flavour) SU(3) expression

$$\sqrt{3} \langle K^0 | H | \eta^0 \rangle = \langle K^0 | H | \pi^0 \rangle$$

If, to allow for some SU(3) breaking, this is modified to

$$\sqrt{3} \langle K^0 | H | \eta^0 \rangle = (1 - \epsilon) \langle K^0 | H | \pi^0 \rangle$$

then, with $\epsilon \sim 0.25$, the correct mass difference is obtained.

Greenberg /79/ and Donoghue et al. /77/ have pointed out that in the exact SU(3) limit the octet state η_8 should be used in place of the physical state η . The Gell-Mann-Okubo mass relation is then satisfied, giving

$$\delta m_{|\pi^0, \eta_8} = 0$$

The SU(3) octet (η_8) and singlet (η_0) states mix to produce the physical η and η' states. Taking this mixing into account, which is equivalent to including the η' as an intermediate state, gives /77/

$$\frac{\delta_m}{\Gamma_S} | \pi^0, \eta, \eta' \rangle = (0.20 + 0.78 \rho^2)$$

where ρ is defined by

$$\langle K_L | H | \eta_0 \rangle = -(\rho\sqrt{2}/\sqrt{3}) \langle K_L | H | \pi^0 \rangle$$

$\rho = 1$ is suggested by the quark model and the $\Delta I = \frac{1}{2}$ enhancement of weak interactions, leading to

$$\delta_m | \pi^0, \eta, \eta' \rangle \approx -2 \delta_m^{\text{expt.}} \quad (3.22)$$

From these estimates it appears that the one particle pseudoscalar intermediate states give a contribution to δ_m of roughly the correct magnitude but of the wrong sign when compared to the experimental result.

The contribution from the two pion intermediate state has the correct sign. This, together with the undetermined three pion contribution, could be enough to overcome the π^0, η, η' contribution and reproduce the experimental result. The semileptonic and vector meson intermediate states are neglected due to their suppression by the $\Delta S = \Delta Q$ rule and angular momentum effects respectively. A summary statement is that the sign of the total dispersive contribution to the $K_L - K_S$ mass difference is undetermined, and its magnitude is consistent with either the experimental result or zero.

In the standard current x current theory of weak interactions

with less than three generations of quarks there is no CP-violation. Therefore, in the years before the Kobayashi-Maskawa (KM) model /39/, CP-violation was thought to occur as a result of a new "superweak" interaction /60/, whose coupling constant was $G_{\text{superweak}} \sim 10^{-6} G_F$. Now that there are three or more generations of quarks, CP-violation finds a natural place in standard weak interactions through a phase in the KM quark mixing matrix. For this reason "superweak" theories are not discussed here.

3.4 $K^0 - \bar{K}^0$ Amplitude: The Box Diagram

In the GWS theory of weak interactions there is an effective local /80/ $\Delta S = 2$ Hamiltonian in the form of the box diagram /36/ (Figure 3.1). The free quark transition amplitude ($\bar{s} d \leftrightarrow \bar{d} s$) is computed using the Feynman rules /12/ producing a function multiplied by a quark operator. This transition amplitude is then taken to be an effective Hamiltonian for the $K^0 - \bar{K}^0$ transition. The free quark amplitude is given by

$$H_{\text{eff.}} = \frac{G_F^2 M_W^2}{16 \pi^2} \sum_{i,j = u,c,t} \lambda_i \lambda_j B_{ij} (\bar{s}_L \gamma_\mu d_L) (\bar{s}_L \gamma^\mu d_L) \quad (3.23)$$

where the λ_i are products of KM matrix elements $\lambda_i = V_{is}^* V_{id}$. The B_{ij} are known functions /81,82/ of the quark masses

$$B_{ii} = \frac{x_i}{4} \left(1 + \frac{1}{(1-x_i)} - \frac{6}{(1-x_i)^2} \right) - \frac{3}{2} \left(\frac{x_i}{1-x_i} \right)^3 \ln(x_i)$$

$$B_{ij} = \frac{x_i x_j}{4} \left\{ \frac{1}{(x_j - x_i)} \left(1 + \frac{6}{(1-x_j)} - \frac{3}{(1-x_j)^2} \right) \ln(x_j) \right. \\ \left. + (x_j \leftrightarrow x_i) - \frac{3}{(1-x_i)(1-x_j)} \right\}$$

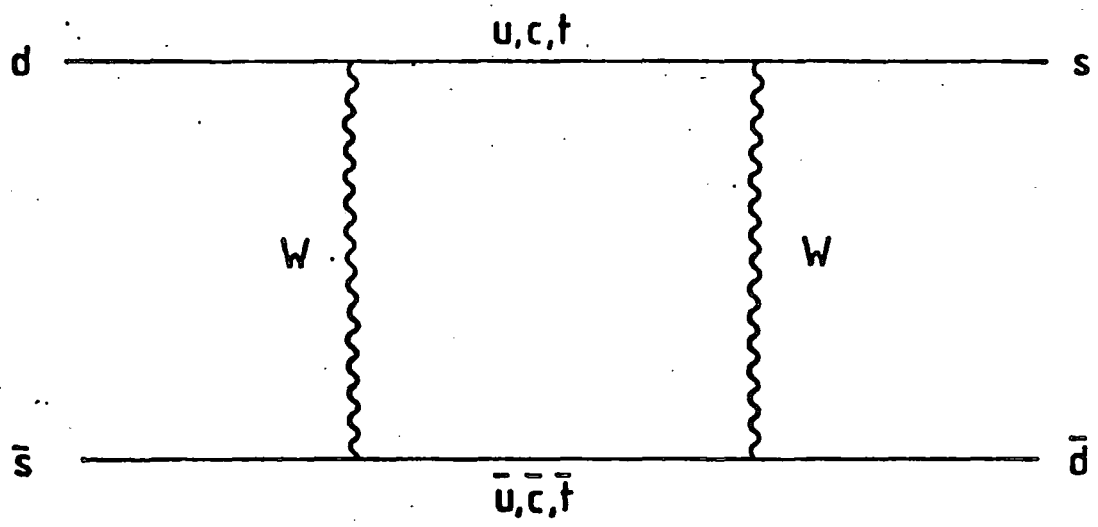


Figure 3.1

The box diagram amplitude for the $K^0 - \bar{K}^0$ transition.

with $x_i = m_i^2 / M_W^2$.

Perturbative QCD corrections to this free quark transition amplitude have been evaluated in the leading logarithmic approximation by Gilman and Wise /83,84/. The effect of these corrections is to multiply each of the functions E_{ij} by a number η_{ij} . The values of these numbers depend on the QCD scale Λ in an effective four quark theory, which is the quantity extracted from QCD analysis of deep inelastic scattering data. The results of this calculation are shown in table 3.1 below. η_{ij} is symmetric and $\eta_{uj} = 1$ for all $j = u, c, t$.

$\Lambda^2 (\text{GeV}^2)$	η_{cc}	η_{tt}	η_{ct}
0.01	0.69	0.59	0.41
0.1	0.99	0.60	0.40

Table 3.1 QCD correction factors for the $\bar{s} d \leftrightarrow \bar{d} s$ transition.

The $K^0 - \bar{K}^0$ transition amplitude is given by

$$\begin{aligned}
 M_B &= \langle \bar{K}^0 | H_{\text{eff.}} | K^0 \rangle \\
 &= \frac{G_F^2 M_W^2}{16\pi^2} \left(\sum_{i,j = u,c,t} \lambda_i \lambda_j B_{ij} \eta_{ij} \right) Q_B
 \end{aligned} \tag{3.24}$$

where Q_B is the hadronic matrix element

$$Q_B = \langle \bar{K}^0 | \bar{s} \gamma^\mu (1 - \gamma_5) d \bar{s} \gamma_\mu (1 - \gamma_5) d | K^0 \rangle$$

The calculation of this matrix element requires non-perturbative techniques not yet available. Instead, Q_B must be estimated in a model. The first estimate was made by Gaillard and Lee in the vacuum saturation (factorization) approximation. In this approach

a complete set of states is inserted between the two currents and the vacuum state is assumed to saturate the matrix element

$$Q_B = \frac{8}{3} \langle \bar{K}^0 | \bar{s} \gamma^\mu (1 - \gamma_5) d | 0 \rangle \langle 0 | \bar{s} \gamma_\mu (1 - \gamma_5) d | K^0 \rangle$$

The factor $8/3$ results from the four possible Wick contractions and the two types of contraction of quark colour indices. Using PCAC this gives

$$Q_B = - \frac{8}{3} \left(\frac{f_K^2 m_K^2}{2m_K} \right)$$

where $f_K = 1.23 m_\pi$ is the kaon decay constant obtained /85/ from the $K^+ \rightarrow \mu^+ \nu$ decay width with the KM matrix element $|V_{us}| = 0.219$. The factor of $(2m_K)^{-1}$ arises from the normalization of the kaon states.

There is, however, no theoretical justification for this method. Shrock and Treiman /85/ have estimated the one pion contribution to this matrix element and find that it is roughly comparable to the vacuum state contribution but opposite in sign. Although Vysotskii's /86/ estimate is somewhat smaller, this raises serious doubts about the reliability of the vacuum saturation method. As a consequence the matrix element has been estimated in a variety of other ways. The result is usually expressed as

$$Q_B = - \frac{4}{3} f_K^2 m_K B \tag{3.25}$$

which is normalised to the vacuum saturation estimate of $B = +1$.

There are three other types of determination of the hadronic matrix element: the quark model approach /87/ which includes the MIT bag /85/, the use of SU(3) and PCAC /88 - 91/ and a general method which views the matrix element as a scalar form factor and which leads only to an upper bound /92/.

Both the QCD correction coefficients γ_{ij} and the hadronic matrix element Q_B depend on the renormalization point μ and this dependence should cancel in the product. Only the coefficients γ_{ij} can be evaluated as a function of μ , while the μ -dependence of the matrix element is unknown since it is calculated in a quark model. However, the μ -dependence of the coefficients γ_{ij} is mild and the final result is approximately μ -independent.

Shrock and Treiman /85/ used the MIT bag model of hadrons /93/ to estimate Q_B . This model incorporates quark and gluon confinement as an assumed property and has achieved a number of successes in describing the static properties of low lying hadrons, such as masses, magnetic moments, charge radii and axial vector coupling constants. The model depends on a set of arbitrary parameters which are determined by a fit to various hadron properties. These determinations have resulted in three different sets of values for the parameters (labelled A, B and C). Set A yields a prediction for the kaon mass which is in very good agreement with experiment, and it is this set that Shrock and Treiman use in their determination of the matrix element. They find $B = 0.42$ and infer, from the known accuracy of bag model calculations of $K \rightarrow 2\pi$ decays, that this result is accurate to within a factor of two.

Colić et al. /87/ have repeated the bag model calculation. In determinations using each of the sets of bag model parameters they found $B = -0.42, 0.055$ and 0.34 . Trampetić /94/ has noted that the first calculation is the same as that of Shrock and Treiman with the exception of the sign of the result.

In addition to the bag model Colić et al. /87/ studied three models based on harmonic oscillator potentials. The first model,

called simply the Harmonic Oscillator (HO) model, is non-relativistic and treats the interquark potential as a harmonic oscillator potential. This model gives $B = 2.86$. In the Relativized Harmonic Oscillator (RHO) model, relativistic corrections are estimated by replacing the Pauli spinors by Dirac ones. The term "relativized" is used instead of "relativistic" because full relativistic invariance is not achieved. The RHO model gives $B = 1.44$. In the Harmonic Oscillator Shell (HOS) model the quarks move relative to a harmonic oscillator potential which is fixed at the centre of the coordinate system. This model gives $B = 0.46$. Of these three models the RHO model is most stable with respect to changes of input parameters. The HO model always gives the same sign for B but the result is strongly dependent on the input parameters. For some values of input parameters the result of the HOS model changes sign in a way which is similar to the behaviour of the MIT bag model.

Another method uses $SU(3)$ and PCAC to relate the $\Delta S = 2$ matrix element under study to experimental information on the $\Delta I = 3/2$ $K^{\pm} \rightarrow \pi^{\pm} \pi^0$ decay. The current algebra approach /88/ yields $|B| = 0.33$ with an estimated 50 % uncertainty /77,89/. The sign of the $K \rightarrow 2\pi$ amplitude cannot be deduced from experiment and hence the sign of B is not determined. However, a model dependent determination of the $K \rightarrow 2\pi$ amplitude predicts a positive sign for B . Both Colic' et al. /95/ and Dupont and Pham /90/ have noticed that it is difficult to reproduce the observed $K^{\pm} \rightarrow \pi^{\pm} \pi^0$ amplitude unless the $\Delta I = 3/2$ operator is suppressed by more than the short distance coefficient $C_4 = 0.4$. This extra suppression would increase the value of B found by Donoghue et al.

This result has been rederived within the framework of chiral

perturbation theory rather than current algebra. In the limit $f_{\pi} = f_K$ Ginsparg and Wise /91/ obtain $B = 0.33$. Dupont and Pham /90/ calculate the $K \rightarrow 2\pi$ amplitudes in chiral perturbation theory with $f_{\pi} = f_K$ and find the same result as would be obtained using the factorization approximation in this limit. Using the SU(3) relation to obtain the matrix element of the $\Delta S = 2$ operator then gives

$$Q_B = -\frac{4}{3} f_{\pi}^2 m_K$$

Taking this literally yields $B = 0.66$. However, the implication is that the factorization (vacuum saturation) method is supported by this analysis and consequently f_{π} should be replaced by f_K to give $B = 1$ /90/.

The vacuum saturation approximation is also supported by a preliminary evaluation of the matrix element Q_B within the framework of lattice QCD. Cabibbo, Martinelli and Petronzio /96/ find $B \sim 1.3$ by this method.

The final approach is that of Guberina et al. /92/ who claim that there is, at present, no reliable calculation of Q_B . They adopt a general method which treats the $\Delta S = 2$ matrix element as the value of a scalar form factor $F(t)$ at $t = 0$. After some extensive manipulation a bound of $|B| \lesssim 2.0 \pm 0.5$ is proposed.

What emerges from all of these calculations is that there is no obvious value for B as estimates range from 0.055 to 2.86 and the sign is undetermined. Therefore, the calculation of the $K^0 - \bar{K}^0$ transition amplitude has a large uncertainty due to this factor.

3.5 $K^0 - \bar{K}^0$ Amplitude: Double Penguin Diagram

In the box diagram amplitude QCD effects were included in the parameters γ_{ij} . However, with the introduction of strong interactions, new effects arise /97/ due to the exchange of gluons. In particular there is a contribution to the $K^0 \rightarrow 2\pi(I=0)$ amplitude from these "penguin" diagrams (Figure 3.2). As a result of the unusual $(V-A) \times (V+A)$ structure of the quark operators arising from these diagrams their matrix elements are thought to be large enough to overcome the small short distance coefficient $C_5 = 0.12$ and give an important (possibly dominant) contribution to the $K^0 \rightarrow 2\pi(I=0)$ amplitude. Since these diagrams are purely $\Delta I = \frac{1}{2}$, a dominant contribution from them is a possible explanation for the $\Delta I = \frac{1}{2}$ enhancement in weak interactions. However, Guberina and Peccei /98/ have shown that this expectation is rather unrealistic.

Hochberg and Sachs /99/ have pointed out that the inclusion of strong interactions leads to a new contribution to the $K^0 - \bar{K}^0$ transition amplitude which they call a "double penguin diagram" (Figure 3.3). In the same way as the box diagram calculation the free quark transition amplitude is used as an effective Hamiltonian for the kaon transition. The $K^0 - \bar{K}^0$ amplitude due to this penguin Hamiltonian is estimated /99/ to be

$$M_P = \frac{G_F^2 m_t^2}{18(4\pi)^4} \left(\lambda_u \ln \left(\frac{m_c^2}{\mu^2} \right) - \lambda_t \ln \left(\frac{m_t^2}{m_c^2} \right) \right)^2 Q_P \quad (3.26)$$

where μ is an infra-red cut off in the quark - W boson loop which is taken to be $\mu \sim 1$ GeV (a typical hadronic scale at which the effects of confinement might become important). Due to renormalization effects the strong interaction coupling constant is evaluated at the

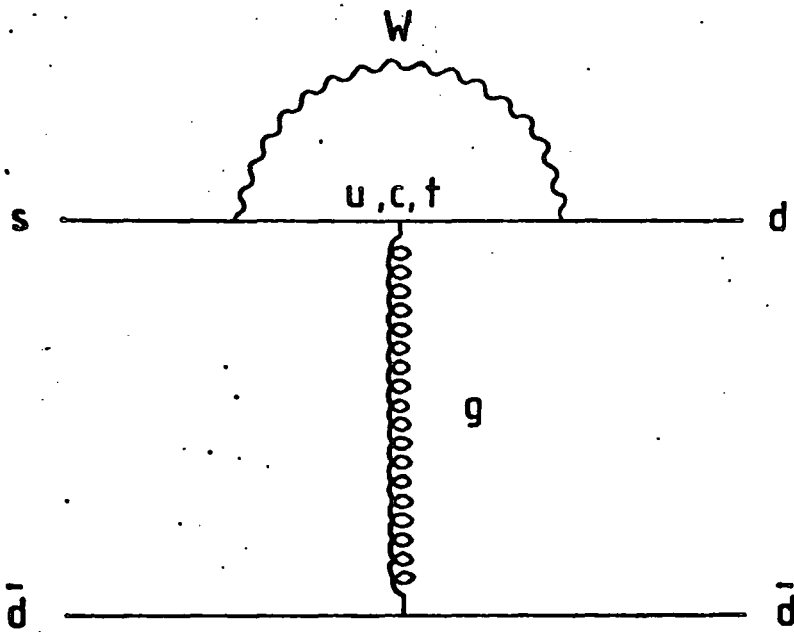


Figure 3.2

The penguin contribution to $K^0 \rightarrow 2\pi$ decays.

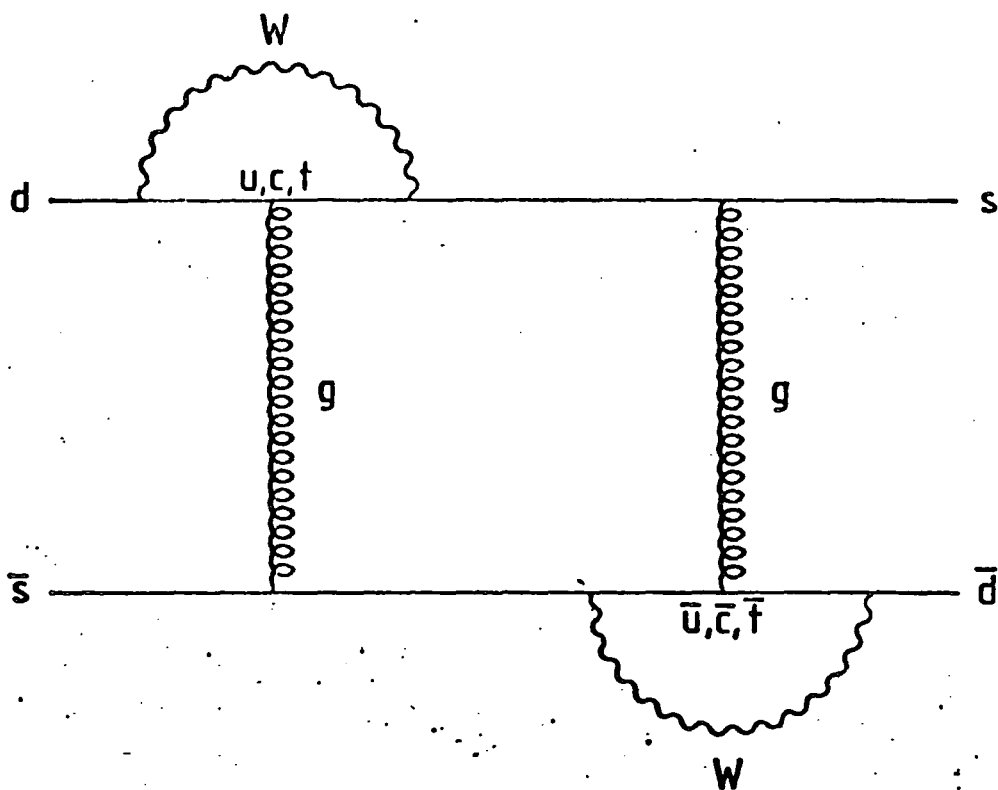


Figure 3.3

The double penguin amplitude for the $K^0 - \bar{K}^0$ transition.

scale μ where $\alpha_s(\mu) = 1/96/$. Q_P is the matrix element of a quark operator

$$Q_P = \langle \bar{K}^0 | \bar{s} \gamma^\mu (1 - \gamma_5) T^a T^b d \bar{s} \gamma_\mu (1 - \gamma_5) T_b T_a d | K^0 \rangle$$

Since the matrix element is taken between colour singlet states, only the colour blind part of the operator, having the same structure as the box diagram operator, will contribute and it can be expressed in terms of the box diagram matrix element /99/

$$Q_P = \frac{73}{9} Q_B \approx -10.8 f_K^2 m_K B \quad (3.27)$$

The double penguin diagram, therefore, has the same uncertainty associated with the non perturbative matrix element as the box diagram. It also contains another uncertainty in the IR cut off μ which controls the cancellation of the two logarithms in the coefficient function. There is no a priori reason why this contribution should be small, particularly since it depends quadratically on the t-quark mass.

The three contributions to the $K^0 - \bar{K}^0$ transition amplitude described above - the dispersive terms, box diagram and double penguin amplitudes - have been used extensively in weak interaction phenomenology. These applications are described in the next chapter.

CHAPTER 4

PHENOMENOLOGICAL APPLICATIONS OF THE $K^0 - \bar{K}^0$ TRANSITION

4.1 Phenomenology: 1966 - 1983

The first application of the $K^0 - \bar{K}^0$ transition amplitude to phenomenology was made by T.N. Truong /73/ in 1966. Assuming that the dominant contribution to the $K_L - K_S$ mass difference came from the 2π ($I = 0$) intermediate state, he derived a relation between the mass difference and the pion phase shift

$$2 \tau_S \delta_m = - \cot \delta_0 (m_K^2) \quad (4.1)$$

The experimental result $2 \tau_S \delta_m \approx -1$ then gives $\delta_0 (m_K^2) \approx 45^\circ$ which is in very good agreement with the experimental measurement /68/ $\delta_0 = 46 \pm 5^\circ$ for this phase. This information was then used to infer the existence of an s-wave di-pion resonance above the mass of the kaon. Unfortunately, corrections to this formula, derived by Rockmore and Yao and by Kang and Land /74,75/, remove the agreement with experiment.

In 1974 Gaillard and Lee /36/ estimated the mass of the c-quark from the $K_L - K_S$ mass difference by considering the $\Delta S = 2$ box diagram amplitude. They calculated the hadronic matrix element using the vacuum saturation approximation ($B = +1$) and determined that the mass of the c-quark was $m_c \approx 1.5$ GeV. This prediction was remarkably confirmed in 1974 with the discovery /100,101/ of the J/ψ resonance at 3.1 GeV and its subsequent interpretation as a

$\bar{c}c$ meson.

Following the success of Gaillard and Lee, phenomenological applications of the $K^0 - \bar{K}^0$ transition amplitude were made using only the direct $\Delta S = 2$ part of the Hamiltonian in the form of the box diagram. The dispersive $(\Delta S = 1)^2$ terms were assumed to cancel out to a large degree. Since in the box diagram the loop integration was taken down to $k = 0$ the remaining small $\pi^0, \eta, 2\pi$, etcetera contributions were thought to be included by a quark - hadron duality /102/. That is, the $u\bar{u}$ intermediate state of the box diagram could be thought of at low energies as a π^0 or η , or with the insertion of a $d\bar{d}$ quark loop as a $\pi^+\pi^-$ state. There were no penguin contributions as they had not yet been thought of.

Using this method information on the Kobayashi-Maskawa (KM) mixing angles was extracted from the $K^0 - \bar{K}^0$ amplitude by many authors /86, 103 - 106/. The box diagram amplitude M_B contains five unknown parameters ($\theta_2, \theta_3, \delta, m_t$ and B) which can be related to two measurable quantities (δ_m and ϵ) via equations (3.17) and (3.18)

$$\delta_m = 2 \operatorname{Re} M_B \quad (4.2)$$

$$\operatorname{Re} \epsilon = - \operatorname{Im} M_B / 2 \delta_m \quad (4.3)$$

These two equations can be solved to find information about two of the unknowns in terms of the remaining three. A standard way of presenting these results is to determine $\sin\theta_2$ and $\sin\delta$ as functions of $\sin\theta_3, m_t$ and B . The results of this analysis are shown in Figures 4.1 and 4.2 for $m_t = 35$ GeV. The solutions are labelled by quadrant in which δ appears using the convention for the KM matrix given in Chapter 2. As m_t is increased solutions 1 and 2 move down while solution 4 moves to the left. A simple consequence of these

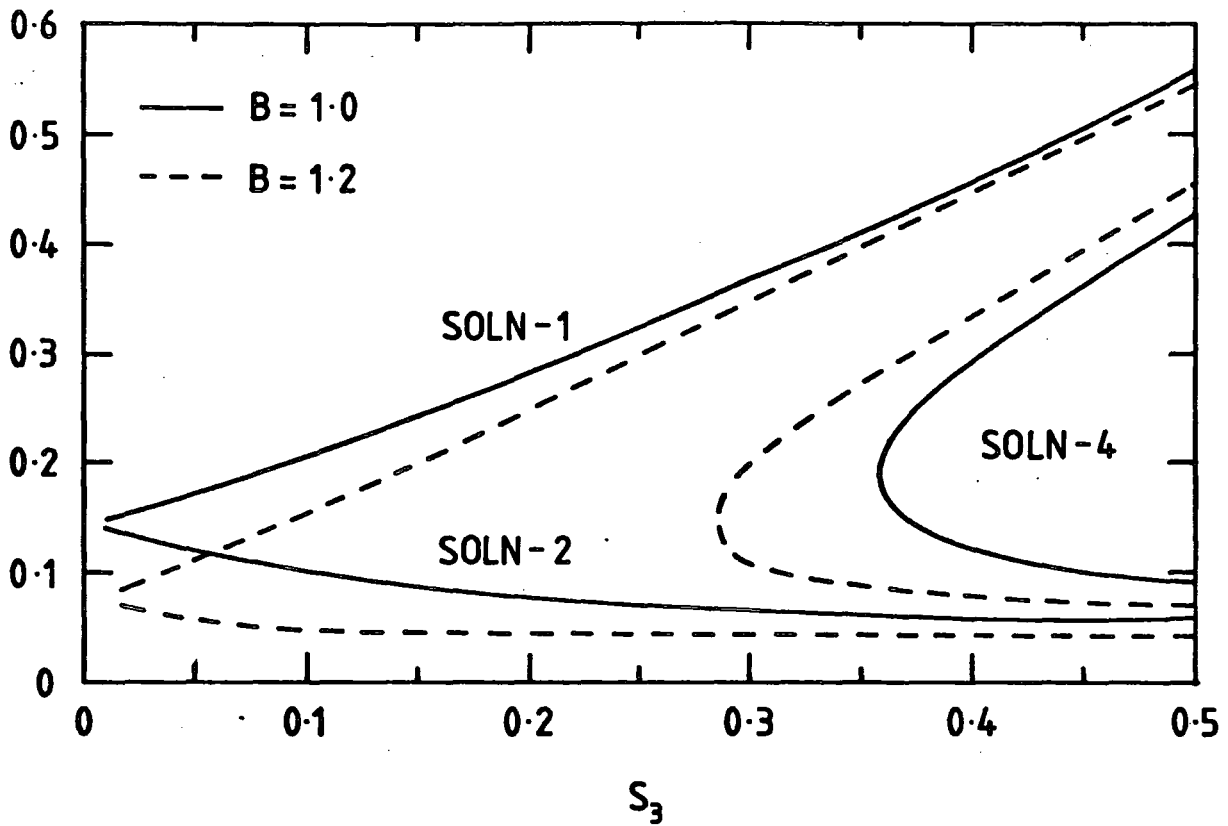


Figure 4.1

The four possible solutions for s_2 as a function of s_3 for $B = 1.0$ and $B = 1.2$.

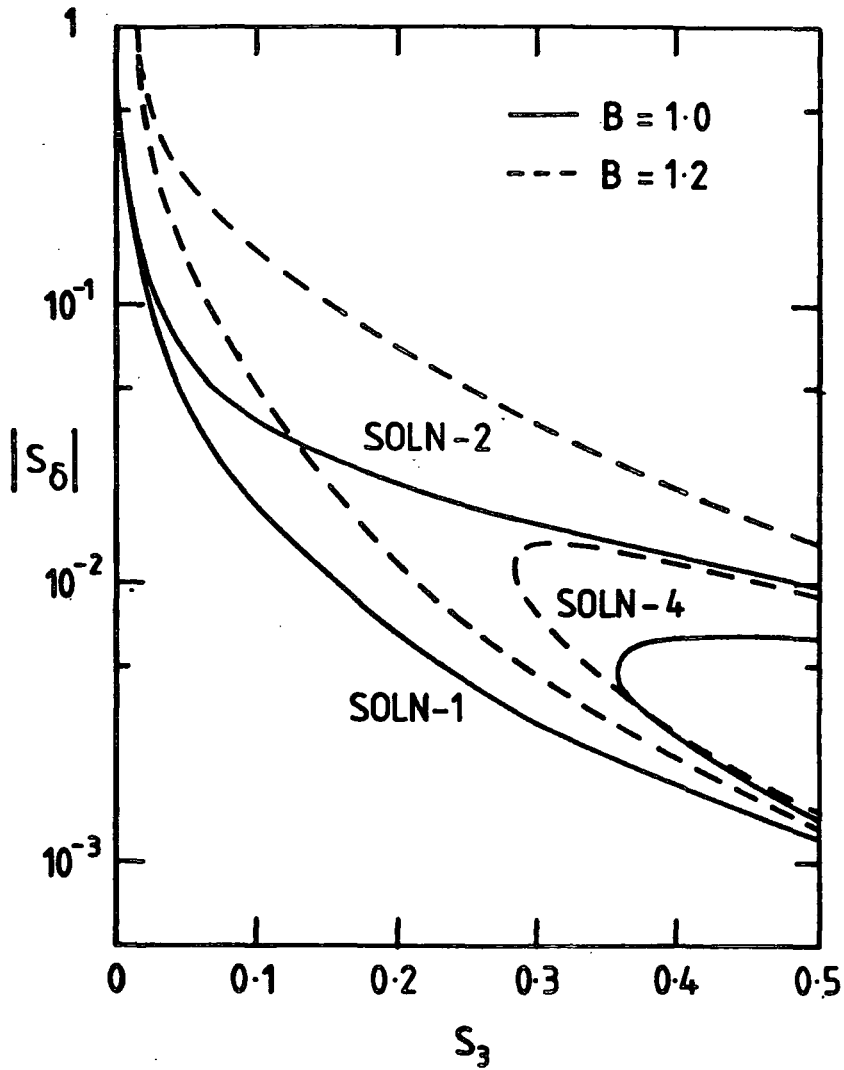


Figure 4.2

The four possible solutions for $|s_\delta|$ as a function of s_3 for $B = 1.0$ and $B = 1.2$.

solutions is that the b-quark is expected /103,104/ to decay in a cascade fashion, $b \rightarrow c \rightarrow s, d$ at least as often as the decay $b \rightarrow u$. This result has been strikingly confirmed by recent measurements on B-meson decay which give /107/

$$\frac{\Gamma(b \rightarrow u)}{\Gamma(b \rightarrow c)} < 0.055 \quad (90 \% \text{ c.l.}) \quad (4.4)$$

Buras /82/ derived an upper bound on the t-quark mass using the box diagram calculation of δ_m together with a calculation of the short distance dispersive $K_L \rightarrow \mu^+ \mu^-$ amplitude. One loop diagrams contributing to this process in the unitary gauge are shown in Figure 4.3 . By normalizing to the decay $K^+ \rightarrow \mu^+ \nu_\mu$ the hadronic matrix element is eliminated by

$$\langle 0 | \bar{s} \gamma_\mu \gamma_5 d + \bar{d} \gamma_\mu \gamma_5 s | K_L \rangle = \sqrt{2} \langle 0 | \bar{s} \gamma_\mu \gamma_5 u | K^+ \rangle$$

giving the ratio of branching fractions for each process to be (neglecting the mass of the muon) /108/

$$\frac{B(K_L \rightarrow \mu^+ \mu^-)_{sd}}{B(K^+ \rightarrow \mu^+ \nu_\mu)} = \frac{G_F^2}{2\pi^4} \frac{1}{|V_{us}|^2} \frac{\tau(K_L)}{\tau(K^+)} \left(\sum_{i=u,c,t} (\text{Re } \lambda_i) G(x_i) \eta_i \right)$$

where /81,82,109/

$$G(x_i) = \frac{3}{4} \left(\frac{x_i}{x_i - 1} \right)^2 \ln(x_i) + \frac{x_i}{4} + \frac{3}{4} \frac{x_i}{1 - x_i}$$

with $x_i = m_i^2/M_W^2$ and η_i is a QCD correction.

The branching ratio $B(K^+ \rightarrow \mu^+ \nu)$ is known ($63.50 \pm 0.16 \%$ /33/) and an upper bound on $B(K_L \rightarrow \mu^+ \mu^-)$ can be found if the assumption is made that the dispersive $K_L \rightarrow \gamma\gamma \rightarrow \mu^+ \mu^-$ contribution is negligible.

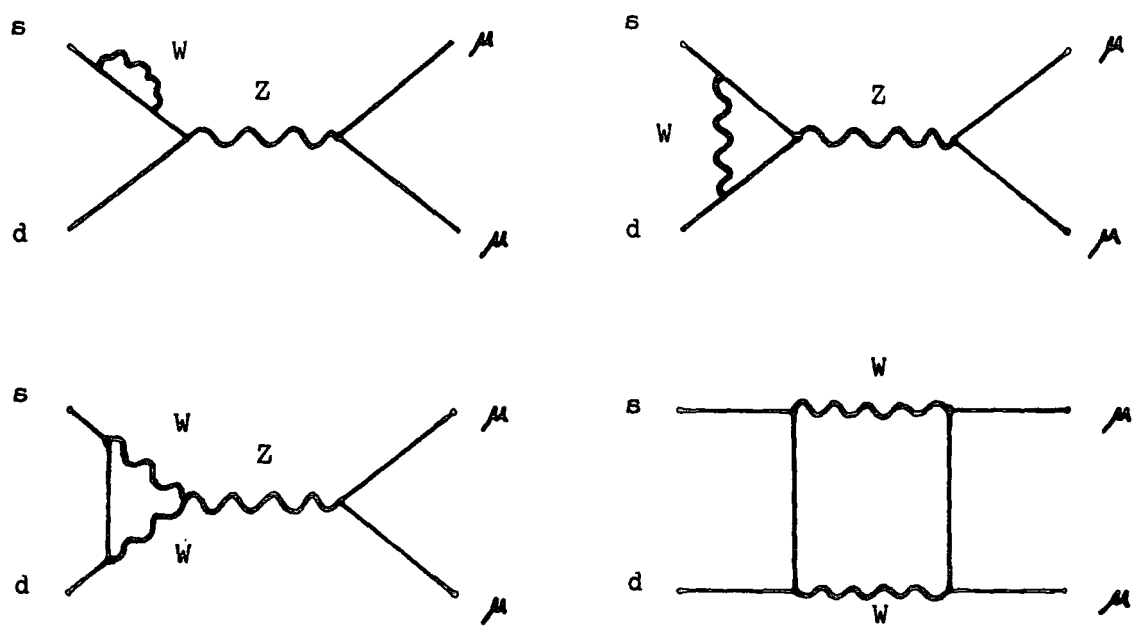


Figure 4.3

One loop contributions to $K_L \rightarrow \mu^+ \mu^-$ in unitary gauge.

This upper bound is /82/

$$B(K_L \rightarrow \mu^+ \mu^-)_{sd} \leq 5.6 \times 10^{-9}$$

which then leads to the inequality

$$\frac{|\operatorname{Re} \lambda_t| G(x_t) \eta}{|V_{us}|} \leq k \quad (4.5)$$

where $k = 0.85 \times 10^{-2}$ /82/ and $\eta = \eta_t$. The contributions of the u- and c-quarks have been neglected because they are orders of magnitude smaller than the right hand side of the inequality.

The box diagram amplitude is used to derive δ_m giving /82/

$$\operatorname{Re} \sum_{i,j = u,c,t} \lambda_i \lambda_j B_{ij} \eta_{ij} B = 4.44 \times 10^{-5}$$

This expression together with the inequality from consideration of the $K_L \rightarrow \mu^+ \mu^-$ decay yields an upper bound on the t-quark mass as a function of the parameter B. Since these equations contain three unknown parameters θ_2 , θ_3 and δ it might appear that by making a suitable choice for their values an arbitrarily large t-quark mass would be allowed. However, this is not the case. Consider the (hypothetical) situation where the box diagram is dominated by the $t\bar{t}$ intermediate state then the above equations give

$$\frac{G^2(x_t)}{B_{tt}} \leq \frac{B \eta_{tt}}{\eta^2} |V_{us}|^2 \times 1.63$$

Since the function $G^2(x_t)/B_{tt}$ increases monotonically with increasing x_t (in the small x_t limit $G(x_t) \sim x_t$ and $B_{tt} \sim x_t$) an upper bound on m_t can be obtained. The upper bound obtained by Buras /82/ is

$m_t \ll 33$ GeV at $B = 0.42$ (the original bag model estimate for the $K^0 - \bar{K}^0$ hadronic matrix element). For $B \sim 1$, m_t is much larger than M_W .

Barger et al. /110/ have questioned the assumption that the dispersive two photon contribution to $K_L \rightarrow \mu^+ \mu^-$ is negligible. They argue that the ratio of dispersive to absorptive two photon contributions is the same for $K_L \rightarrow \mu^+ \mu^-$ as for $\eta \rightarrow \mu^+ \mu^-$. The magnitude of the absorptive contribution is known in each case from unitarity arguments. Since the purely weak contribution $\eta \rightarrow Z \rightarrow \mu^+ \mu^-$ is known to be at most 10^{-4} times the experimental rate it can be ignored and, therefore, the dispersive two photon contribution can be determined from the experimental $\eta \rightarrow \mu^+ \mu^-$ rate. Unfortunately, there are two separate measurements of the $\eta \rightarrow \mu^+ \mu^-$ rate which do not agree. The branching fraction as given by Hyams et al. /111/ is $(2.2 \pm 0.8) \times 10^{-5}$, whereas that given more recently by Dzhelyadin et al. /112/ is $(6.5 \pm 2.1) \times 10^{-6}$. The Particle Data Group /33/ adopts the more recent measurement. Due to a sign ambiguity in the derivation each of these measurements eventually leads to two values for the parameter k of equation (4.3). For the original measurement the values are $k = (1.24 \pm_{-0.48}^{+0.57}) \times 10^{-2}$ and $(2.62 \pm_{-0.48}^{+0.57}) \times 10^{-2}$; for the more recent one the values are $k = (1.38 \pm_{-0.33}^{+0.54}) \times 10^{-2}$ and $(0.00 \pm_{-0.00}^{+0.57}) \times 10^{-2}$. Barger et al. /110/ conclude that the upper bound on m_t is relaxed, with $m_t \ll 75$ GeV for $B = 0.4$.

As Bergström et al. /113/ have pointed out, the comparison of $K_L \rightarrow \mu^+ \mu^-$ with $\eta \rightarrow \mu^+ \mu^-$ may not be correct since the former is a $|\Delta S| = 1$ transition for which there can be extra pole contributions to the amplitude. Because of these uncertainties it is usual /105,114/ to take the ratio of dispersive to absorptive two photon contributions as an unknown parameter. Until this parameter is better known, no

interesting bounds result from the consideration of $K_L \rightarrow \mu^+ \mu^-$ decay /114/.

In the context of left - right symmetric models (LRS models) the box diagram contains additional contributions arising from the exchange of one or more gauge bosons (W_R) associated with the extra gauge group $SU(2)_R$ (Figure 4.4). Equating the real part of the total transition amplitude to half the $K_L - K_S$ mass difference Beall, Bander and Soni /115/ deduced a lower bound on the mass of the W_R boson

$$M_{W_R} \gtrsim 1.6 \text{ TeV}$$

This calculation was performed using the vacuum saturation estimate for the matrix elements of the two distinct quark operators which arise. Trampetic repeated /94/ the calculation using MIT bag model and harmonic oscillator estimates for the matrix elements and arrived at a similar conclusion.

Nohapatra, Senjanovic and Tran /117/ noted that LRS models necessarily contained a neutral Higgs particle which changed flavour leading to a tree level contribution to the $K^0 - \bar{K}^0$ amplitude. Cancellations between this term and the contributions involving W_R lead to a lowering of the bound to

$$M_{W_R} \gtrsim 300 \text{ GeV}$$

This result depends upon particular values of the KM mixing angles being allowed. Recent data from the CUSB collaboration /107/ shows

$$\frac{\Gamma(b \rightarrow u e \nu)}{\Gamma(b \rightarrow c e \nu)} < 0.055 \quad (90 \% \text{ c.l.})$$

which rules out the particular values required and the lower bound

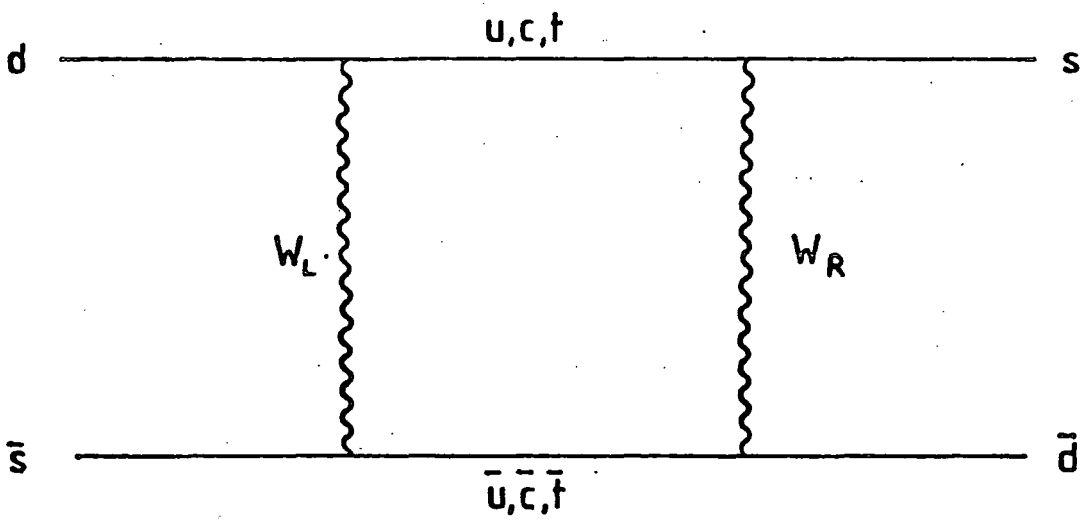


Figure 4.4

$W_L - W_R$ box diagram contribution to $K^0 - \bar{K}^0$ in an $SU(2)_R \times SU(2)_L \times U(1)$ gauge theory.

returns /118/ to the value of Beall et al. /115/ and Trampetic /94/.

As an example of the type of bounds which can be derived from rare kaon decays in supersymmetric models, Lahanas and Nanopoulos /118/ have repeated the analysis of Buras /82/. They find that, in a locally supersymmetric theory, the t-quark mass is inversely related to squark masses. If the masses of squarks are greater than 20 GeV as indicated by searches at PETRA and PEP, then the t-quark mass must be less than 100 GeV. This calculation is, of course, subject to the same uncertainties as the original calculation in the standard model by Buras.

4.2 B-Meson Decay

A major uncertainty in the calculation of short distance effects in rare kaon transitions is the value of the quark mixing angles which appear in the amplitudes. However, recent measurements on B-meson decay provide a means of determining these angles. The experimental data consists of lifetime measurements, an upper bound on a ratio of partial widths and measurements of the semileptonic branching ratios for B-meson decay.

In 1982 the JADE experiment at PETRA determined an upper bound on the lifetime /119/ of

$$\tau_B < 1.4 \times 10^{-12} \text{ s} \quad (90 \% \text{ c.l.}) \quad (4.6a)$$

Recently two experiments at the PEP accelerator have measured the B-meson lifetime. The results are

$$\tau_B = (1.8 \pm 0.6 \pm 0.4) \times 10^{-12} \text{ s} \quad (4.6b)$$

from the MAC detector group /120/ and

$$\tau_B = (1.20^{+0.45}_{-0.36} \pm 0.30) \times 10^{-12} \text{ s} \quad (4.6c)$$

from the MARK II detector group /121/.

Experiments at the Cornell Electron Storage Ring (CESR) have measured the ratio of partial widths $\Gamma(b \rightarrow ue\nu)/\Gamma(b \rightarrow ce\nu)$ and the semileptonic branching ratio. The source of B-mesons is the $\Upsilon(4S)$ (or Υ''') $b\bar{b}$ state which is just above flavour threshold. In semileptonic decays the momentum spectrum of the final state electrons is harder in the case of $b \rightarrow ue\nu$ than in the case of $b \rightarrow ce\nu$. Using the model of Altarelli et al./122/ for semileptonic B-meson decay, the CUSB collaboration /107/ find that the spectrum agrees well with that predicted for $b \rightarrow ce\nu$. They find no evidence for the decay $b \rightarrow ue\nu$. From this they obtain the upper limit

$$\frac{\Gamma(b \rightarrow ue\nu)}{\Gamma(b \rightarrow ce\nu)} < 0.055 \quad (90 \% \text{ c.l. }) \quad (4.4)$$

Based on the analysis of Altarelli et al. /122/, the CUSB collaboration have also measured the semileptonic branching ratio for $B \rightarrow e\nu X$ and obtain /107/

$$B(B \rightarrow e\nu X) = (13.2 \pm 0.8 \pm 1.4) \% \quad (4.7)$$

This agrees well with the results of the CLEO collaboration who find /123/

$$B(B \rightarrow e\nu X) = (12.7 \pm 1.7 \pm 1.3) \%$$

and

$$B(B \rightarrow \mu\nu X) = (12.2 \pm 1.7 \pm 3.1) \%$$

A theoretical analysis of B-meson decay can be made in two ways. The first involves a calculation of the total decay width. Since the b-quark is heavy compared to the scale of strong interactions, B-meson decay can be approximated by the decay of a free b-quark (Figure 4.5). Then

$$\Gamma = \Gamma(b \rightarrow c) + \Gamma(b \rightarrow u)$$

where /124/

$$\Gamma(b \rightarrow c) = \Gamma_0 |V_{bc}|^2 \left\{ 1.11 + 1.53 \eta_0 (|V_{ud}|^2 + |V_{us}|^2) + 0.57 \eta_0 (|V_{cd}|^2 + |V_{cs}|^2) \right\}$$

and

$$\Gamma(b \rightarrow u) = \Gamma_0 |V_{bu}|^2 \left\{ 2.33 + 3 \eta_0 (|V_{ud}|^2 + |V_{us}|^2) + 1.53 \eta_0 (|V_{cd}|^2 + |V_{cs}|^2) \right\}$$

In each case the first term in the brackets comes from the semileptonic decay into e, μ or τ . $\Gamma_0 = (G_F^2 m_b^5 / 192 \pi^3)$ and η_0 is a QCD correction whose value is /124/ $\eta_0 \approx 1.1$. This approximation is good to the extent that non-spectator diagrams (Figure 4.6) contribute to the decay. However, it is not easy to calculate non-spectator effects reliably, as is shown by the unsuccessful attempts to calculate the semileptonic branching ratio /125/. Penguin contributions to B-meson decay are thought to be negligible /126/.

The second method, which avoids the problems of non-spectator and penguin diagrams, is to calculate only the semileptonic width and use the experimentally measured branching ratio to determine the lifetime /122,125/. The analysis of Altarelli et al. /122/ involves free b-quark decay with corrections for soft gluon and bound state effects.

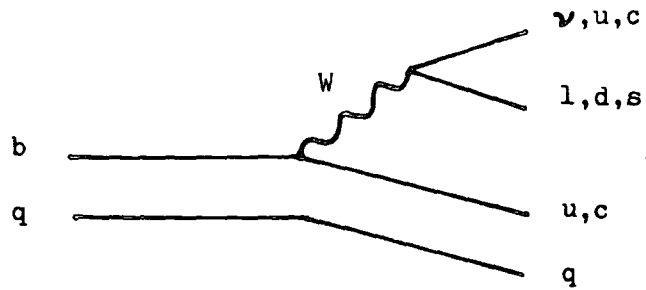


Figure 4.5

Free b-quark decay (spectator diagrams).

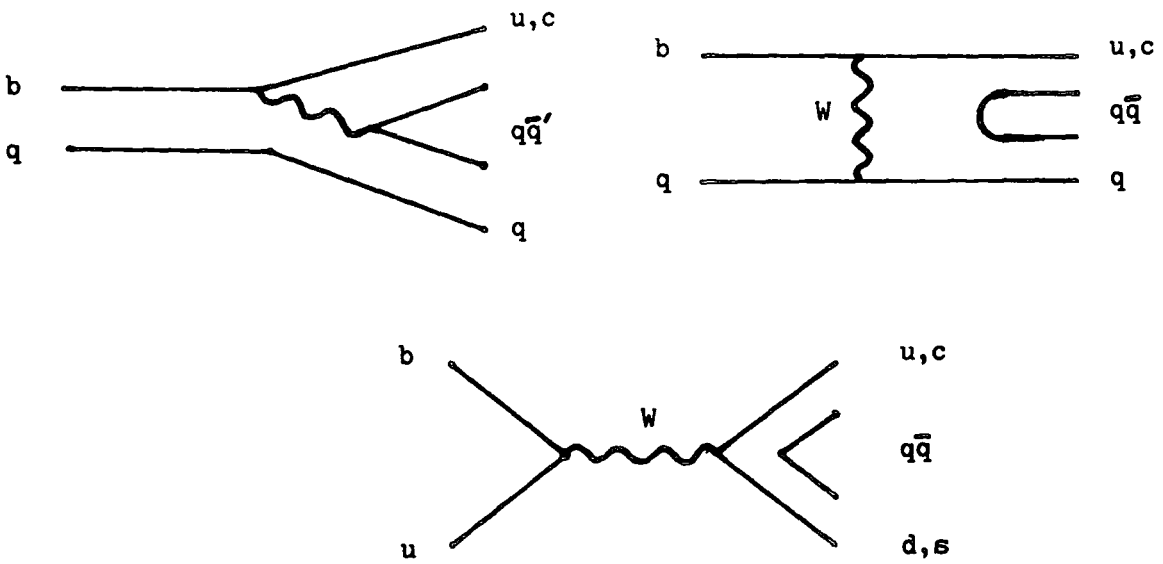


Figure 4.6

Non-spectator contributions to B-meson decays.

The consequences of the b-quark being in a bound state are modelled by giving the spectator quark a gaussian momentum distribution with mean spread p_F . This method gives good agreement with the observed spectrum in D-meson decay for $0 \leq p_F \leq 300$ MeV /122/.

The B-meson lifetime is calculated from

$$\tau_B = B_{SL} / \Gamma_{SL}$$

where B_{SL} is the semileptonic branching ratio and Γ_{SL} is the semileptonic width given by /122/

$$\Gamma_{SL} = \Gamma_0 (Z_c |V_{bc}|^2 + Z_u |V_{bu}|^2) \quad (4.8)$$

Z_u and Z_c are phase space factors, calculated by Altarelli et al. /122/, which depend on the amount of Fermi motion given to the quarks in the B-meson:

$$\begin{aligned} Z_u &= 0.94 \quad ; \quad Z_c = 0.46 \quad \text{for } p_F = 0 \text{ MeV} \\ Z_u &= 0.86 \quad ; \quad Z_c = 0.41 \quad \text{for } p_F = 150 \text{ MeV} \\ Z_u &= 0.73 \quad ; \quad Z_c = 0.33 \quad \text{for } p_F = 300 \text{ MeV} \end{aligned}$$

Taking the phase space factors for $p_F = 150$ MeV, the above expression for the semileptonic width can be used to translate the CUSB result on the ratio of partial widths into a bound on a ratio of KM matrix elements

$$\frac{\Gamma(b \rightarrow u)}{\Gamma(b \rightarrow c)} = \frac{Z_u}{Z_c} \left| \frac{V_{bu}}{V_{bc}} \right|^2 < 0.055$$

giving

$$\left| \frac{V_{bu}}{V_{bc}} \right| < 0.16 \quad (4.9)$$

This bound together with the measurements of the B-meson lifetime can be used to restrict the KM angles θ_2 and θ_3 to a small range /127,128/. Since the $b \rightarrow u$ contribution is so small it can be neglected and equation (4.6) can be used to determine $|V_{cb}|$. With $m_b = 5$ GeV and $1.4 \times 10^{-12} > \tau_B(s) > 0.6 \times 10^{-12}$ an allowed range is derived

$$0.05 < |V_{cb}| < 0.076$$

From equation (4.9) this gives

$$|V_{ub}| \leq 0.012, 0.008$$

for the upper and lower limits respectively, or

$$s_3 \leq 0.05, 0.035 \tag{4.10a}$$

Using (for small s_2, s_3)

$$|V_{cb}| = |c_1 c_2 s_3 - s_2 c_3 e^{-i\delta}| = |s_3 - s_2 e^{-i\delta}|$$

it can be shown that s_2 is bounded by

$$|V_{cb}| - s_3 \leq s_2 \leq |V_{cb}| + s_3$$

or

$$0.015 \leq s_2 \leq 0.13 \tag{4.10b}$$

The CP-violating phase δ cannot be determined from this information.

Combining these results with the other data given in section 2.2 leads to the following determination of the KM matrix elements /129/

$$|V| = \begin{pmatrix} 0.9723 - 0.9737 & 0.228 - 0.234 & 0.000 - 0.008 \\ 0.228 - 0.234 & 0.9704 - 0.9726 & 0.042 - 0.067 \\ 0.003 - 0.016 & 0.041 - 0.066 & 0.9977 - 0.9991 \end{pmatrix}$$

where the unitarity of the KM matrix has been used with the assumption of six quark flavours. In the generalized case with more than six flavours, the ranges of values for $|V_{ij}|$ are given by /129/

$$|V| = \begin{pmatrix} 0.9709 - 0.9757 & 0.228 - 0.234 & 0.000 - 0.013 \\ 0.21 - 0.27 & 0.78 - 1.00 & 0.042 - 0.067 \\ 0.00 - 0.12 & 0.00 - 0.58 & 0.000 - 0.999 \end{pmatrix}$$

The new information from B-meson decay is important for this work because it gives independent constraints on two of the variables in the $K^0 - \bar{K}^0$ transition amplitude. This reduces the uncertainty in determinations of the remaining parameters.

4.3 Phenomenology: 1983 - 1984

4.3.1 Limits on B

The calculation of the hadronic matrix element in the $K^0 - \bar{K}^0$ transition amplitude requires non-perturbative techniques not yet available. Instead, the matrix element is calculated in a model with the vacuum saturation approximation ($B = +1$) being used to set the scale and sign. Colić et al. /87/, using a variety of models, have found values of B ranging from 2.86 to 0.055. The MIT bag model calculation had given /85/ $B = 0.42$ but a repetition of this calculation by Colić et al. showed it to be unstable in magnitude and even in sign with one calculation giving $B = -0.42$. Although it is clear that $B < 0$ will not reproduce the correct sign for $\delta m = m_S - m_L$ in the four quark model, the extra freedom in the six quark model means that such solutions cannot, a priori, be ruled out /105/.

In attempts to bound the t-quark mass the decay $K_L \rightarrow \mu^+ \mu^-$ is considered together with δm and ϵ . In addition to the problem with the electromagnetic contribution to the dispersive part of $K_L \rightarrow \mu^+ \mu^-$, both Buras /82/ and Barger et al. /110/ stressed the sensitive dependence of their calculations on B. Once m_t is fixed the size of B becomes the most significant phenomenological issue in the study of the perturbative $K^0 - \bar{K}^0$ transition amplitude. The experimental constraints on the KM matrix elements can be used to bound B above and below and to restrict its sign /106/.

The data to be fitted are the $K_L - K_S$ mass difference and the CP-violation parameter. Following the success of Gaillard and Lee /36/ in determining m_c and of the many determinations of the quark mixing angles /86, 103 - 106/, these are related to the real and imaginary parts of the box diagram amplitude M_B by

$$\delta m = 2 \operatorname{Re} M_B \quad (4.2)$$

$$\operatorname{Re} \epsilon = - \operatorname{Im} M_B / 2 \delta m \quad (4.3)$$

The value of s_1 is fixed at $s_1 = 0.228$ and s_3 is varied in the range of 0.0 to 0.5. For each s_1, s_3 pair chosen there are up to four s_2, s_3 pairs which fit the data for B positive or negative. The solutions are labelled by the quadrant in which δ appears.

In reference 106 the t-quark mass was taken to be $m_t = 35 \pm 5$ GeV following an analysis of UA1 data /57/ by Barger et al. /56/ which indicated that this was a likely value. The QCD corrections were taken to be $\eta_{uj} = 1$, $\eta_{cc} = 0.99$, $\eta_{tt} = 0.60$ and $\eta_{ct} = 0.40$. The solutions for these values of the parameters and B positive are illustrated in Figures 4.1 and 4.2. They are found in quadrants 1, 2 and 4 and there are two solutions in quadrant 4.

As positive B decreases from $B = 1$ the trend is that the s_2 curves for solutions 1 and 2 move up and solution 4 moves to the right until by $B \sim 0.5$ no part of solution 4 remains in the acceptable range $s_3 < 0.5$. A characteristic of solution 1 in this region is that s_2 is always larger than s_3 and for both solutions $|s_3|$ is small except for small values of s_3 .

As B increases from $B = 1$ the s_2 curves fall for solutions 1 and 2 and solution 4 moves to the left until $B \approx 1.3$ when the solution 4 curve starts to move to the right as B continues to increase. By about $B = 1.4$ in solution 1 s_2 becomes equal to s_3 for some values of s_3 and by $B = 2$ s_2 is always less than s_3 . A characteristic of both solutions 1 and 2 is that the minimum value of s_3 corresponding to $|s_3| = 1$ increases as B increases until it moves beyond $s_3 = 0.5$ in solution 2 for $B = 1.7$ and in solution 1 it is about 0.28 for $B = 3.0$ (Figure 4.7).

The negative B solutions are presented in Figure 4.8 for $B = -0.4$. Four solutions are found, two in the first quadrant and two almost identical ones in the fourth quadrant. As in the case for positive B the solutions move to the right as $|B|$ decreases. These solutions illustrate how easy it is to fit the data in this model, but as the value of $|V_{ub}/V_{cb}|$ in all cases never drops below 0.35 they are eliminated by the experimental bound $|V_{ub}/V_{cb}| < 0.16$. The predicted ratio does decrease as $|B|$ decreases but the solutions move outside the acceptable s_3 range before the experimental value is reached.

The bound on $|V_{ub}/V_{cb}|$ is important as it eliminates solutions 4 for positive B as well as negative B and it establishes an upper bound on B in solutions 1 and 2. Before seeing how B is bounded, it is instructive to examine the ratio

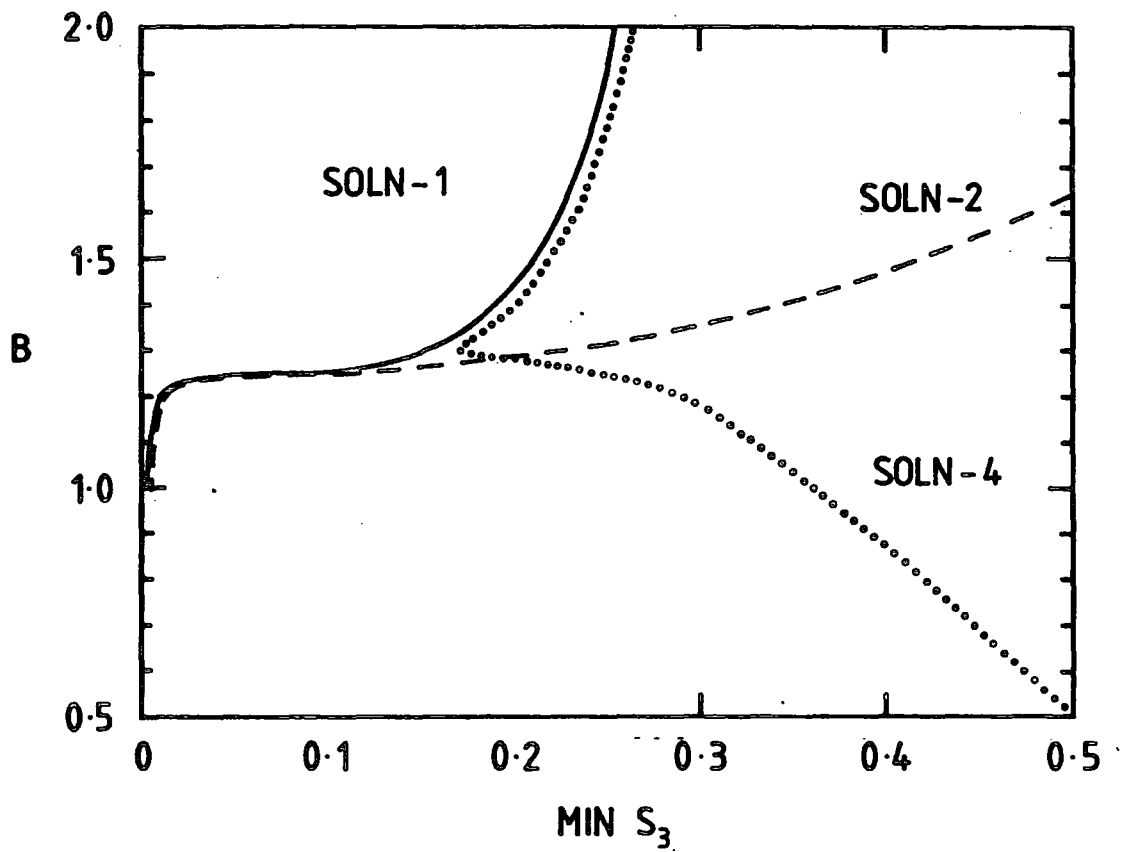


Figure 4.7

B plotted against the minimum value of s_3 . For solutions 1 and 2 only, the minimum s_3 corresponds to $|s_\delta| = 1$.

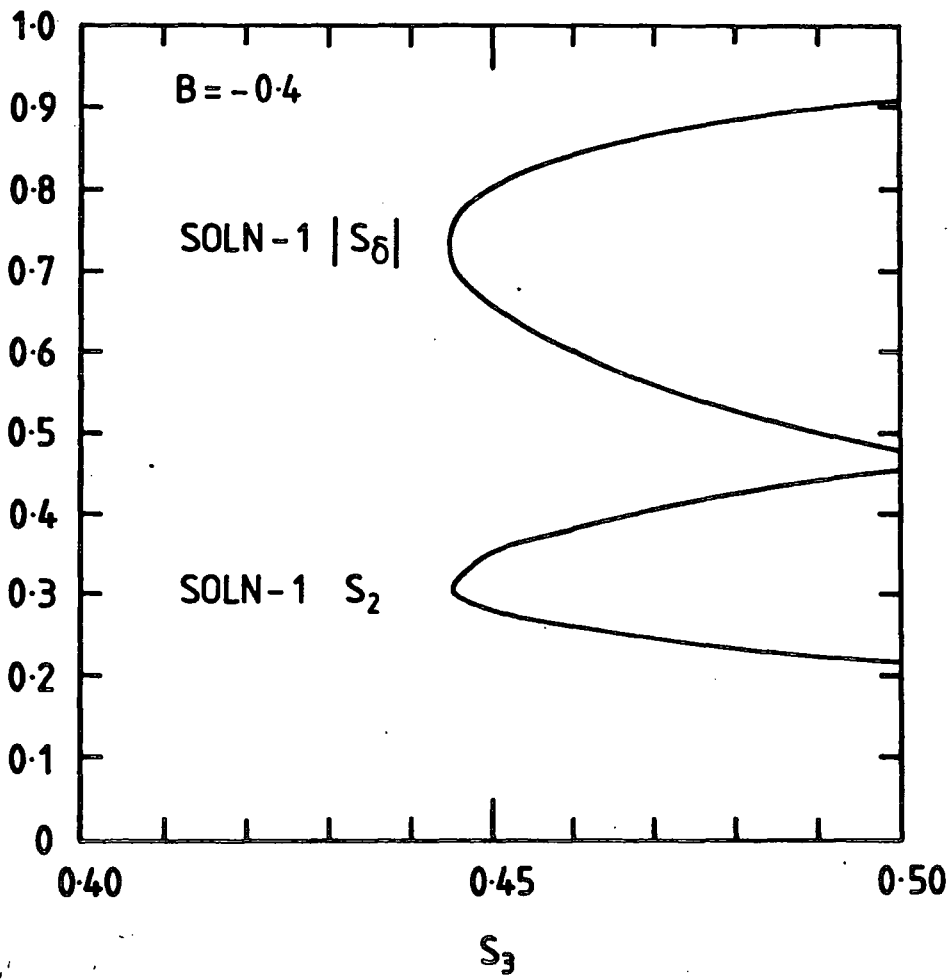


Figure 4.8

The two first quadrant solutions for s_2 and $|s_\delta|$ as a function of s_3 for $B = -0.4$. The two fourth quadrant solutions are essentially identical to these.

$$\left| \frac{V_{ub}}{V_{cb}} \right| = \left| \frac{s_1 s_3}{c_1 c_2 s_3 - s_2 c_3 e^{-i\delta}} \right|$$

There are three areas of interest and two arise for $s_2 \approx s_3$ in the region where $|s_\delta|$ is small. For solution 1 this arises for $B > 1$ and the ratio can be very large indeed (unless $|s_\delta| \sim 1$) and the solution is easily eliminated in this region. For solution 2 $s_2 \approx s_3$ can occur for any value of B but as δ is in the second quadrant the ratio becomes $\sim \frac{1}{2}s_1 = 0.114$. The third case arises for solution 2 with $B > 1$. As B increases the values of s_2 become very small and the ratio approaches $s_1 = 0.228$. The importance of the experimental bound $|V_{ub}/V_{cb}| < 0.16$ in eliminating these solutions and in bounding B is clear.

For a particular value of B the bound on the ratio of KM matrix elements places an upper bound on the allowed values of s_3 . As B increases the maximum value of s_3 allowed decreases as illustrated in Figure 4.9 . By $B \approx 1.23$ in both solutions 1 and 2 the maximum value of s_3 allowed coincides with the minimum value of s_3 at which $|s_\delta| = 1$ and that is the upper bound on B . No solution with larger B satisfies the bound on the ratio.

If the bound on the ratio $|V_{ub}/V_{cb}|$ were to fall the bound on B would be slightly reduced. If an earlier bound of $|V_{ub}/V_{cb}| < 0.4$ were used the upper bound would move to $B < 3.0$ for solution 1 and for solution 2 it would be $B < 1.5$ which emphasizes the importance of the present value.

This analysis has been repeated /130/ for $20 \leq m_t(\text{GeV}) \leq 300$ and there is essentially no change in the upper bound on B over this range. However, the upper bound is sensitive to the values of the QCD

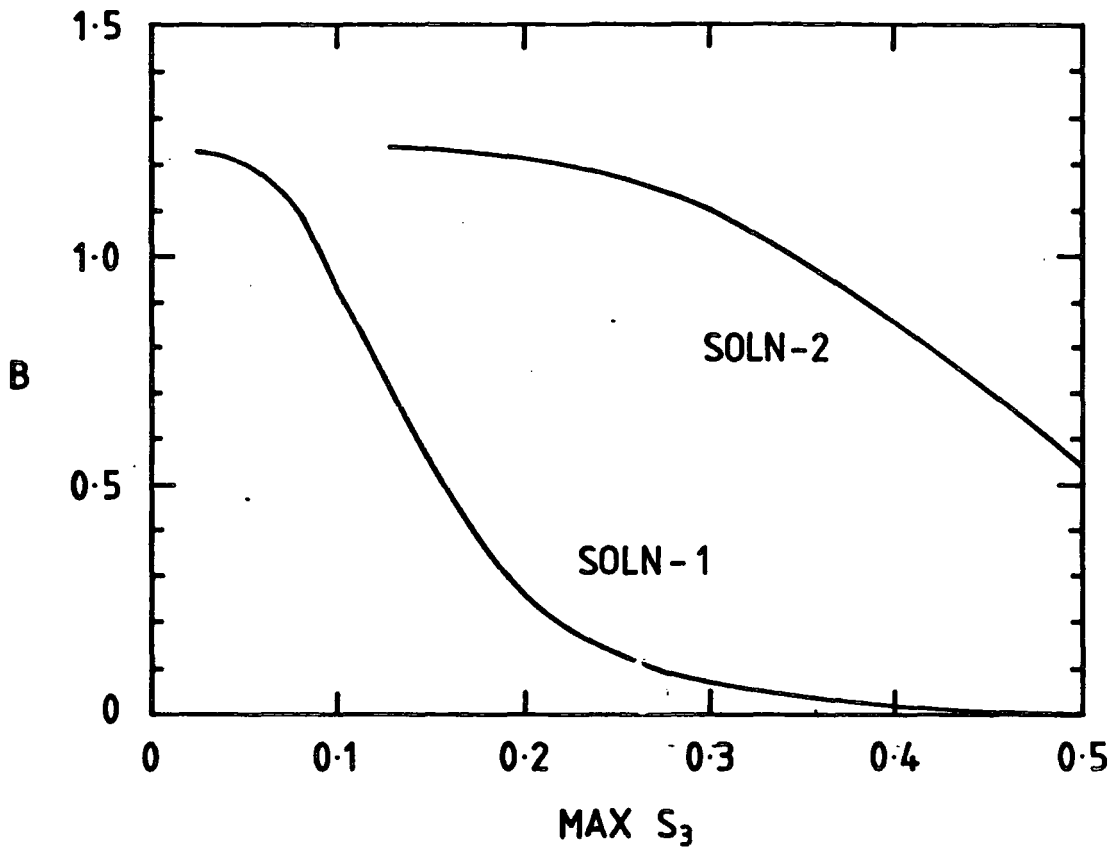


Figure 4.9

B plotted against the maximum value of s_3 allowed by the constraint on $|V_{ub}/V_{cb}|$. No fourth quadrant solutions are permitted.

corrections η_{ij} . If these are given the values for $\Lambda_{QCD} \approx 0.1$ GeV ($\eta_{cc} = 0.69$, $\eta_{tt} = 0.59$, $\eta_{ct} = 0.41$) then the upper bound is as high as $B < 1.7$.

A lower bound on B is harder to establish than the upper one as the ratio $|V_{ub}/V_{cb}|$ is not restrictive and other information on the KM matrix elements must be used. The bound $0.2 < |V_{cd}| < 0.24$, for example, restricts B to $B > 0.05$ for solution 1 but to limit solution 2 requires the combination of $|V_{cd}| > 0.2$ and $|V_{cs}| > 0.8$ to give $B > 0.04$. If the lower bound on $|V_{cs}|$ is closer to the CDHS value of 0.59 then the $|V_{cd}|$ bound alone gives $B > 0.02$. The lower bound on B is quite sensitive to the lower bound on $|V_{cd}|$ with $B > 0.04$ for $|V_{cd}| > 0.21$. The most general conclusion /106/ is that the lower bound on B is $B > 0.04$ from the experimental data on the KM matrix elements.

Another way of looking at the lower bound on B is to use the parameter k arising in the analysis of the $K_L \rightarrow \mu^+ \mu^-$ decay (equation (4.5)). Barger et al. /110/ estimate k by comparison with the decay $\eta \rightarrow \mu^+ \mu^-$. The more recent experimental determination /112/ of the branching fraction for this decay yields the two values $k = (1.38^{+0.54}_{-0.33}) \times 10^{-2}$ or $k = (0.00^{+0.57}_{-0.00}) \times 10^{-2}$ due to a sign ambiguity. By the reverse of the argument that Buras /82/ used to bound m_t , these values give the bounds $0.1 < B < 0.4$ and $0.7 < B < \infty$ respectively for $m_t = 35$ GeV.

In summary, experimental data on the KM matrix elements places bounds on the size and sign of the hadronic matrix element in the $K^0 - \bar{K}^0$ transition amplitude. $B < 0$ is eliminated together with the possibility of having the phase δ in the fourth quadrant for B positive or negative. For the solutions with δ in the first or second quadrants, B is bounded by $0.04 \lesssim B \lesssim 1.7$. This last result depends critically on the starting

assumption that the box diagram is the dominant contribution to the real part of the $K^0 - \bar{K}^0$ transition amplitude.

4.3.2 Bounds on t-Quark Mass

Experimental information on B-meson decay /107,119 - 121/ together with standard calculations of δm and ϵ can be used to place a lower bound on the mass of the t-quark /114,124,127,128,130/. This is in contrast to the (uncertain) upper bound which resulted from consideration of $K_L \rightarrow \mu^+ \mu^-$ decay.

In reference 130 a lower bound on the t-quark mass m_t is derived as a function of the parameter B assuming that the box diagram is the dominant contribution to both the real and imaginary parts of the kaon mass matrix. The B-meson lifetime is calculated using the expression of Altarelli et al. /122/ for the semileptonic width and the experimentally measured branching ratio. The phase space factors are allowed to vary over the ranges $0.73 \leq Z_u \leq 0.94$ and $0.33 \leq Z_c \leq 0.46$ calculated /122/ for $0 \leq p_F \leq 300$ GeV and the branching ratio for $B \rightarrow X e \nu$ is varied over the experimentally allowed range /107/ $0.108 \leq B_{SL} \leq 0.154$. Additionally the mass of the b-quark is allowed to vary over the reasonable range $4.8 \leq m_b \text{ (GeV)} \leq 5.2$.

The lower bound on m_t is obtained as follows. For fixed m_t the $K_L - K_S$ mass difference δm and the CP-violation parameter ϵ are used to find solutions for the KM parameters $\sin\theta_2$ (s_2) and $\sin\delta$ (s_δ) as a function of $\sin\theta_3$ (s_3). The experimental constraint $|V_{bu}/V_{bc}| < 0.16$ is then used to eliminate $B > 1.23$, $B < 0$ and solution 4 (using the QCD corrections for $\Lambda_{QCD} = 0.33$ GeV). These results were originally obtained /106/ for $m_t = 35 \pm 5$ GeV, however they do not change in the range $20 \leq m_t \text{ (GeV)} \leq 300$. This ratio of KM matrix elements also

places an upper bound on s_3 in the remaining solutions. Figures 4.10 and 4.11 show this limit for $B = 1$ and a range of m_t . As B decreases this bound becomes less restrictive as shown in Figure 4.9. There is also a lower bound on s_3 which is the value at which $|s_3| = 1$. This does not change appreciably with B in the range considered.

For the allowed values of s_3 the KM matrix elements are calculated and used to find the B-meson lifetime τ_B . Taking into account the theoretical and experimental uncertainties, a range of predictions for τ_B is obtained. For solution 1 τ_B decreases with decreasing s_3 , but for solution 2 τ_B decreases with increasing s_3 . Therefore, an experimental lower bound on τ_B determines a minimum s_3 in solution 1 and a maximum s_3 in solution 2. The limits on τ_B are $\tau_B < 1.4 \times 10^{-12}$ s from JADE /119/ and $\tau_B > 0.54 \times 10^{-12}$ s from MARK II /121/.

In solution 1, for small m_t , the minimum s_3 allowed by the MARK II result lies above the maximum s_3 determined by the ratio $|V_{ub}/V_{cb}| < 0.16$. As m_t increases the minimum s_3 falls until it meets the maximum s_3 : this determines the smallest allowed value for m_t in solution 1. This situation is illustrated in Figure 4.10 for $B = 1$. As B is decreased the maximum s_3 curve rises and the curve for the minimum s_3 allowed by τ_B moves to the right. The combined result is that the minimum value of m_t increases.

The case for solution 2 is slightly different: for large m_t , the maximum s_3 allowed by the B-meson lifetime is above the minimum s_3 defined by $|s_3| = 1$ (Figure 4.11). As m_t is decreased this maximum decreases until it meets the minimum s_3 : this determines the minimum m_t for solution 2. As B decreases the trend is for the maximum s_3 curve to move to the right, leading to an increased lower bound on m_t . There is no significant change in the minimum s_3 curve for the

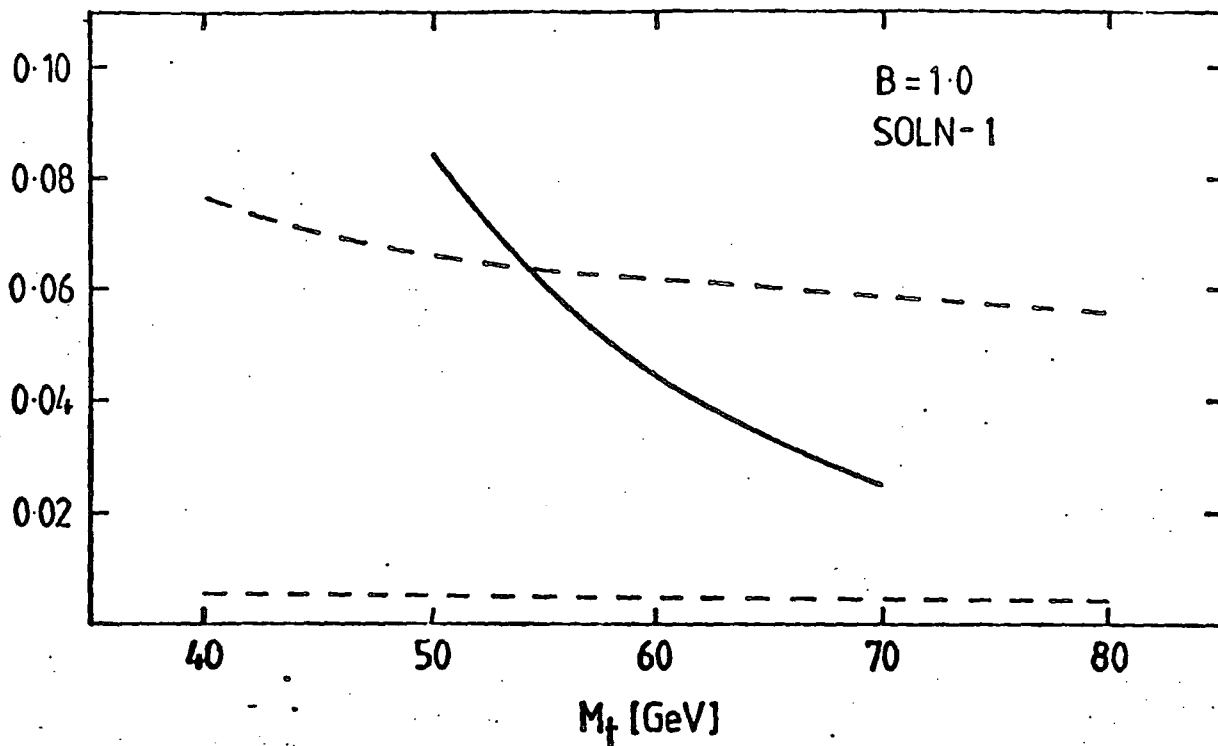


Figure 4.10

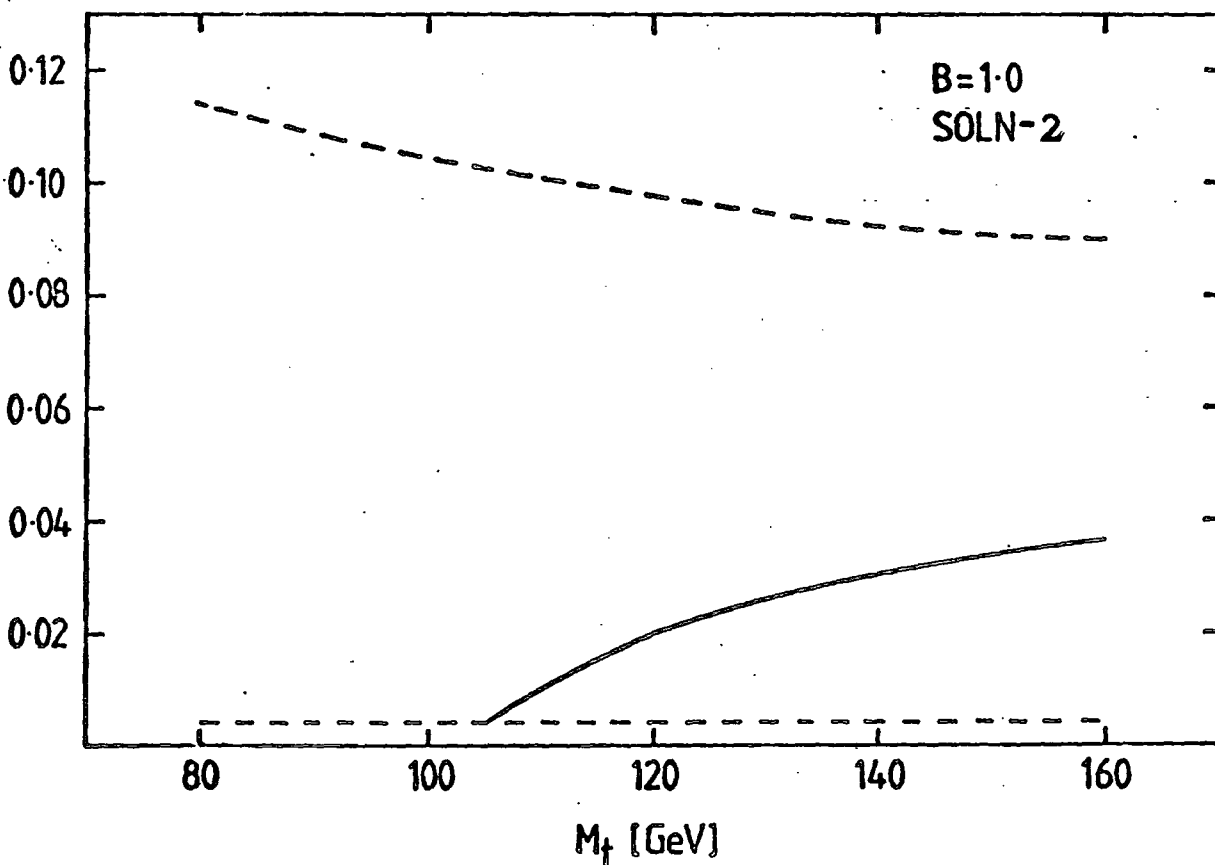


Figure 4.11

In solution 1 (2) a minimum (maximum) s_3 is determined by a minimum τ_B . The solid line shows the variation of this minimum (maximum) with m_t . The dotted lines are maximum s_3 from $|V_{ub}/V_{cb}| < 0.16$ and minimum s_3 from $|s_8| = 1$. Minimum m_t occurs where solid and dotted lines cross.

range of B considered.

The results for the lower bound on m_t as a function of B are shown in Figures 4.12 and 4.13. For Figure 4.12 the QCD corrections ($\Lambda = 0.33$ GeV) to the $K^0 - \bar{K}^0$ transition amplitude have been included. The corresponding result where these corrections have been omitted are shown in Figure 4.13. A comparison of the two figures shows that the bound on m_t is sensitive to the presence or absence of such corrections. If the QCD corrections for $\Lambda = 0.1$ GeV were used, the curves would be shifted to the right until $B_{\max} \approx 1.7$.

Alternatively, if the mass of the t -quark were known, these results would determine an allowed range for B . For example, $m_t = 40$ GeV would restrict the size of the hadronic matrix element to $0.8 \leq B \leq 1.2$. There is a limit on the t -quark mass of $m_t \leq 300$ GeV /131/ from consideration of radiative corrections to the parameter $\rho = M_W^2 / M_Z^2 \cos^2 \theta_W$ /132/. From Figures 4.12 and 4.13 it can be seen that this result places a lower bound, $B \geq 0.2$, on the size of the hadronic matrix element.

It is possible to obtain an upper bound on m_t by considerations similar to those used to find the lower bound. However, the result is much larger than the limit derived from radiative corrections to ρ .

The results of this calculation are sensitive to changes in the semileptonic branching ratio and the lower limit on the B -meson lifetime. The lower bound on m_t would be strengthened if the maximum possible branching ratio decreased or if the minimum allowed lifetime increased. For example, for $B_{SL} \leq 0.12$ and $\tau_B \geq 1.0 \times 10^{-12}$ s the lower bound on m_t in Figure 4.12 would rise to 160 GeV for solution 1 and 400 GeV for solution 2 at $B = 1.0$. The corresponding results when the QCD corrections are omitted from the $K^0 - \bar{K}^0$ transition amplitude are 85 GeV and 210 GeV.

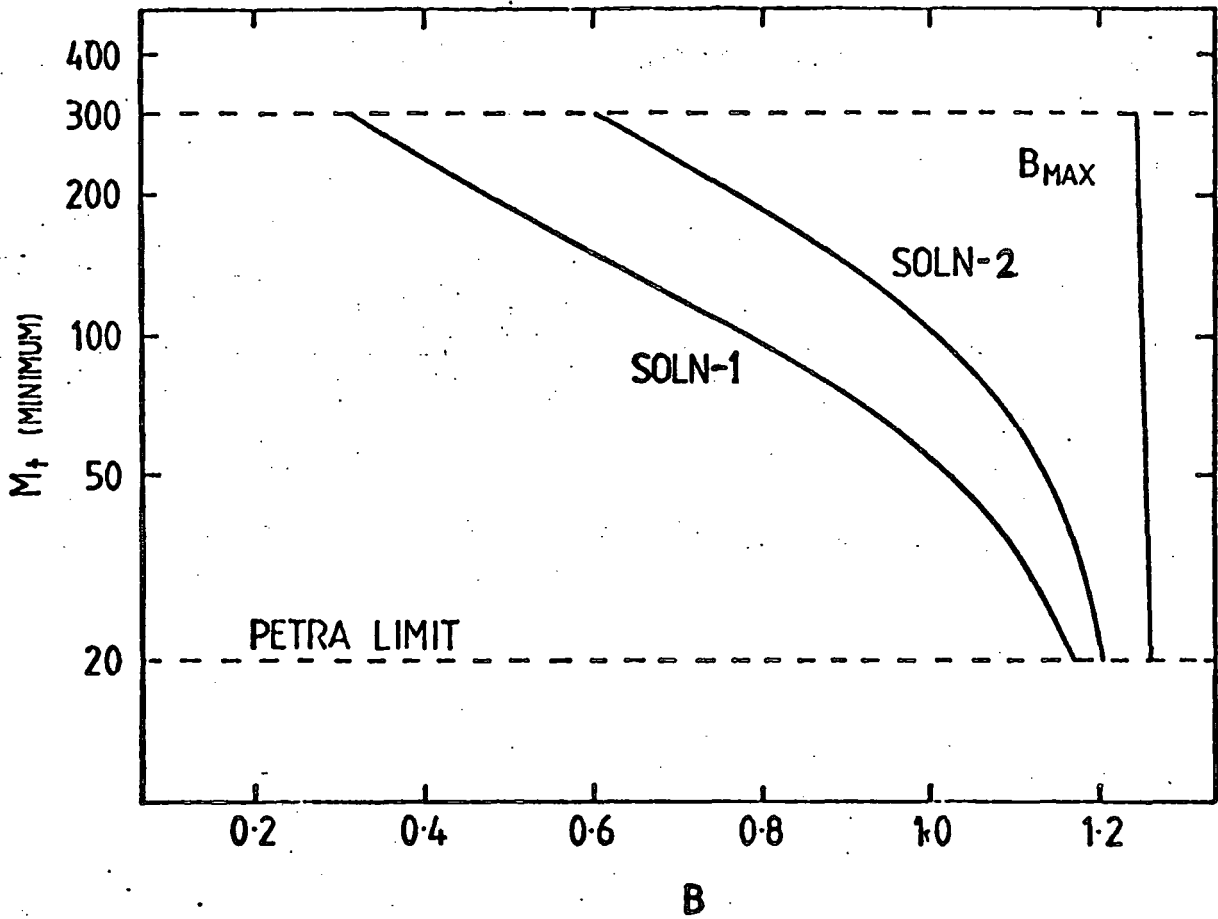


Figure 4.12

The minimum value of m_t in solutions 1 and 2 when the constraint $\delta m = 2 \operatorname{Re} M_B$ is satisfied (QCD corrections η_{ij} are included). The upper bound on the size of the hadronic matrix element (B_{\max}) is also shown.

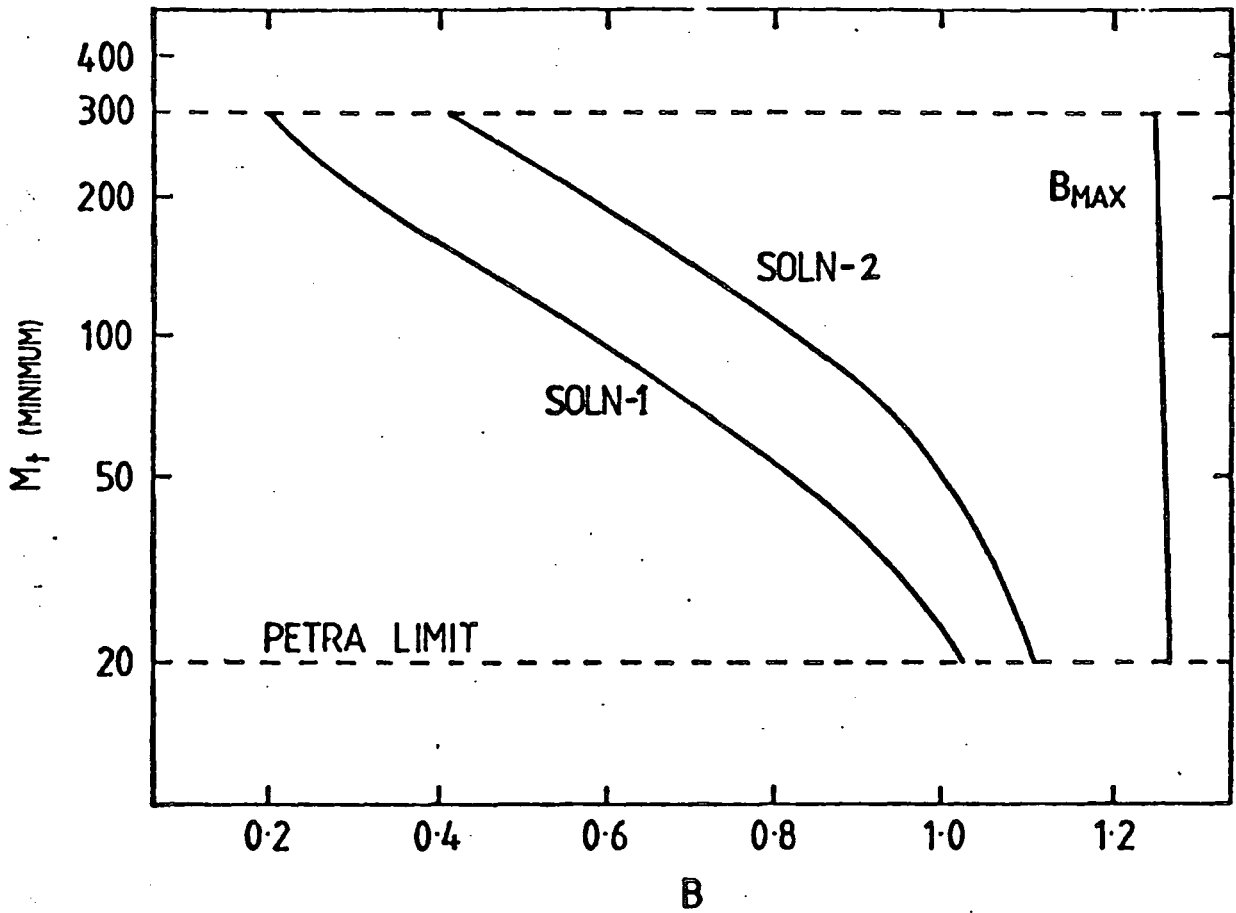


Figure 4.13

The minimum value of m_t in solutions 1 and 2 when the constraint

$\delta_m = 2 \text{Re}M_B$ is satisfied (QCD corrections γ_{ij} are omitted).

B_{max} is also shown.

These results illustrate an observation originally made by Ellis and Hagelin /133/ that for small B (~ 0.4) the short distance contribution to δ_m from the box diagram is totally inadequate unless the t-quark mass is very large indeed. For this reason it is thought /124/ that the real part of the transition amplitude may be dominated by the long distance dispersive contributions of section 3.3 . However, the imaginary part of the $K^0 - \bar{K}^0$ mass matrix is not greatly affected in the convention in which the $K^0 \rightarrow \pi\pi(I=0)$ amplitude is real and a significantly less constraining lower bound can be obtained by consideration of the CP-violation parameter only /114,124, 127,128/.

Ginsparg, Glashow and Wise /124/ derived a lower bound on m_t as a function of τ_B using this method. They took the size of the hadronic matrix element as given by $B = 0.37$. This analysis was extended to cover $B = \frac{1}{3}, \frac{2}{3}, 1$ by Buras et al. /114/ who also included the small effect of CP-violation in the $K^0 \rightarrow \pi\pi(I=0)$ amplitude (A_0) from penguin diagrams. As a result of penguin contributions A_0 is not real in the KM model. In order to regain the Wu-Yang convention in which A_0 is real a redefinition of kaon fields by a phase ξ is performed. This redefinition changes the relation between the CP-violation parameter and the $K^0 - \bar{K}^0$ transition amplitude to

$$\text{Re } \epsilon = -\frac{1}{2} \left(\frac{\text{Im} M_B}{\delta_m} - \xi \frac{2 \text{Re} M_B}{\delta_m} \right) \quad (4.11)$$

Buras et al. use $\xi = -0.54 s_2^c s_3 s_\delta$ as found by Gilman and Hagelin /134/. The effect of this extra term is to slightly increase the lower bound on m_t (see Figure 4.14), but this is much less than the effect of including the constraint $\delta_m = 2 \text{Re} M_B$.

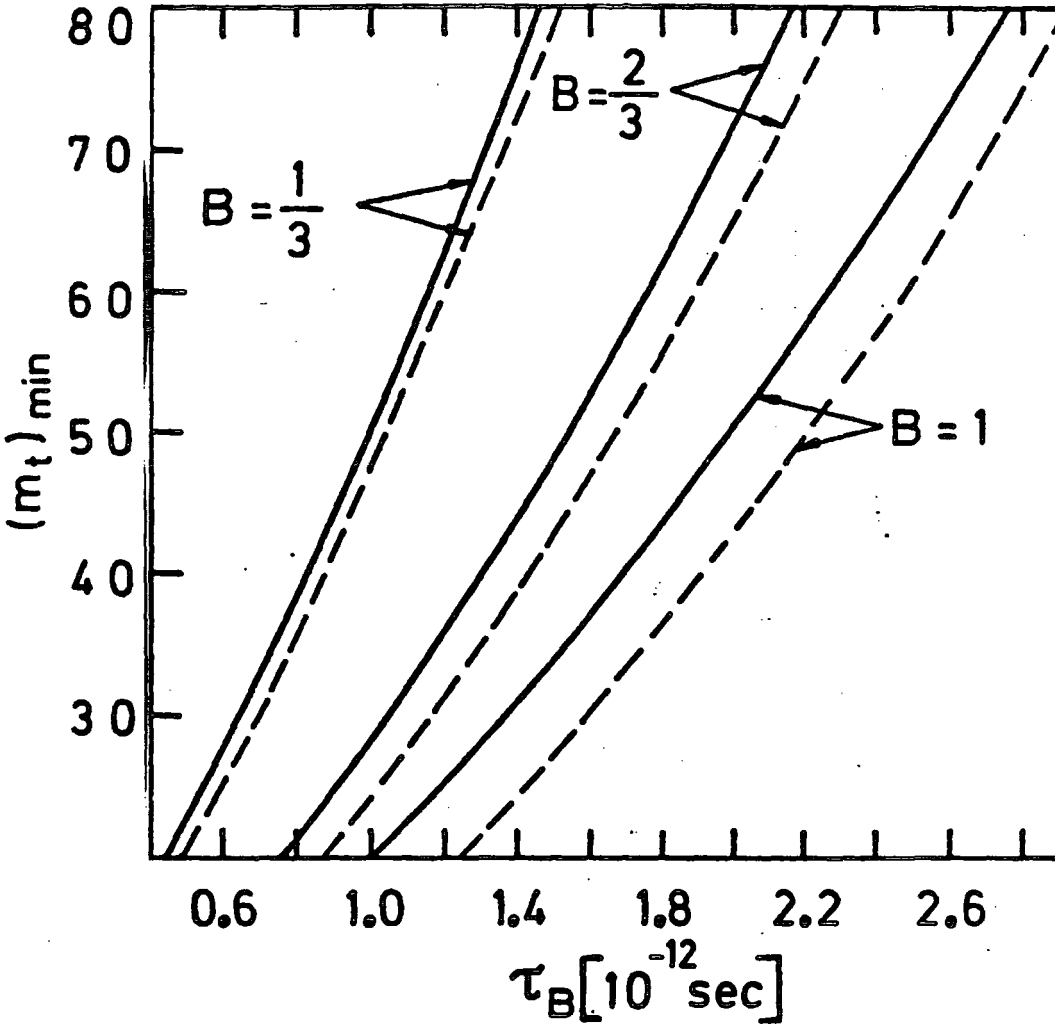


Figure 4.14

The lower bound on m_t as a function of τ_B for $\Gamma(b \rightarrow u)/\Gamma(b \rightarrow c) = 0.05$ and δ in either quadrant 1 or quadrant 2. The constraint $\delta m = 2 \operatorname{Re} M_B$ is not imposed. The solid (dashed) lines correspond to the inclusion (omission) of the ξ -term in the expression for $\operatorname{Re} \xi$.

4.3.3 Maximal CP-Violation

The phase δ is responsible for CP-violation in the KM model and the term "maximal CP-violation" describes the case where $|s_\delta| = 1$. Analysis of the $K^0 - \bar{K}^0$ mass matrix, based on the box diagram amplitude only, revealed /103, 105, 106/ that this situation occurs for s_3 very small unless $B > 1.2$ or δ is in the fourth quadrant. Both these cases are ruled out by the experimental bound on the ratio $|V_{ub}/V_{cb}|$.

By including contributions from double penguin amplitudes and low energy dispersive terms, Hochberg and Sachs /99/ find that large s_3 can be consistent with maximal CP-violation. Taking $B = 0.5$ and $m_t = 30$ GeV they find that $(s_1 = 0.23, s_2 = 0.18 \times 10^{-2}, s_3 = 0.28, s_\delta = 1)$ is a consistent set of the KM parameters. However, the small value of s_2 in this solution and similar ones ensures that $|V_{ub}/V_{cb}|$ is approximately given by $|s_1| = 0.228$ and these solutions can, therefore, be ruled out. The lower bound on the B-meson lifetime, $\tau_B > 0.6 \times 10^{-12}$ s from MARK II, eliminates such a large value for s_3 anyway.

The constraint $\delta_m = 2 \text{Re}M_B$ has a significant effect on the phenomenological analysis of the neutral kaon mass matrix, as is shown in the preceding sections. If this constraint is dropped the bounds derived are considerably weakened. It is, therefore, of interest to attempt to discover the relative sizes of each of the possible contributions to the $K^0 - \bar{K}^0$ transition amplitude. Such an analysis is performed in the following chapter.

CHAPTER 5

ANALYSIS OF THE $K^0 - \bar{K}^0$ TRANSITION AMPLITUDE

5.1 Introduction

The $K^0 - \bar{K}^0$ transition amplitude has been a useful source of information about weak interactions. The first phenomenological success was the prediction of the c-quark mass by Gaillard and Lee /36/. This success was followed by several analyses placing bounds on the parameters /91,99,103,104,106,134,135/ of the Kobayashi-Maskawa (KM) matrix /39/ and attempts to determine the mass of the t-quark (m_t) /82,110,114,124,130/. These analyses are based on different assumptions about the $K^0 - \bar{K}^0$ mass matrix which leads in some cases /114,124,130/ to a large variation in the result. For this reason a better understanding of the $K^0 - \bar{K}^0$ mass matrix itself is desirable.

In general the $K^0 - \bar{K}^0$ transition amplitude can be written /60/ as the sum of a local $\Delta S = 2$ Hamiltonian (H_2) and the time ordered product of two local $\Delta S = 1$ Hamiltonians (H_1):

$$M = \langle \bar{K}^0 | H_2 | K^0 \rangle + \sum_n \frac{\langle \bar{K}^0 | H_1 | n \rangle \langle n | H_1 | K^0 \rangle}{m_K - E_n} \quad (5.1)$$

Following Gaillard and Lee, one method is to consider only the direct $\Delta S = 2$ part in the form of the box diagram and to assume that the dispersive ($\Delta S = 1$)² terms cancel out. However, calculations of individual dispersive terms /71 - 79,99/ indicate that they are substantial which makes such a cancellation seem unlikely. There is

also a possibly large additional contribution to the $\Delta S = 2$ Hamiltonian from a penguin operator /99/. As a result this approach has been questioned /99, 114, 124, 136, 137/.

Measurements of the B-meson partial decay widths /107/ and lifetime /119 - 121/ can be used to determine the contribution to the transition amplitude from the $\Delta S = 2$ Hamiltonian /127, 128/. In this way the large theoretical variation in the size and sign of the dispersive contribution can be limited phenomenologically.

It is sometimes stated that the dispersive amplitudes must give a positive contribution to the $K_L - K_S$ mass difference /77, 127/ ("positive" means here a positive contribution to $(-\delta m) > 0$). This statement is based on the assumption of a small value for the $K^0 - \bar{K}^0$ hadronic matrix element and the absence of penguin diagrams. However, if the matrix element is given a larger value (such as occurs in the Relativized Harmonic Oscillator model /87/) and/or penguin contributions are included, it can be shown that situations exist within the Standard Model where the dispersive amplitudes must give a negative contribution /128/.

5.2 The Box Diagram Contribution

In the GWS theory of weak interactions there is an effective local $\Delta S = 2$ Hamiltonian in the form of the box diagram /36/ (Figure 3.1). In the approximation where the masses and momenta of the external quarks are neglected, the $K^0 - \bar{K}^0$ transition amplitude due to this Hamiltonian is given by

$$M_B = -B \frac{G_F^2 M_W^2 f_K^2 m_K}{12 \pi^2} \sum_{i,j = u,c,t} \lambda_i \lambda_j B_{ij}^B \eta_{ij} \quad (5.2)$$

where the B_{ij} are known functions of the quark masses /81,82/. The η_{ij} are the perturbative QCD corrections due to Gilman and Wise /84/ and are numbers less than or equal to one.

The λ_i are products of KM matrix elements, $\lambda_i = V_{is}^* V_{id}$, which are a major uncertainty in the calculation of the $\Delta S = 2$ Hamiltonian. However, B -meson decay data provide a means of restricting the variation in the quark mixing angles to the very small range /127,128/

$$\begin{aligned} \sin\theta_2 &< 0.13 \\ \sin\theta_3 &< 0.05 \end{aligned} \tag{5.3}$$

The number B parametrizes the size of the hadronic matrix element of a quark operator

$$\begin{aligned} Q_B &= \langle \bar{K}^0 | \bar{s} \gamma^\mu (1 - \gamma_5) d \bar{s} \gamma_\mu (1 - \gamma_5) d | K^0 \rangle \\ &= -\frac{4}{3} f_K^2 m_K B \end{aligned} \tag{5.4}$$

The result is normalized to the vacuum saturation approximation ($B = +1$) of Gaillard and Lee /36/. Various approaches have been used to estimate this matrix element /85 - 92,96/ but there is no general agreement on a best value for B . In general B is positive and lies in the range $0.055 \leq B \leq 2.86$. However, the MIT bag model with one set of input parameters gives $B = -0.4$ /87/. A theoretical upper bound on the magnitude of the matrix element has been derived by Guberina et al. /92/ who find $|B| \leq 2.0 \pm 0.5$. In what follows B is normally taken to be positive with $B \leq 2.5$, but $B < 0$ is considered at various points.

In standard notation the CP-violation parameter ϵ is given by

$$\text{Re } \epsilon = - \text{Im} K / 2 \delta m \tag{5.5}$$

where M is the $K^0 - \bar{K}^0$ transition amplitude which is not yet identified with that arising from the box diagram. The $K_L - K_S$ mass difference is related to the $K^0 - \bar{K}^0$ transition amplitude by

$$\delta m = 2 \operatorname{Re} M \quad (5.6)$$

With the identification $\operatorname{Im} M = \operatorname{Im} M_B$ the constraints on the KM angles from B-meson decay imply a lower bound on the t-quark mass as a function of B /114, 124, 127, 130/. Up to the inclusion of penguin diagrams this is a good approximation since long distance contributions to $\operatorname{Im} M$ are limited by the experimental bound on $|\epsilon'/\epsilon|$ (section 5.3). The function $\operatorname{Re} M_B$ can now be calculated for allowed combinations of B and m_t and for all values of s_2 and s_3 in equation (5.3). The result is presented in Figure 5.1. The ratio $R_B = 2 \operatorname{Re} M_B / \delta m$ is shown for $0.6 \times 10^{-12} \text{ s} \leq \tau_B \leq 1.4 \times 10^{-12} \text{ s}$ and $20 \leq m_t (\text{GeV}) \leq 80$ and is independent of these variations. The reason for this is that the B-meson decay data (even in their least stringent form) constrain s_2 and s_3 to be sufficiently small that the t-quark decouples and an effective four quark theory remains:

$$M_B = - \frac{B G_F^2 f_K^2 m_K}{12\pi^2} \sin^2 \theta_c \cos^2 \theta_c \left\{ m_c^2 \eta_{cc} + m_u^2 - \frac{2 m_u^2 m_c^2}{m_c^2 - m_u^2} \ln \left(\frac{m_c^2}{m_u^2} \right) \right\} \quad (5.7)$$

In equation (5.7) the quark mixing has been restricted to a dependence on $\theta_1 = \theta_c = \theta_{\text{Cabibbo}}$ and the functions B_{ij} have been written in the approximate form /85, 103/ valid for $m_u, m_c \ll M_W$. Figure 5.1 shows $R_B \approx 0.8 \times B$ which is obtained from equation (5.7) using $m_u = 0.3 \text{ GeV}$, $m_c = 1.5 \text{ GeV}$ and $\eta_{cc} = 0.99$ /84/. The effect of changing any of these parameters is easily calculable from equation (5.7).

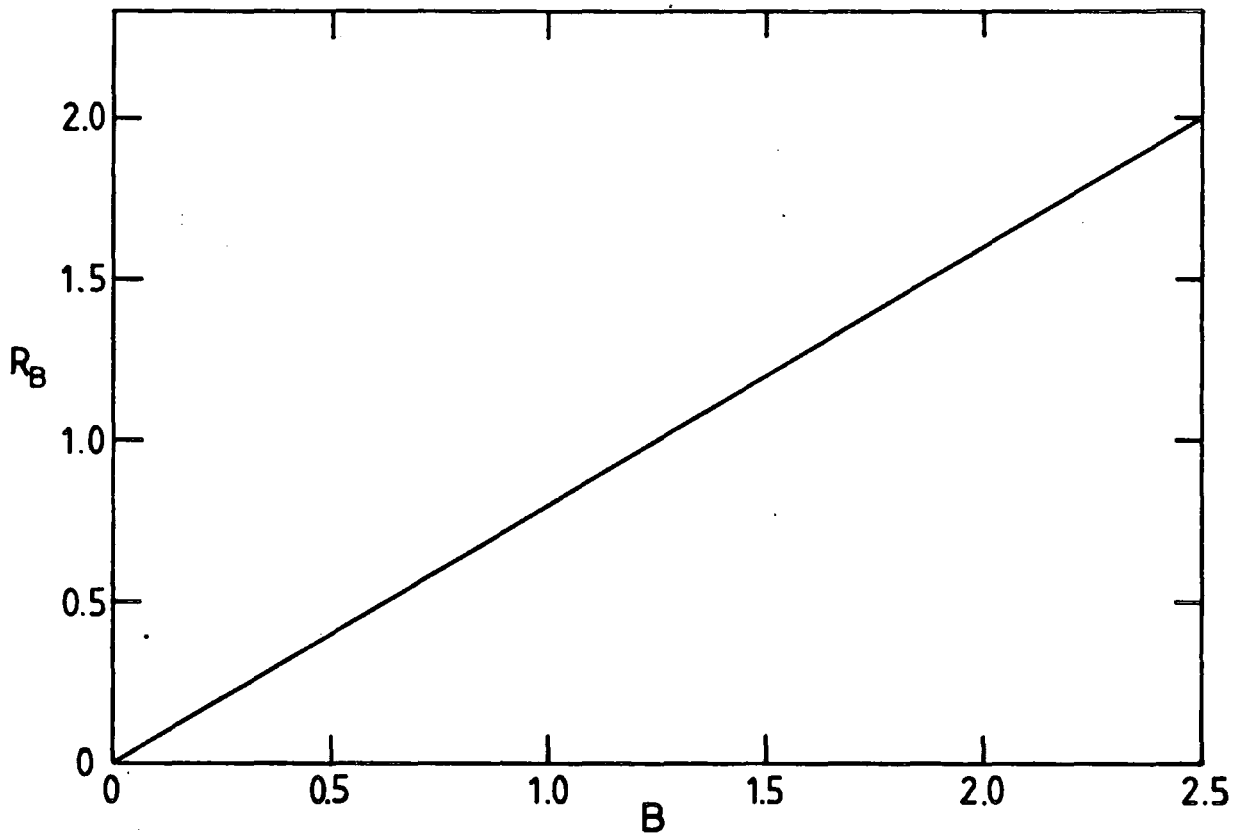


Figure 5.1

The contribution of the box diagram to the $K_L - K_S$ mass difference for $\tau_B > 0.6 \times 10^{-12}$ s. $R_B = 2 \text{Re}M_B / \delta m$ where δm is the experimental value.

The significance of the long B -meson lifetime ($\tau_B \gg 0.6 \times 10^{-12}$ s) is demonstrated by Figure 5.2. With $\tau_B = 0.1 \times 10^{-12}$ s the KM angles are not so restricted and a significant variation in R_B is allowed. This is due to the effect of the t -quark which increases the value of R_B/B . The reason for the dramatic increase in the lower bound on m_t when the constraint $\delta m = 2 \operatorname{Re} H_B$ is included /130/ is clear: for small values of B , m_t must be much larger than M_W in order to overcome the smallness of the mixing angles.

For the choice of quark masses and QCD corrections given above, the box diagram reproduces the experimental $K_L - K_S$ mass difference when $B \approx 1.2$. This is the source of the upper bound on B derived in reference 106 (recall, the contribution of the t -quark is positive). If B is smaller than this value the box diagram is insufficient, but for B at its theoretical upper limit ($B = +2.5$) the calculation gives twice the experimental result.

For B positive the KM CP-violating phase δ is excluded from the region $\pi < \delta < 2\pi$ by equations (5.3) and (5.5). However, for B negative the phase is excluded from $0 < \delta < \pi$. The solutions of equation (5.5) with $3\pi/2 < \delta < 2\pi$ and $\pi < \delta < 3\pi/2$ for $B < 0$ are identical to the solutions with $0 < \delta < \pi/2$ and $\pi/2 < \delta < \pi$ respectively for $B > 0$. This corresponds to $B \sin \delta > 0$ as found by Gilman and Hagelin from $|\epsilon'/\epsilon|$ /134/. $B < 0$, of course, gives the wrong sign for the mass difference. However, contributions from other sources such as long distance terms and penguin operators may be enough to compensate for this.

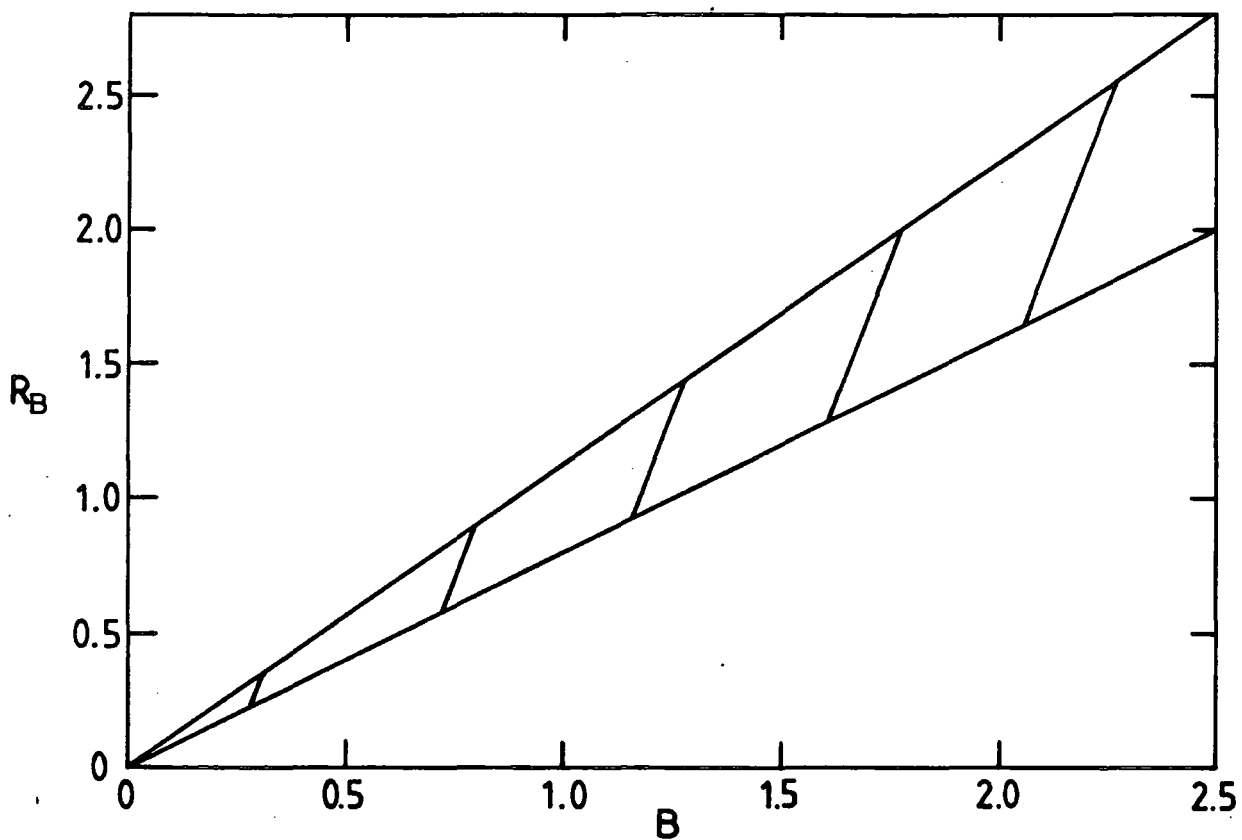


Figure 5.2

The contribution of the box diagram to the $K_L - K_S$ mass difference for $\tau_B = 0.1 \times 10^{-12}$ s . The shaded region is allowed.

5.3 Penguin Diagram Contributions

In the box diagram amplitude QCD effects were included in the parameters η_{ij} . However, with the introduction of strong interactions, new effects arise /97/ due to the exchange of gluons. These are the penguin diagrams.

In particular there is a CP-violating contribution to the $K^0 \rightarrow 2\pi(I=0)$ amplitude /98,138/ from such diagrams (Figure 3.2). In order to regain the Wu-Yang convention /60/ where this decay amplitude is real, a redefinition of the kaon fields by a phase ξ is performed ($|K^0\rangle \rightarrow e^{-i\xi}|K^0\rangle$; $|\bar{K}^0\rangle \rightarrow e^{i\xi}|\bar{K}^0\rangle$). This redefinition changes the relation between the CP-violation parameter and the $K^0 - \bar{K}^0$ transition amplitude to

$$\text{Re } \epsilon = - (\text{Im} M_B - 2\xi \text{Re} M_B) / 2\delta \quad (5.8)$$

where $\xi < 0$ /135/. This redefinition also introduces a phase $e^{-i\xi}$ to the $K^0 \rightarrow 2\pi(I=2)$ amplitude A_2 giving $\text{Im} A_2 \approx -\xi |A_2|$ and hence /134/

$$\left| \frac{\epsilon'}{\epsilon} \right| = \frac{|\xi|}{\sqrt{2}|\epsilon|} |A_2/A_0| \approx 15.6 |\xi| \quad (5.9)$$

where the experimental values of $|A_2/A_0| = 1/20$ /139/ and $|\epsilon| = 2.27 \times 10^{-3}$ have been used. The experimental result /68/ $\epsilon'/\epsilon = -0.003 \pm 0.014$ gives $|\xi| \leq 10^{-3}$.

Although this redefinition of fields has a significant effect on the lower bound for the t-quark mass /114/, the result of section 5.2 concerning $\text{Re} M_B$ is not changed. This is a consequence of the smallness of the mixing angles θ_2 and θ_3 which ensures that the c-quark dominates the real part of the $K^0 - \bar{K}^0$ transition amplitude.

Hochberg and Sachs /99/ have pointed out that the inclusion of

strong interactions leads to a new contribution to the $\Delta S = 2$ Hamiltonian which is topologically distinct from the box diagram. This is the double penguin diagram (Figure 3.3). The $K^0 - \bar{K}^0$ transition amplitude due to this part of the Hamiltonian is estimated to be /99/

$$M_P = - \frac{73}{9} \left(\frac{4}{3} f_K^2 m_K B \right) \frac{G_F^2 m_t^2}{18(4\pi)^4} \left(\lambda_u \ln \left(\frac{m_c^2}{\mu^2} \right) - \lambda_t \ln \left(\frac{m_t^2}{m_c^2} \right) \right)^2 \quad (5.10)$$

where μ is an infra red cut off taken to be $\mu \sim 1$ GeV. Although the amplitude is only logarithmically dependent on the cut off, it is quite sensitive to the actual value of μ which controls the cancellation of the two logarithms. For $\mu = 1$ GeV the cancellation is quite good, but for $\mu = 0.7$ GeV the penguin amplitude becomes much larger. However, this effect can be reduced by a simultaneous adjustment of the effective c-quark mass.

The double penguin amplitude has a real part which contributes to the $K_L - K_S$ mass difference and an imaginary part which contributes to the CP-violation:

$$\text{Re } \mathcal{E} = - (\text{Im} M_B + \text{Im} M_P(\mu)) / 2 \delta m \quad (5.11)$$

where the \mathcal{E} -term from single penguin diagrams has been neglected. The lower bound on m_t obtained from this equation and the constraints from B-meson decay are shown in Figure 5.3 as a function of the parameter B. This can alternatively be viewed as a lower bound on $|B|$ as a function of m_t . For $\mu = 1$ GeV and $m_c = 1.5$ GeV, the lower bound on m_t is significantly lower in the region of small B than the value obtained from the box diagram alone (compare Figure 4.14). The difference is about 10 GeV at $B = \frac{1}{3}$ for $\tau_B = 1.0 \times 10^{-12}$ s. This is due to the

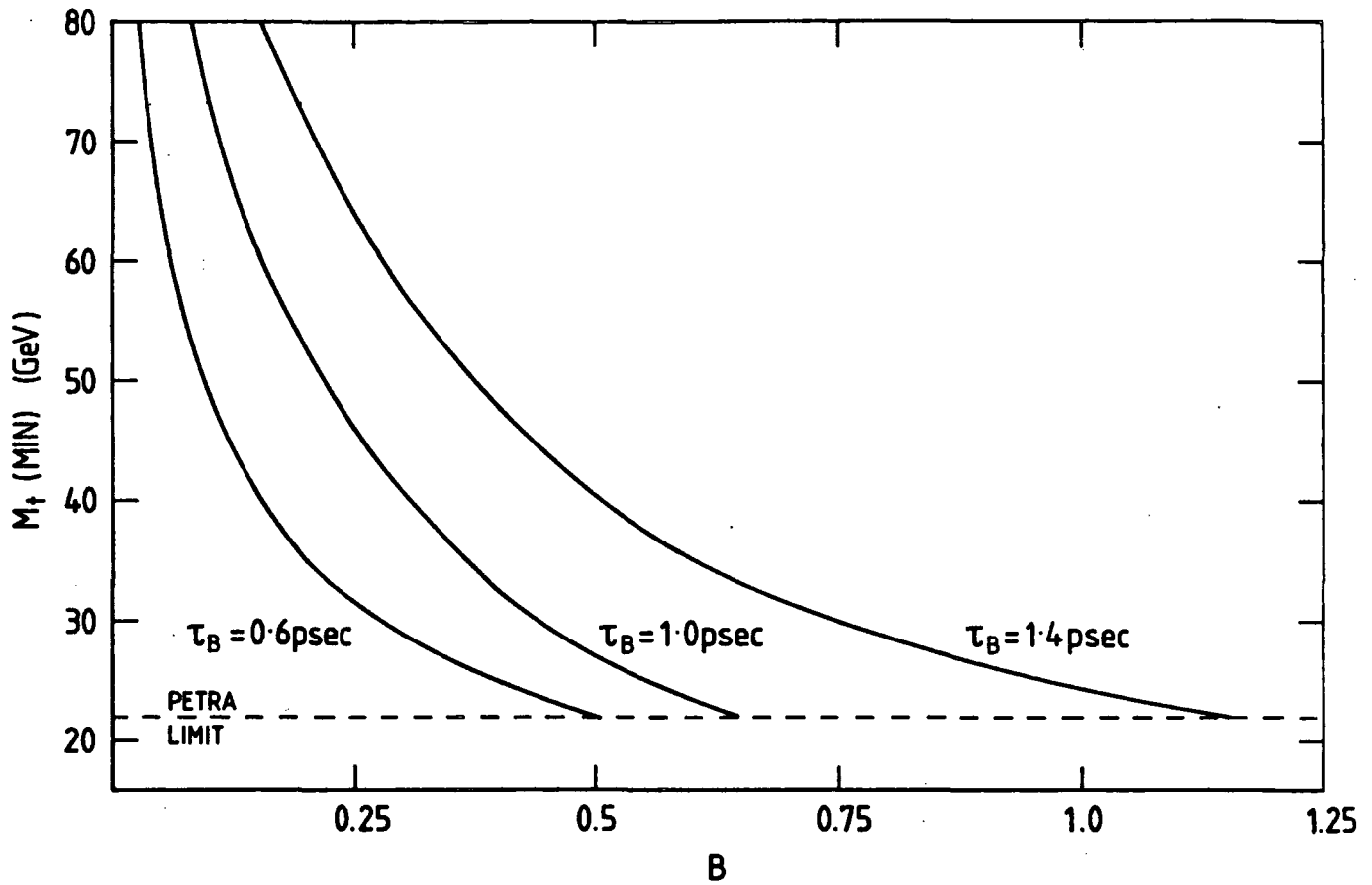


Figure 5.3

Lower bound on m_t for $\tau_B = (0.6, 1.0, 1.4) \times 10^{-12}$ s . The IR cut off in the double penguin amplitude is $\mu = 1.0$ GeV . For $\mu = 0.7$ GeV the curves are slightly lower.

relative importance of the double penguin diagram in this region, arising from its quadratic dependence on m_t and the large value for this parameter needed to fit the observed CP-violation.

The prediction of the real part of the box diagram (Figure 5.1) is unchanged due to the c-quark dominance of this amplitude. However, the double penguin amplitude provides an additional contribution to the mass difference of $2 \text{Re}M_P$. The ratio $R_P = 2 \text{Re}M_P / \delta m$ is shown in Figures 5.4 and 5.5 for $m_t = 25, 40, 60$ GeV, $m_c = 1.5$ GeV and two values for μ . $m_t = 25$ GeV is just above the current PETRA lower bound /55/ of $m_t > 22$ GeV. The result is independent of τ_D (equivalently θ_2 and θ_3) over the allowed range.

It can be seen that the double penguin amplitude gives a large, possibly dominant, contribution to the $\Delta S = 2$ Hamiltonian of the same sign as the box diagram. The sum of the box diagram and double penguin amplitudes reproduces the observed $K_L - K_S$ mass difference for B in the range 0.3 to 1.0. If B is negative, then a very large positive contribution from long distance dispersive terms is required to compensate for this. The long distance contributions are considered in the next section.

5.4 Dispersive Contributions to δm

In the $K^0 - \bar{K}^0$ transition amplitude, equation (5.1), there is a piece which is the time ordered product of two $\Delta S = 1$ transitions. It is this piece which contains the "long distance" dispersive amplitudes: $K^0 \leftrightarrow \pi\pi \leftrightarrow \bar{K}^0$; $K^0 \leftrightarrow \pi^0, \eta, \eta' \leftrightarrow \bar{K}^0$; $K^0 \leftrightarrow \rho, \omega, A_1 \leftrightarrow \bar{K}^0$; etcetera. These amplitudes were previously neglected on the assumption that their sum is small. As shown in the previous sections, it is easy

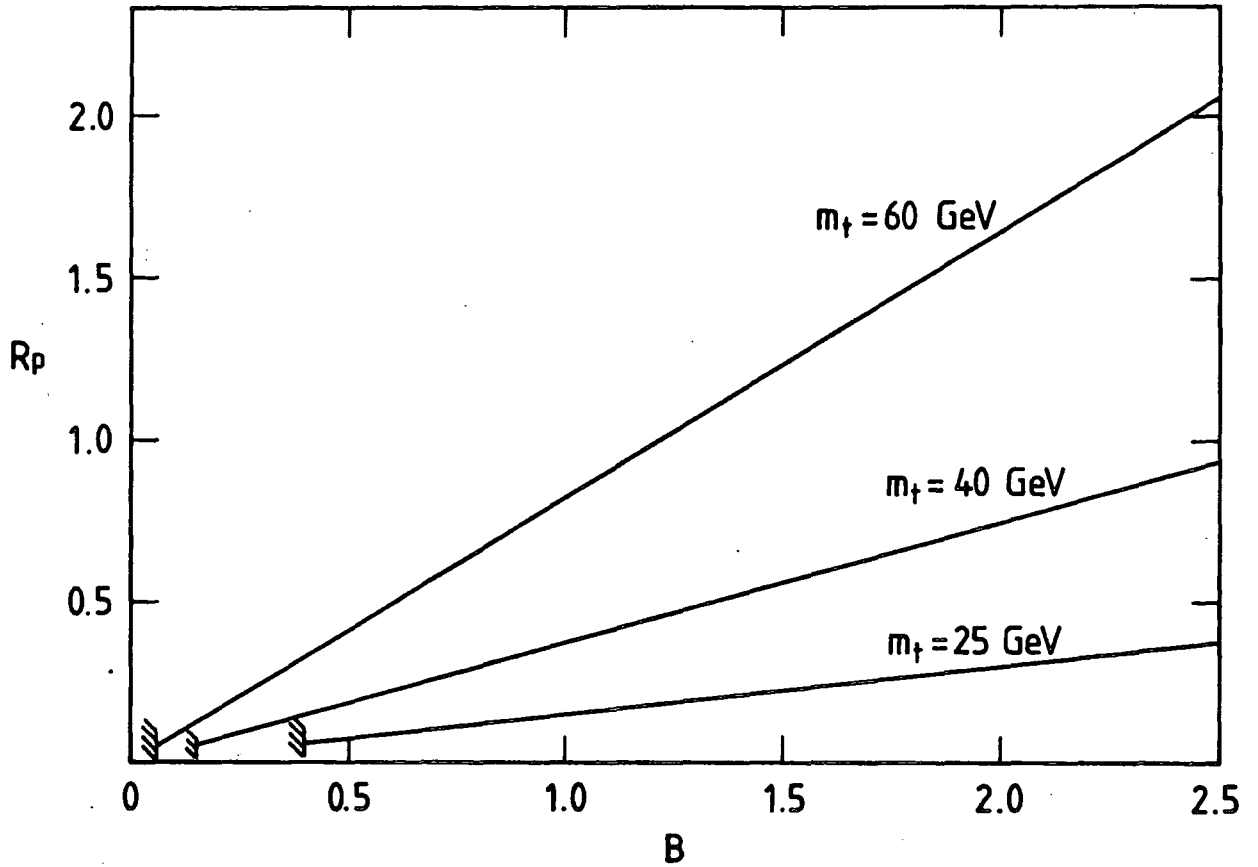


Figure 5.4

The contribution of the double penguin amplitude ($\mu = 1.0$ GeV) to the $K_L - K_S$ mass difference. $R_P = 2 \text{Re}M_P / \delta_m$.

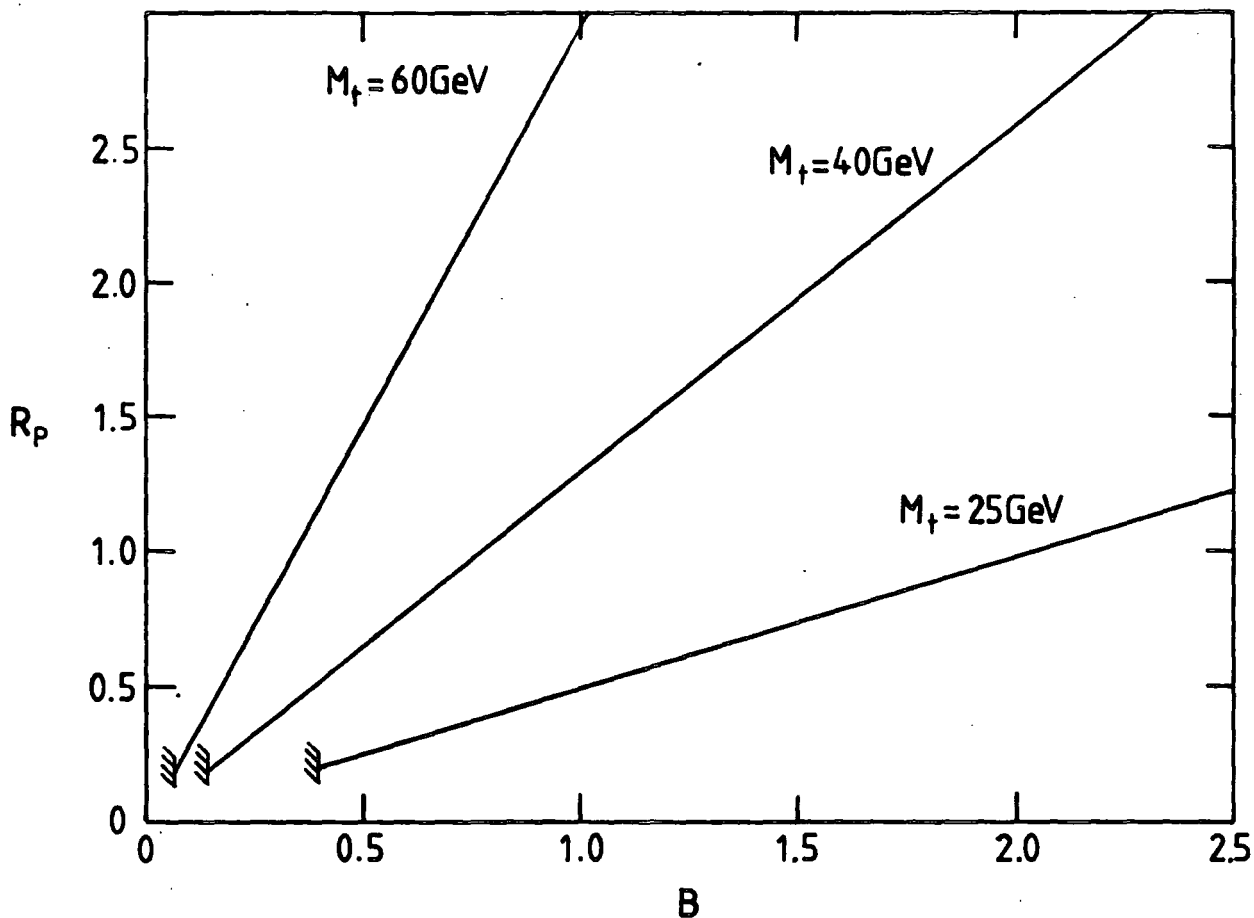


Figure 5.5

The contribution of the double penguin amplitude ($\mu = 0.7 \text{ GeV}$) to the $K_L - K_S$ mass difference.

to reproduce the observed value of δm without including any long distance pieces. However, estimates of the separate contributions /71 - 79/ indicate that their magnitudes are of the same order as the observed mass difference (see section 3.3). Although contributions of both signs occur, the large magnitudes of the individual terms indicates that an exact cancellation is unlikely.

The calculation of the amplitude from one particle pseudoscalar intermediate states by Itzykson et al. /78/ gives a contribution opposite in sign to the observed mass difference. In terms of the ratio $R_D = 2 \text{Re}M(\text{dispersive})/\delta m$, they find $R_D = -1.4$. The negative sign is supported by the analysis of Donoghue et al. /77/ who give $R_D(\pi^0, \gamma, \gamma') \approx -2$. The contribution of the two pion intermediate state is uncertain in magnitude but is probably positive /77/. Using a subtracted dispersion relation for the kaon self energy, Donoghue et al. /77/ find $R_D(\pi\pi) = 0.64$ with an ultra violet cut off of $\Lambda = 0.7 \text{ GeV}$ rising to $R_D(\pi\pi) = 1.4$ for $\Lambda = 1 \text{ GeV}$. A perturbation theory calculation leads to a somewhat larger result, being $R_D(\pi\pi) = 1.4$ for $\Lambda = 0.7 \text{ GeV}$ and $R_D(\pi\pi) = 2.8$ for $\Lambda = 1 \text{ GeV}$. The contributions due to one particle vector intermediate states are thought to be small /71/ due to angular momentum effects.

In the standard approach involving the box diagram an integral over a loop momentum k is performed. For small k the contribution of the u -quark accounts for at least part of the low energy dispersive terms. To avoid double counting an IR cut off, $\lambda \sim 1 \text{ GeV}$, should be introduced. The main effect of this is to remove the u -quark contribution from $\text{Re}M_B$. As the overall contribution of the u -quark is negative, the contribution of the box diagram to the $K_L - K_S$ mass difference is increased by $\sim 20\%$. It is possible that the dispersive contribution

is negative reflecting this variation on the quark level, as is indicated by the large negative contribution from the π^0, η, η' intermediate states /77,78/.

C.T.Hill /137/ assumed penguin dominance of the $\Delta S = 1$ Hamiltonian in order to obtain a clear separation of short distance box diagram and long distance dispersive contributions to δ_{π} . With the introduction of the $\Delta S = 2$ penguin operator this separation of long and short distance effects is no longer clear. The variation of the double penguin amplitude with IR cut off μ appears to compensate the opposing variation of the two pion long distance contribution with UV cut off Λ . However, as all the cut offs are independent (being artefacts of specific calculations), these effects are only qualitative.

It is usually stated that the dispersive amplitudes must give a positive contribution to the $K^0 - \bar{K}^0$ transition /77,127/. This statement is based on the assumption of a small value for B and the absence of penguin diagrams. However, if the matrix element is given a larger value (such as occurs in the Relativized Harmonic Oscillator (RHO) model) and/or penguin contributions are included, it can be shown that situations exist within the standard model where the dispersive amplitudes must give a negative contribution.

Donoghue et al. /88/ find $B = 0.33$ with an estimated 50 % uncertainty /77,89/ by relating the $\Delta S = 2$ matrix element to the $\Delta I = 3/2$ $K^+ \rightarrow \pi^+ \pi^0$ amplitude. In the absence of $\Delta S = 2$ penguin contributions this determines $R_D \sim +0.7$. However, in the case where there is a large penguin contribution, $R_D < 0$ is a possibility even for such a small value of B. For example, $\mu = 0.7$ GeV, $m_c = 1.5$ GeV and $m_t = 60$ GeV leads to $R_D \sim -0.3$.

Colić et al. /95/ and Dupont and Pham /90/ have noted that it is difficult to reproduce the experimental $K^+ \rightarrow \pi^+ \pi^0$ amplitude unless the $\Delta I = 3/2$ operator is suppressed by more than the short distance coefficient $C_4 \approx 0.4$. This would tend to increase the value for B obtained by Donoghue et al. /88/. For this reason a larger value for B should not be ruled out. A larger value for B is given by the RHO model of Colić et al. /87/ ($B = 1.4$). This model is the most stable of those considered. Its results are supported by a preliminary evaluation of the matrix element on the lattice /96/ ($B \sim 1.3$) and by an analysis of the $\Delta I = 3/2$ $K^+ \rightarrow \pi^+ \pi^0$ amplitude by Dupont and Pham /90/ ($B \gtrsim 1$). For $B = 1.4$ and $m_t = 40$ GeV, $m_c = 1.5$ GeV, $\mu = 1$ GeV, the observed $K_L - K_S$ mass difference is reproduced when $R_D \approx -0.6$, and much larger (negative) dispersive contributions are possible.

5.5 Conclusions

In the Standard Model the $K^0 - \bar{K}^0$ transition amplitude is the sum of three contributions: the box diagram, the double penguin and the $(\Delta S = 1)^2$ dispersive terms. Recent data on B-meson decay can be used to determine the magnitude of the box diagram contribution as a function of the parameter B . The box diagram alone is sufficient to reproduce the observed $K_L - K_S$ mass difference for $B \sim 1.2$ to 1.5 .

The double penguin amplitude also gives a possibly large contribution to δm which depends on m_t and an IR cut off μ . If B is small and the penguin contribution is not large, then the dispersive contribution to δm must be positive (i.e. $R_D > 0$) as is usually stated. However, when the magnitude of the hadronic matrix element is given by the RHO model ($B = 1.4$), the sum of the box and penguin amplitudes is too large and the dispersive terms must supply a negative contribution.

Improved measurements of the t-quark mass and B-meson lifetime would place better limits on the magnitudes of the box diagram and penguin amplitudes by determining a minimum value for $|A|$. This would then give a better indication of the magnitude and sign of the dispersive amplitude. For example, the present measurements of $m_t \leq 50$ GeV /58/ and $\tau_B > 0.6 \times 10^{-12}$ s /121/ give $|B| \geq 0.1$ whereas $m_t = 40$ GeV and $\tau_B = 1.4 \times 10^{-12}$ s gives $|B| \geq 0.5$ which leads to $R_D < 0.4$ for $B > 0$. On the theoretical side the most important advance would be an accurate and generally accepted calculation of the hadronic matrix element.

Due to these large uncertainties in the calculation of the $K_L - K_S$ mass difference, it is difficult to obtain useful constraints on new theories of weak interactions from this parameter. An optimistic approach might be to apply the criterion that $R_N = 2 \text{ReM}(\text{new contribution})/\delta m$ should be bounded by $|R_N| \leq 1$. On the whole, more reliable constraints would be obtained by considering the new contributions to CP-violation in the theory.

CHAPTER 6

CONCLUSIONS

In the preceding chapters the significance of the strangeness changing neutral currents $K^0 \leftrightarrow \bar{K}^0$, $K_L \rightarrow \mu^+ \mu^-$ and $K^0 \rightarrow n\pi$ has been discussed. These processes are the part of the general class of flavour changing neutral currents (FCNCs) which is presently the most useful due to the availability of experimental data. The observed suppression of FCNCs could lead, in principle, to precise phenomenology in weak interactions, since small changes in the theory could lead to large changes (on this scale) for the predictions of FCNC amplitudes. Unfortunately, this possibility is not realised in the case of the kaon amplitudes mentioned above. The problem occurs in the necessity of relating theoretical predictions which are given in terms of quarks to experimental data on hadrons.

The most widely used FCNC is the $K^0 - \bar{K}^0$ transition amplitude, $M(K^0 - \bar{K}^0)$, and possible contributions to this amplitude from Standard Model (SU(3)xSU(2)xU(1)) sources were reviewed in chapter 3. The contributions fall into two classes: "long" and "short" distance. The short distance contributions are the box diagram and double penguin amplitudes, which are given initially in terms of a quark transition amplitude. The relation between this and the hadronic $K^0 - \bar{K}^0$ transition amplitude is parametrized by a number B which is derived from the hadronic matrix element of a four quark operator. A perturbative

calculation of this matrix element is not possible and so it is estimated in a variety of models. These give a range $0.05 \leq B \leq 2.9$ and in one case $B < 0$. There is also a theoretical upper bound of $|B| \leq 2.0 \pm 0.5$. As no consensus on a preferred value for B has been reached, it was left as a free parameter in most of the phenomenological analyses described in chapters 4 and 5. The long distance amplitudes involve only hadrons from the outset, and so their contribution to $M(K^0 - \bar{K}^0)$ is correspondingly uncertain.

Theoretical calculations of $M(K^0 - \bar{K}^0)$ can be related to two pieces of data. The real part of the amplitude is equal to half the $K_L - K_S$ mass difference (δm) and the imaginary part is proportional to the CP-violation parameter (ϵ). From these relations one can attempt to determine the values of any unknown parameters in the theoretical prediction. The results can be used to check the consistency of the theory for describing other weak interaction processes.

One way of proceeding is to assume that the short distance box diagram dominates both the real and imaginary parts of the amplitude. This assumption was pioneered by Gaillard and Lee, who used it to successfully estimate the mass of the c-quark. Buras, also following this method, placed an upper bound on the t-quark mass. He used the box diagram calculation of δm together with a short distance calculation for the dispersive $K_L \rightarrow \mu^+ \mu^-$ amplitude to obtain the bound $m_t \leq 33$ GeV at $B = 0.4$. The result depends sensitively on B and for $B = 1$ the upper bound is above M_W . However, even if $B = 0.4$, various uncertainties in the calculation of the $K_L \rightarrow \mu^+ \mu^-$ amplitude raise the bound to above M_W . This, together with the uncertainties in the calculation of δm , means that a reliable upper bound on m_t cannot be obtained by this method.

This calculation has been repeated in the context of a supersymmetric theory, giving $m_t < 100$ GeV. However, this calculation is subject to the same uncertainties as the one in the Standard Model.

Measurements of the B-meson lifetime and partial decay widths can be used to place bounds on the elements of the quark mixing matrix as shown in chapter 4. This information, in conjunction with a calculation of the $K^0 - \bar{K}^0$ mass matrix yields a lower bound on the t-quark mass. This lower bound depends critically on the assumptions made for the calculation of the $K^0 - \bar{K}^0$ amplitude.

If only the imaginary part of the amplitude is considered to be dominated by the box diagram, then the lower bound on m_t lies below M_W for $\tau_B < 1.4 \times 10^{-12}$ s (the upper limit from JADE) and $B > 0.33$. The minimum value of m_t reaches the lower bound from PETRA data ($m_t > 22$ GeV) for $B \geq 1$ and $\tau_B \leq 1.0 \times 10^{-12}$ s.

This calculation was repeated in chapter 4 with the additional constraint that the $K_L - K_S$ mass difference was given by the real part of the box diagram amplitude. For $B > 1$, the lower bound on m_t is comparable to the results of the previous calculation. However, for values of B much less than this, the lower bound is dramatically increased. For example, $m_t > 150$ GeV at $B = 0.4$. This result may indicate that the real part of the $K^0 - \bar{K}^0$ transition amplitude is dominated by long distance contributions.

Penguin diagrams affect these calculations in two ways. Firstly, the relation between ξ and the imaginary part of $M(K^0 - \bar{K}^0)$ is defined in the Wu-Yang convention where the $K^0 \rightarrow 2\pi (I = 0)$ amplitude is real. Penguin diagrams give an imaginary contribution to this decay amplitude which can be rotated away by a suitable redefinition of the kaon fields. This affects the calculation of $\text{Im}M(K^0 - \bar{K}^0)$ and gives a

slight increase in the lower bound for m_t . Secondly, including the contribution to $\text{Im}M(K^0 - \bar{K}^0)$ from the double penguin diagram lowers the minimum value of m_t as shown in Chapter 5. The addition of the real part of the double penguin amplitude also makes it easier to reproduce the experimental value for δ_m at small B without any long distance contributions.

Under the assumption that the box diagram was the dominant contribution to both parts of $M(K^0 - \bar{K}^0)$, an upper bound on the parameter B was obtained in Chapter 4, using the constraints on the quark mixing from B -meson decay. This upper bound was $B \ll 1.2$ to 1.7 depending on the magnitude of the QCD corrections to the box diagram amplitude. The maximum value for B occurs when the t -quark contribution (which is always positive) is entirely suppressed by small mixing matrix elements and the c - and u -quark contributions reproduce the experimental value for δ_m . No phenomenological upper bound (below the present theoretical upper bound of $B \ll 2.5$) can be obtained under other assumptions.

Before the results from CESR and PEP on B -meson decay were available, there was a considerable freedom in the allowable values for the quark mixing angles. Analyses of the $K^0 - \bar{K}^0$ mass matrix, based on the box diagram calculation alone, determined that the decay $b \rightarrow u$ would be less frequent than the decay $b \rightarrow c$. This prediction was confirmed at CESR. In these analyses the CP-violating phase δ was restricted to lie in the range $0 < \delta < \pi$ or in a small region in the fourth quadrant, which was subsequently excluded by the experimental result $\Gamma(b \rightarrow u) / \Gamma(b \rightarrow c) < 5.5\%$.

These results were obtained for $B > 0$ which was required by the box diagram calculation of δ_m . If a large contribution to δ_m from long distance amplitudes is present, $B < 0$ is possible. The constraint on δ

from $\text{Im}(K^0 - \bar{K}^0)$ is then $B \sin \delta > 0$. This result is not affected by the introduction of the double penguin amplitude.

The analyses described above are based on different assumptions about the $K^0 - \bar{K}^0$ mass matrix which leads in some cases (such as the lower bound on m_t) to a large variation in the result. For this reason a better understanding of the $K^0 - \bar{K}^0$ mass matrix itself is desirable. The possible contributions to δ_m from Standard Model sources were examined in Chapter 5.

The data on the B-meson lifetime and ratio of partial widths restricts the quark mixing angles θ_2 and θ_3 to be sufficiently small that the t-quark decouples from the box diagram. The box diagram contribution to δ_m is then given by the four quark model calculation. The major uncertainty in this is the value of B. For B in the range 1.2 to 1.7 (depending on the QCD corrections to this amplitude) it was found that the box diagram alone gave the experimental value for δ_m . The Relativized Harmonic Oscillator (RHO) model gives B in this range (B = 1.4).

The double penguin amplitude gives a contribution to the $K_L - K_S$ mass difference which is the same sign as the box diagram. Its contribution is uncertain in magnitude but is possibly substantial. The sum of these two short distance amplitudes was shown to give the correct value for δ_m when B was in the range $0.3 \leq B \leq 1.0$.

From these results it can be seen that there is no compelling phenomenological reason to include a large contribution from long distance dispersive amplitudes. However, if B is found theoretically to be small (~ 0.3 say) and the double penguin amplitude is negligible, then the dispersive contribution (to $-\delta_m$) must be positive and relatively large. If, on the other hand, B is nearer to the RHO result of 1.4 and/or

the penguin contribution is large, then the dispersive amplitudes must give a negative contribution. Both these possibilities are allowed by the theoretical calculations of the long distance amplitudes.

Due to these large uncertainties in the calculation of δ_m , more reliable constraints on unknown parameters can be obtained by considering only the CP-violating, imaginary part of $M(K^0 - \bar{K}^0)$. However, an optimistic approach, in the case of extensions to the Standard Model, might be to assume that the magnitude of new contributions to δ_m should be smaller than the experimental result. In the case of the Left-Right Symmetric model, this would lead to a lower bound on the mass of the new gauge boson being $M_{WR} \gg 1.6$ TeV as given in Chapter 4.

The usefulness of the $K^0 - \bar{K}^0$ mass matrix as a constraint on weak interaction physics would be considerably improved by an accurate and generally accepted calculation of the hadronic matrix element $\langle B \rangle$. On the experimental side, more precise measurements of the B-meson lifetime and the t-quark mass would be advantageous. Data on other FCNCs, such as $B^0 - \bar{B}^0$ mixing is eagerly awaited.

REFERENCES

1. C.N.Yang and R.L.Mills, Phys. Rev. 96, 191 (1954)
2. H.D.Politzer, Phys. Rep. 14C, 129 (1974)
3. M.R.Pennington, Rep. on Prog. in Phys. 46, 393 (1983)
4. R.M.Barnett and D.Schlatter, Phys. Lett. 112B, 475 (1982)
5. R.M.Barnett, Phys. Rev. Lett. 48, 1657 (1982)
6. I.J.R.Aitchison and A.J.G.Hey, "Gauge Theories in Particle Physics", Adam Hilger Ltd, Bristol (1982)
7. S.L.Glashow, Nucl. Phys. 22, 579 (1961)
8. S.Weinberg, Phys. Rev. Lett. 19, 1264 (1967)
9. A.Salam, Proc. 8th Nobel Symp., Almqvist and Wiksell, Stockholm (1968), p.367
10. P.Higgs, Phys. Rev. Lett. 12, 132 (1964); 13, 508 (1964)
F.Englert and R.Brout, Phys. Rev. Lett. 13, 321 (1964)
G.S.Guralnik, C.R.Hagen and T.W.B.Kibble, Phys. Rev. Lett. 13, 585 (1964)
11. G.'t Hooft, Nucl. Phys. B33, 173 (1971); B35, 167 (1971)
12. M.Clements et al., Phys. Rev. D27, 570 (1983)
13. J.E.Kim et al., Rev. Mod. Phys. 53, 211 (1981)
14. C.H.Llewellyn-Smith and J.F.Wheater, Phys. Lett. 105B, 486 (1981)
15. M.Banner et al., UA2 collab., Phys.Lett. 122B, 476 (1983)
16. G.Arnison et al., UA1 collab., Phys. Lett. 129B, 273 (1983)
17. H.Fritzsch and P.Minkowski, Phys. Rep. 73C, 67 (1981)
18. H.Georgi and S.L.Glashow, Phys. Rev. Lett. 32, 438 (1974)
19. W.J.Marciano and A.Sirlin, Phys. Rev. Lett. 46, 163 (1981)

20. F.Langacker, Phys. Rep. 72C, 165 (1981)
21. E.Fiorini, Proc. Int. Symp. on Lepton and Photon Interactions
at High Energies, Cornell (1983)
22. R.M.Bionta et al., Phys. Rev. Lett. 51, 27 (1983)
23. J.C.Pati and A.Salam, Phys. Rev. Lett 31, 661 (1973)
24. M.A.B.Bég et al., Phys. Rev. Lett. 38, 1252 (1977)
25. J.F.Donoghue and B.R.Molstein, Phys. Lett. 113B, 382 (1982)
26. P.Fayet and S.Ferrara, Phys. Rep. 32C, 249 (1977)
27. P. van Nieuwenhuizen, Phys. Rep. 68C, 191 (1981)
28. J.Ellis, D.V.Nanopoulos and K.Tanvakis, Phys. Lett. 121B, 123 (1983)
29. G.Senjanović, Proc. IV Adriatic Meeting, Dubrovnik (1983)
30. F.E.Close, "An Introduction to Quarks and Partons", Academic (1979)
31. N.Cabibbo, Phys. Rev. Lett. 10, 531 (1963)
32. R.E.Shrock and L.-L.Wang, Phys. Rev. Lett. 41, 1692 (1978)
33. Particle Data Group, Phys. Lett. 111B, 1 (1982)
34. S.L.Glashow, J.Iliopoulos and L.Maiani, Phys. Rev. D2, 1285 (1970)
35. S.L.Glashow and S.Weinberg, Phys. Rev. D15, 1958 (1977)
36. M.K.Gaillard and B.W.Lee, Phys. Rev. D10, 897 (1974)
37. M.H.Shaevitz, Proc. Int. Symp. on Lepton and Photon Interactions
at High Energies, Cornell (1983)
38. V.A.Lubimov et al., Phys, Lett. 94B, 266 (1980)
V.A.Lubimov, Proc. Eur. Phys. Soc. HEP 83, Brighton (1983)
39. M.Kobayashi and T.Maskawa, Prog. Theor. Phys. 49, 652 (1973)
40. V.Barger, W.F.Long and S.Pakvasa, Phys. Rev. Lett. 42, 1585 (1979)
41. R.E.Shrock, S.B.Treiman and L.-L.Wang, Phys. Rev. Lett.
42, 1589 (1979)
42. L.Maiani, Proc. Int. Symp. on Lepton and Photon Interactions
at High Energies, Hamburg (1977)

43. S.W.Herb et al., Phys. Rev. Lett. 39, 252 (1977)
44. P.Avery et al., CLEO report no. CLEO-84-6 (1984)
45. G.L.Kane and H.E.Peskin, Nucl. Phys. B195, 29 (1982)
46. K.Kleinknecht and B.Renk, Z. Phys. C16, 7 (1982)
47. S.Pakvasa, Proc. XXI Int. Conf. on High Energy Phys., Paris (1982)
48. S.L.Adler, Phys. Rev. 177, 2426 (1969)
49. J.S.Bell and R.Jackiw, Nuovo Cim. 60A, 47 (1969)
50. D.G.Sutherland, Nucl. Phys. B2, 433 (1967)
M.Veltman, Proc. Roy. Soc. A301, 107 (1967)
51. R.Jackiw, in "Current Algebra and its Application", S.B.Treiman,
R.Jackiw and D.J.Gross, Princeton (1972), p.97
52. D.J.Gross and R.Jackiw, Phys. Rev. D6, 477 (1972)
53. H.Georgi and S.L.Glashow, Phys. Rev. D6, 429 (1972)
54. C.Bouchiat, J.Iliopoulos and Ph.Meyer, Phys. Lett. 38B, 519 (1972)
55. M.Althoff et al., Phys. Lett. 138B, 441 (1984)
56. V.Barger, A.D.Martin and R.J.N.Phillips, Phys. Lett. 125B, 339 (1983)
57. G.Arnison et al., UA1 collab., Phys. Lett. 122B, 103 (1983)
58. D.DiBitonto, Proc. 7th Eur. Symp. on Antiproton Interactions,
Durham (1984)
59. M.Gell-Mann and A.Pais, Phys. Rev. 97, 1387 (1955)
60. L.Wolfenstein, Proc. School of Phys. "E.Majorana", ed. A.Zichichi,
Academic (1969), p.218
61. P.K.Kabir, "The CP-Puzzle", Academic, London (1968)
62. J.H.Christenson et al., Phys. Rev. Lett. 13, 138 (1964)
63. A.Abashian et al., Phys. Rev. Lett. 13, 243 (1964)
64. W.Fry and R.G.Sachs, Phys. Rev. 109, 2212 (1958)
65. Y.B.Zel'dovich, Zh. éksp. teor. Fiz. 30, 1168 (1956)
66. S.B.Treiman and R.G.Sachs, Phys. Rev. 103, 1545 (1956)

67. W.Melhop et al., Proc. XIII Int. Conf. on High Energy Phys.,
Berkeley (1967)
68. K.Kleinknecht, Proc. XVII Int. Conf. on High Energy Phys.,
London (1974)
69. W.Norse and K.Kleinknecht, Proc. Europhys. Conf. on "Flavour
Mixing in Weak Interactions", "E.Majorana"
Centre, Erice, Sicily (1984)
70. P.Pavlopoulos, CERN preprint, CERN - EP/84 - 49 (1984)
71. S.Oneda, Y.S.Kim and D.Korff, Phys. Rev. 136B, 1064 (1964)
72. V.Barger and E.Kazes, Phys. Rev. 124, 279 (1961)
73. T.N.Truong, Phys. Rev. Lett. 17, 1102 (1966)
74. R.Rockmore and T.Yao, Phys. Rev. Lett. 18, 501 (1967)
75. K.Kang and D.J.Land, Phys. Rev. Lett. 18, 503 (1967)
76. K.Nishijima, Phys. Rev. Lett. 12, 39 (1964)
77. J.F.Donoghue, E.Golowich and B.R.Holstein, Phys. Lett. 135B, 481 (1984)
78. C.Itzykson, H.Jacob and G.Mahoux, N. Cim. Suppl. 5, 978 (1967)
79. D.F.Greenberg, Nuovo Cim. LVIA, 597 (1968)
80. E.Witten, Nucl. Phys. B122, 109 (1977)
81. T.Inami and C.S.Lim, Prog. Theor. Phys. 65, 297 (1981); 65,
1772 Erratum (1981)
82. A.J.Buras, Phys. Rev. Lett. 46, 1354 (1981)
83. F.J.Gilman and M.B.Wise, Phys. Lett. 93B, 129 (1980)
84. F.J.Gilman and M.B.Wise, Phys. Rev. D27, 1128 (1983)
85. R.E.Shrock and S.B.Treiman, Phys. Rev. D19, 2148 (1979)
86. M.I.Vysotskii, Yad. Fiz. 31, 1535 (1980); Sov. J. Nucl. Phys. 31,
797 (1980)
87. P.Colić et al., Nucl. Phys. B221, 141 (1983)
88. J.F.Donoghue, E.Golowich and B.R.Holstein, Phys. Lett. 119B, 412 (1982)

89. C.H.Llewellyn-Smith, Proc. Int. Symp. on Lepton and Photon Interactions at High Energies, Cornell (1963)
90. Y.Dupont and L.L.Pham, Phys. Rev. D29, 1368 (1984)
91. P.Ginsparg and H.B.Wise, Phys. Lett. 127B, 265 (1983)
92. B.Guberina, B.Machet and E. de Rafael, Phys. Lett. 126B, 269 (1983)
93. A.Chodos et al., Phys. Rev. D9, 3471 (1974)
94. J.Trampetić, Phys. Rev. D27, 1565 (1983)
95. P.Colić, J.Trampetić and D.Tadić, Phys. Rev. D26, 2286 (1982)
96. N.Cabibbo, G.Martinelli and R.Petronzio, CERN report no. CERN - TH.3774 (1984)
97. N.A.Shifman, A.I.Vainshtein and V.I.Zakharov, Nucl. Phys. B120, 316 (1977)
98. B.Guberina and R.D.Peccei, Nucl. Phys. B163, 289 (1980)
99. D.Hochberg and R.G.Sachs, Phys. Rev. D27, 606 (1983)
100. J.J.Aubert et al., Phys. Rev. Lett. 33, 1404 (1974)
101. J.E.Augustin et al., Phys. Rev. Lett. 33, 1406 (1974)
102. V.Barger, Private Communication.
103. V.Barger et al., Phys. Rev. Lett. 42, 1585 (1979)
104. R.E.Shrock et al., Phys. Rev. Lett. 42, 1589 (1979)
105. L.-L.Chau, W.-Y.Keung and M.D.Tran, Phys. Rev. D27, 2145 (1983)
106. F.D.Gault and J.N.Webb, Z. Phys. C22, 93 (1984)
107. C.Klopfenstein et al., Phys. Lett. 130B, 444 (1983)
108. R.E.Shrock and M.B.Voloshin, Phys. Lett. 87B, 375 (1979)
109. E.Ma and A.Pramudita, Phys. Rev. D22, 214 (1980)
110. V.Barger et al., Phys. Rev. D25, 1860 (1982)
111. B.D.Hyams et al., Phys. Lett. 29B, 128 (1969)
112. R.I.Dzhelyadin et al., Phys. Lett. 97B, 471 (1980)
113. L.Bergström et al., Phys. Lett. 134B, 373 (1984)

114. A.J.Euras, W.Szymanski and H.Steger, Nucl. Phys. B230, 529 (1984)
115. G.Beall, H.Bander and A.Soni, Phys. Rev. Lett. 48, 646 (1982)
116. R.N.Mohapatra, G.Senjanović and N.D.Tran, Phys. Rev. D20, 546 (1983)
117. F.J.Gilman and M.H.Reno, Phys. Lett. 127B, 426 (1983)
118. A.E.Lahanas and D.V.Nanopoulos, Phys. Lett. 129B, 461 (1983)
119. V.Bartel et al., Phys. Lett. 114B, 71 (1982)
120. E.Fernandez et al., Phys. Rev. Lett. 51, 1022 (1983)
121. N.S.Lockyer et al., Phys. Rev. Lett. 51, 1316 (1983)
122. G.Altarelli et al., Nucl. Phys. B200, 365 (1982)
123. K.Chadwick et al., Phys. Rev. D27, 475 (1983)
124. P.H.Ginsparg, S.L.Glashow and M.B.Wise, Phys. Rev. Lett. 50,
1415 (1983); 51, 1395 Erratum (1983)
125. S.Stone, Proc. Int. Symp. on Lepton and Photon Interactions at
High Energies, Cornell (1983)
126. J.Cortes, X.Y.Pham and A.Tounsi, Phys. Rev. D25, 188 (1982)
127. L.-L.Chau and W.-Y.Keung, Phys. Rev. D29, 592 (1984)
128. J.N.Webb, Durham report DTP/84/12 (1984); DTP/34/26 (1984)
129. K.Kleinknecht and B.Renk, Phys. Lett. 130B, 459 (1983)
130. J.N.Webb, Durham report DTP/83/22 (1983)
131. G.Altarelli, Proc. NATO Adv. Summer Inst., Munich (1983)
132. M.B.Einhorn et al., Nucl. Phys. B191, 146 (1981)
133. J.Ellis and J.S.Hagelin, Nucl. Phys. B217, 189 (1983)
134. F.J.Gilman and J.S.Hagelin, Phys. Lett. 126B, 111 (1983)
135. F.J.Gilman and J.S.Hagelin, Phys. Lett. 133B, 443 (1983)
136. L.Wolfenstein, Nucl. Phys. B160, 501 (1979)
137. C.T.Hill, Phys. Lett. 97B, 275 (1980)
138. F.J.Gilman and M.B.Wise, Phys. Lett. 83B, 83 (1979)
139. T.J.Devlin and J.O.Dickey, Rev. Mod. Phys. 51, 237 (1979)

